Studies on Chaos and Fractal of Discrete Nonlinear Control Systems

Yasuda, Toshihiko

(Degree)
博士（工学）

(Date of Degree)
1995-03-15

(Date of Publication)
2008-03-25

(Resource Type)
doctoral thesis

(Report Number)
乙1914

(JaLCDOI)
https://doi.org/10.11501/3105515

(URL)
https://hdl.handle.net/20.500.14094/D2001914

KOBE UNIVERSITY
DOCTORAL DISSERTATION

STUDIES ON CHAOS AND FRACTAL OF DISCRETE NONLINEAR CONTROL SYSTEMS

(離散型非線形制御システムのカオスとフラクタルに関する研究)

January 1995

TOSHIHIKO YASUDA

Acknowledgements

The author would like to express his special thanks to Professor Emeritus Yoshifumi Sunahara of Kyoto Institute of Technology for his supervisions, suggestions and continuous encouragement during the long years that the preparation of this thesis was in progress.

The author would like to express his sincere thanks to Professor Kazumasa Hirai of Kobe University for his encouragement and helpful advises. Thanks are also extended to Prof. Keisuke Ito, Prof. Shinzo Kitamura and Prof. Masao Ikeda of Kobe University for their comments on this thesis.

The author would like to thank Dr. Yoji Morita of Kyoto Gakuen University and Dr. Tokuo Fukuda of Otemon Gakuin University for their valuable suggestions and advises. Thanks are also extended to many members of Professor Sunahara's laboratory of Kyoto Institute of Technology, and furthermore staff members of Shiga Prefectural Junior College, for their helpful advises and encouragement.

The author expresses his deep appreciation to his wife, Mrs. Kiyoe Yasuda for her constant encouragement and patience.

This thesis is dedicated to my parents, Mr. Yukio Yasuda and Mrs. Masumi Yasuda.

Abstract

In this thesis, first, fractal boundaries of the invariant set are investigated, in connection with a class of one-dimensional discrete nonlinear dynamical systems. The evaluation of the Hausdorff dimension of the boundary brings us existing conditions of fractal boundaries, i.e., it is analytically shown that if periodic points with period three exist, then fractal boundaries of the invariant set appear. Furthermore, by introducing the notation of the symbolic dynamics, mechanisms yielding fractal invariant set are clarified.

The results obtained are applied to explore the invariant set of a class of one-dimensional nonlinear sampled-data control systems and it is demonstrated that the set of initial conditions, under which the state variable is finite, exhibits the fractal structure. Fractal basin boundaries of coexisting final states are also explored. These results reveal that in order to determine the sampling period, it is necessary to take into account the structure of the invariant set.

Based on results obtained in one-dimensional systems, fractal boundaries of the invariant domain of a class of predator-prey systems are discussed. The existing conditions and the yielding mechanisms of fractal boundaries are clarified, concerned with the Volterra-Lotka type two-dimensional difference equations. The invariant domain treated here is a set of initial conditions, under which the prey and predator coexist.

Secondly, based on the fact that chaotic oscillations are often not desirable in some physical systems, for example, biological population systems, the stabilization scheme of the chaotic behavior is investigated in a class of predator-prey systems, by introducing mathematical models with control inputs, where the harvesting or supplying of predators is adopted as control inputs. Furthermore, noting that the chaotic system often exhibits fractal boundaries of the invariant domain, the influences of control inputs, which stabilize the system, on fractal structures of the invariant domain are discussed.

Throughout this thesis, numerical experiments are carried out in order to show the validity of the results.

Contents

Chapter 1

Introduction

1.1 Historical Background

Chaos and fractals are distinct but closely related subjects that many mathematicians and engineers look to as a new way for understanding apparent complexity of nature and as a challenging field in engineering applications. Mathematical studies on chaos demonstrate that deterministic system – some of them surprisingly simple – can behave in seemingly unpredictable fashion. Fractals – a term coined by B. Mandelbrot in the 1970s [Man75],[Man77] – offer an alternative to the smooth curves of Euclidean geometry and yield a geometry representing the true nature of trees, clouds, and coastlines [Fed88]. Both subjects have come the fore in recent years with the advent of high-speed computers and computer graphics, which allow scientists to explore new territory and literally see the intricate structures of simple differential or difference equations. The aim of this section is to present a historical background of the chaos and fractal theory.

1.1.1 Chaos

(a) Classical Studies on Dynamical Systems and Discovery of Chaos

For many years, a great number of scientists are fascinated by problems concerned with dynamical systems. Among such problems, Newton's studies on celestial mechanics, especially those on the motions of the bodies in the solar system, are notable, which yield studies on models described by differential equations.

For linear ordinary differential equations, a relatively complete theory was developed

by the great mechanicians and mathematicians of the eighteenth and nineteenth centuries. However, nonlinear systems remained largely inaccessible, apart from successful applications of perturbation methods to weakly nonlinear problems, where the most famous applications are demonstrated in celestial mechanics. Poincaré's work [Poi90a],[Poi90b],[Poi99] in the late-nineteenth century is the origin of a qualitative approach to studies on nonlinear differential equations. One could assume naively that deterministic motion is rather regular and far from being chaotic because successive states evolve continuously from each other. However, H. Poincaré (1854-1912) was already aware that the nonintegrable three-body problem of classical mechanics can lead to completely chaotic trajectories [Poi90b] . He also found various important concepts, which are fundamental for investigating chaotic phenomena such as a homoclinic point, the Poincaré map, bifurcation theory and so on. A qualitative study of nonlinear dynamical systems, proposed by Poincaré, was continued by G. D. Birkhoff (1884-1944) [Bir35]. Furthermore, about sixty years later, Kolmogorov [Kol54], Arnold [Arn63] and Moser [Mos67] formulated the so-called KAM theorem, which is significant for investigating chaos in slightly nonintegrable Hamiltonian systems.

Besides Hamiltonian systems, before the concept of chaos in deterministic systems was established, complicated behavior exhibited by deterministic systems were observed by some scientists. M. L. Cartwright and J. E. Littlewood found a certain second order nonlinear differential equation with a forcing term exhibiting a complicated behavior [CL45]. N. Levinson simplified this equation and presented a deterministic second order piecewise linear ordinary differential equation, that a Bernoulli shift is embedded in a solution process [Lev49]. In this sense, Levinson showed that a stochasticity can be observed in a solution process of a deterministic system. From this point of view, Kalman found that in a certain solution set of a nonlinear difference equation, a Markov process can be embedded [Kal56]. A number of outstanding problems, including the famous horseshoe model, are outlined by Smale's classic paper [Sma67].

Concerned with fluid dynamics, in 1963, the meteorologist E. N. Lorenz found that even a simple set of three coupled first order nonlinear differential equations, which are derived as an approximation of the Navier-Stokes equation, can lead to completely chaotic

trajectories [Lor63]. He discovered one of the first examples of deterministic chaos in dissipative systems. The importance of *strange attractors* in the study of turbulence was suggested by Ruelle and Takens [RT71]. On the other hand in biological population dynamics, R. May indicates the existence of simple mathematical model exhibiting chaotic behavior [May74]. The study on electrical circuits, by Y. Ueda, led to discover an extraordinarily beautiful set of strange attractors [Ued79].

(b) Simple Mathematical Models Exhibiting Chaos in Discrete Systems

Stimulated by discoveries of chaotic phenomena presented in previous subsection, during the past three decades, there has been an explosion of researches, concerned with the complicated phenomena in nonlinear dynamical systems. At the first stage of studies on chaos theory, an important role was played by one or two-dimensional simple and deterministic maps, in order to understand the basic nature of chaotic phenomena.

Simplest mathematical objects which can display chaotic behavior are given by a class of nonlinear one-dimensional maps [GOI77], [CE80], [GM80], [Ott81], [Pre83], [GH83], [Sch84], [Dev89], [TS86]. Although the famous definition of chaos is provided by the statement *period 3 implies chaos* of Li and York [LY75], there are many definitions of chaos in a dynamical system [Blo78], [OO80], [Dev89], [Ott81], [BPV84]. Oono and Osikawa (1980) [OO80] enumerated physical intuitive pictures of chaos appearing in one-dimensional difference equations. The excellent theorem concerned with the existence of periodic orbits was shown by Sarkovskii (1964) [Sar64], [Guc79]. Furthermore, conditions for existence of stable periodic orbits were demonstrated by Singer [Sin78]. In order to discuss the stochasticity of chaos, relationship between chaotic processes and Bernoulli shift was studied by using symbolic dynamics [Bil65], [AA68], [Fei78], [FOY83].

A well-studied two-dimensional map is the so-called Hénon map [Hen76], [BC91]. The attractor of Hénon map has scale invariance and fractal structure as a Cantor set. Irregular behavior of measure preserving mapping, for example, the baker transformation, were discussed in Lasota and Mackey [LM85]. Various properties of strange attractors were illustrated by using the horseshoe map [Sma67], [SV81], [GH83], [TS86]. Methods for

detecting chaos in higher-dimensional systems was presented by Marotte [Mar78] and Diamond [Dia76]. Furthermore, Marotte's theorem was generalized by Shiraiwa and Kurata [SK79].

Lyapunov exponents measure the exponential attraction or separation in time of two adjacent trajectories in phase space with different initial conditions. A positive Lyapunov exponent indicates a sensitive dependence of a trajectory on initial conditions and a chaotic motion in a dynamical system with bounded trajectories. Therefore, Lyapunov exponents is often adopted as a tool for diagnosing whether or not a system is chaotic [Ose68], [SN79], [WSSV85], [GPL90], [ABK91]. Furthermore, influences of noises on chaos are also evaluated by using Lyapunov exponents [MH81], [SMY88], [SMYK83], [SMY84], [MY91]. In this thesis, the usefulness of Lyapunov exponents will be shown in numerical experiments of Chap.5.

(c) Chaos Observed in Various Research Fields

There exist widespread interest in the engineering and applied science with respect to *strange attractors*, *chaos* and *dynamical systems theory*. In recent years – due to new theoretical results, the availability of high speed computers, and refined experimental techniques – it has become clear that a chaotic phenomenon is abundant in nature and has far-reaching consequences in many branches of science. Some nonlinear systems which display chaos are listed as follows:

- Elastic structures and mechanical systems [HM83], [Moo92]
  - Various types of beam and arch
    [MH79], [Moo80a], [Moo80b], [Hol82], [MS83], [Moo84], [MH85], [SY85], [PMM88], [CM90]
  - Three-dimensional strings [Mil84b], [ORr91]
  - Multiple-well potential problems [ML85a], [ML85b], [LM90a], [LM90b]
  - Duffing's equation
    [Ued79], [Ued80a], [Ued80b], [Ued85], [DP86], [UNHS88], [NS89], [KP91b]

- Bouncing ball problem [WB81], [Hol82], [LL83], [TA86]
- Pendulum problems
  [Mcl81], [LK81], [DBHL82], [RS84], [Mil84a], [HH86], [GW85], [MCH87], [SS89]
- Vibration with friction [FM89], [PS90], [FM92a], [FM92b]
- Loose-fitting gears [SXC89], [PK90], [CS90], [KP91a]
- Impact Print Hammer [Hen83]
- Robotic mechanisms [Bel90]
- Cutting process [Gra86], [Gra88]

- Fluid systems [Swi83], [Tat86]
  - Rayleigh-Bernard convection
    [Lor63], [BDMP80], [DBC82], [Lib87], [HE87]
  - Taylor-Couette flow [BSS*83], [Swi83], [BSSW84], [BS87]
  - Fluid drop chaos [Sha84]
  - Chaotic fluid flow on Jupiter [Mar88], [MSS89]
- Acoustic systems [LC81], [MCL86], [Gib88], [LH91]
- Electrical and electronic circuits and systems [ES90]
  - Circuits described by Duffing type equation
    [Ued79], [Ued80a], [Ued80b], [Ued85]
  - Circuits described by Van der Pol type equation
    [UA81], [Guc80]
  - Diode circuit [Lin81], [SY82], [RH82]
  - Chua circuit – Double scroll [Mat84], [MCT84], [MCT85], [CKM86]
  - Phase-locked loop circuit [EC88], [EC89], [EC90], [End90], [EIC90],
  - the Josephson junction device [CP82], [Mag83],[SS85]

- Optical systems
  - Laser systems [Hak75], [Hak85], [MSA87]
  - Optical devices and light systems [HKGS82], [HB86]
- Chemical systems [AAR*87b]
  - Belousov-Zhabotinski reaction [SWS82], [AAR87a]
  - Reaction-diffusion system [Rmb76a], [Rmb76b], [VRS90]
- Biological systems [DHF87], [GM88]
- Other topics
  - Neural networks [ATT90]
  - Numerical analysis [YM79], [YU81], [Ush82], [Hat90]
  - Earthquake model [CL89]
  - Economic systems [Che88]
  - Chaos synchronization and secure communications [PC90],[KHE*92],[IM92], [IMHC93],[IM93],[Ush94],

In the above list, the control system and the biological population system are omitted, since these two research fields are closely related to this thesis and the following subsections give outlines of chaotic phenomena observed in these two fields.

(d) Chaos in Control Systems

It is well-known that the feedback mechanism often generates chaotic phenomena [Spa80], [Spa81], [adHW83], [Hol85], [HU90], [GM91]. Great interest has recently been aroused in the study of chaotic behavior and strange attractors in various types of control systems:

- Sampled-data control systems
  [Kal56], [UH83], [UH84],[UH85a], [HA88], [Hir90]

- PWM control systems [BBW80], [UH85b]
- Adaptive control systems [RAC85], [MB86], [MB88], [SB88]
- Digital control systems – Chaotic rounding error [UH87a], [UH87b]

Recent progress has been made in using nonlinear behavior to advantage in the design of control system. For example, the new concepts of *controlling chaos* illustrate how one might constructively use the exponentially divergent nature of chaotic orbits and the extreme sensitivity of these systems with respect to small perturbations, in order to design useful systems [OGY90], [SOGY90], [HH91], [RGOD92], [SGOY93], [KSK*93].

(e) Chaotic Dynamics of Biological Populations and Control Inputs

A central task for population biologist is to clarify the underlying mechanisms that regulate natural populations so that no one species of plant or animal increases without bound. Such studies lead us to consider simple equations that might describe the dynamics of natural populations if environmental noise and uncertainty could be stripped away.

One of the oldest problems in mathematical ecology is the explanation of oscillatory behavior observed in many interacting animal populations. The Volterra-Lotka model [Lot25], [Vol26], although too simple to be realistic, provided a first attempt at this explanation. A more realistic explanation has been given by May [May73], based on a limit-cycle theorem of Kolmogorov.

As emphasized in the early 1970s, nonlinearities, in simple models for the regulation of plant and animal populations, can lead to chaotic dynamics [May74]. Therefore, complex dynamics - including chaos - is likely to be abundant in population biology and population genetics, even in seemingly simple situations [BFL75], [May76], [GOI77], [SS80], [May87].

The classical work of Volterra on fish populations in the Adriatic sea was one of the earliest studies of effects of harvesting on populations. Possibilities of reducing a pest population by harvesting and of accidentally wiping out a useful population by harvesting are two important aspects which have been studied. Another important area involves the economic aspects of harvesting [Cla76]. The formulation of the problem of maximizing

the discounted value of a harvest as an optimal control problem has led to results of considerable use in fisheries management. There have been many studies on the effect of harvesting or enrichment according to a specified strategy on a population system, and much is known about effects of constant-rate and constant-effort harvesting on equilibrium population sizes and stability [Bra76], [BSJ76], [Lud79], [LV79], [BS79], [BS85].

1.1.2 Fractal

A widespread interest in fractal geometry is generated by Benoit B. Mandelbrot, with his creative work [Man77], [Man82]. A book *The Fractal Geometry of Nature* (1982) written by Mandelbrot contains both the elementary concepts and an unusually broad range of new and rather advanced ideas. The advent in recent years of inexpensive computer power and graphics has led to the study of nontraditional geometrical objects in many fields of science. The concept of fractals has caught the imagination of scientists in many fields and a enormous numbers of papers and books discussing fractals in various contexts were published [Man82], [Fal85], [Tak86], [PT86], [PR86], [Bar88], [Fed88], [PS88], [Fal90], [Dev90], [Edg90], [Che91], [Moo92].

Many of the fractals and their descriptions go back to classical mathematics and mathematicians as follows:

- Cantor set [Can83]
- Space-filling curves – Peano and Hilbert curves [Pea90], [Hil91]
- Koch curve [vK04], [vK06]
- Sierpinski gasket and carpet [Sie16]
- Julia set [Jul18]
- Hausdorff dimension [Hau19].

Mandelbrot demonstrated that these early mathematical fractals in fact have many features in common with shapes found in nature and proposed the following definition of a

fractal [Man82]:

A fractal is a shape made of parts similar to the whole in some way.

It is now accepted that many geometric objects in nature have fractal-like shapes and surfaces such as coastlines, clouds, mountain ranges, certain trees and leaves [Man82], [Fed88]. In a recent book, Barnsley [Bar88] showed how one can recreate these shapes using iterated maps and made a very nice connection between the static fractal objects and the dynamical equations.

The horseshoe map is the simplest example of an iterative dynamics in the plane that leads to fractal properties. Another example for which one can calculate the fractal properties is the baker's transformation on two-dimensional space [FOY83]. Other examples of iterated maps which produce fractal distribution of points are found in Mira [Mir87] and Barnsley [Bar88].

(a) Fractal Dimension of Strange Attractors

There are two principal applications of fractal mathematics to nonlinear dynamics: characterization of strange attractors and measurement of fractal boundaries in initial condition and parameter space.

In order to characterize strange attractors, three definition of fractal dimension are often used : averaged pointwise dimension, correlation dimension and Lyapunov dimension. With the aid of methods for discretizing the signals, for example, discretization of phase-space variable, Poincaré maps or embedding space method [Moo92], the fractal dimension of the strange attractor was measured in the following systems:

- Two-well potential problem – Duffing-Holmes equation [ML85b]
- Periodically excited circuit [Lin85]
- Long, thin cantilevered beam [CM90]
- Rayleigh-Benard convection [MABD83], [BPV84]
- Taylar-Couette flow [LPC81], [Swi85]

- Surface waves in a fluid [CG85]
- Chua's circuit [MCT85]

Furthermore, the correlation dimension has been successfully used by many experimentalists, for example, Malraison et al. [MABD83], Swinney [Swi85], Ciliberto and Gollub [CG85] and, Moon and Li [ML85b]. An extensive study of this definition of dimension has been given by Grassberger and Proccacia [GP83]. The information dimension, which is a measure of the unpredictability in a system, is discussed by Farmer et al. [FOY83], Grassberger and Proccacia [GP83] and Shaw [Sha81],[Sha84]. Some relation ship between fractal dimension were made by Kaplan and York [KY78], Grassberger and Proccacia [GP83],[GP84].

(b) Fractal Boundaries

Studies on analytic maps $f : \mathbf{C} \rightarrow \mathbf{C}$ with the complex variable $x + iy \in \mathbf{C}$, including beautiful fractal pictures of the Julia and Mandelbrot sets, have demonstrated the intimate connection between dynamical systems and fractals, and furthermore how incredible patterns of complexity can occur from simple mathematical models [PR86], [Dev89].

In dynamical systems, modeled by various kind of differential or difference equations, it happens that the solution processes are attracted to various stable sets, which in the simplest case consist of single point. These stable sets, for example, equilibrium positions, periodic or limit cycle motions, are called attractors in the mathematics of dissipative dynamical systems. In nonlinear systems, it is possible that more than one attractor coexist in a phase space and each attractor has its own *basin of attraction* – the set of points that are drawn to that attractor. Therefore, the final state of the system depend on the initial condition.

In classical problems, we expect the basin boundary to be a smooth, continuous line or surface. However, it has been discovered that in many nonlinear systems, basins interweave among each other in extremely complicated fashion and basin boundaries exhibit fractal structure [GOY83], [MGOY85a], [MGOY85b]. If the basin boundary is fractal, then small uncertainties in initial conditions may lead to uncertainties in the outcome

of the system and predictability in such systems is not always possible. In the following physical systems, the fractal basin boundary is observed:

- Periodically forced particle in a two-well potential [ML85a], [LM90b]
- Phase-locked loop circuits [EC90]

Grebogi et al. have also studied a phenomenon called *boundary basin metamorphosis*, in which a change in some parameter of a dynamic process causes the basin boundary to snap from a smooth curve into fractal form – a kind of mathematical phase change [GOY86].

A criterion for the existence of fractal basin boundaries was derived by Holmes [GH83]), using a method by Melnikov [Mel63]. In the case of the forced motion of a particle in a two-well potential, it turn out that this criterion gives a very good indication of fractal basin boundaries [ML85a].

1.2 Problem Statement

As stated in previous sections, studies on chaos and fractal phenomena in nonlinear dynamical systems are significant from the both scientific and engineering view points.

Noting that the basin of attraction, for example, is an invariant set of the dynamical system, the invariant set is one of the main subject in the dynamical system theory. The first problem of this thesis is to clarify

- the existing conditions of fractal boundaries of invariant sets and
- the mechanisms yielding fractal boundaries of invariant sets,

concerned with one and two dimensional nonlinear discrete dynamical systems, which represent models of sampled-data control systems and biological population systems.

Secondly, based on the fact that chaotic oscillations are often not desirable in some physical systems, for example, biological population systems,

- the stabilization scheme of the chaotic behavior

is investigated in a class of discrete dynamical systems, which present predator-prey systems, by introducing mathematical models with control inputs. Furthermore, noting that the chaotic systems often have fractal invariant sets, the influences of control inputs, stabilizing the system, on fractal structures of the invariant set are discussed.

1.3 Summary of Contents

In this thesis, fractal boundaries and the stabilization of chaotic behavior are studied in deterministic nonlinear discrete dynamical systems, i.e., there exists a prescription, in terms of difference equations, for calculating their future behavior from given initial conditions.

In Chapter 2, the existing conditions of fractal boundaries of invariant set are demonstrated by calculating the Hausdorff dimension of boundaries in a class of one-dimensional nonlinear dynamical systems described by first order difference equation. The relation between periodic points with period three and fractal boundaries is investigated in this chapter. Furthermore, noting that the basin of attraction is an invariant set of the system, the theoretical results are applied to explore the basin boundaries of a class of one-dimensional nonlinear sampled-data control systems.

The mechanism yielding fractal boundaries of invariant sets, discussed in Chapter 2, is presented in Chapter 3. The five different mechanisms are represented by using the concept of the symbolic dynamics.

Based on results obtained in Chapter 3, fractal boundaries of invariant domain of a class of predator-prey systems are discussed in Chapter 4. The existing conditions and the yielding mechanisms are clarified, concerned with the Volterra-Lotka type two-dimensional difference equations. The invariant domain treated in this chapter is a set of initial conditions, under which the prey and predator coexist.

Chapters 5 and 6 are devoted to the investigation of the stabilization of chaotic behavior, observed in the predator-prey system, whose fractal boundaries of the invariant domain are discussed in Chapter 4. The mathematical models with control inputs are

derived by using the stock-recruitment concept. It is shown through the stability analysis that the constant and constant rate harvestings or supplyings of predators contribute to prevent oscillating behavior of the system. Furthermore, influences of control inputs on fractal boundaries of the invariant domain are discussed.

Throughout all chapters, except Chapter 7 which is devoted to the discussion and the summary of results, numerical experiments are carried out in order to show the validity of the results.

Chapter 2

Hausdorff Dimension of Fractal Boundaries of Invariant Sets in One-Dimensional Discrete Dynamical Systems

2.1 Introductory Remarks

In a certain class of nonlinear dynamical systems, recognizing that the asymptotic behavior of the system depends on the initial condition, in order to assign the final state of the system, it is required to estimate the basin, that is, a set of initial conditions under which the system state converges to a final state. Recently, it has been shown that there exists the basin with extremely complicated boundaries called fractal [MGOY85a]. If basin boundaries are fractal, then it is difficult to decide whether an initial condition is included in the basin or not in the neighborhood of the basin boundary. Namely, it is difficult to preassign the final state of the system from initial conditions. Hence, the fractal structure of basin boundaries are generally undesirable in engineering systems. In order to prevent the appearance of fractal basin boundaries, it is necessary to clarify existing conditions of fractal basin boundaries.

In this chapter, by discussing the Hausdorff dimension of the basin boundary, existing conditions of fractal basin boundaries are demonstrated, concerned with a class of one-

dimensional discrete dynamical systems of the form [YS93], [YS94a], [YS94b]:

$$\begin{aligned} x_{n+1} &= f(x_n),\ n = 0, 1, 2, \cdots, \\ x_n &\in \mathbf{R}^1,\ f : \mathbf{R}^1 \to \mathbf{R}^1. \end{aligned} \tag{2.1}$$

First of all, in order to clarify existing conditions of fractal basin boundaries, it is shown that the basin is an invariant set of the system, From this fact, existing conditions of fractal basin boundaries are converted into those of fractal boundaries of the invariant set. Secondly, based on the fact that, in one-dimensional systems, if the Hausdorff dimension of the basin boundary is greater than 0, then the basin boundary is said to be fractal and any magnification of the boundary does not bring us a simple structure of the boundary [MGOY85a], a lower bound of the Hausdorff dimension of basin boundaries is calculated and existing conditions of fractal basin boundaries are clarified.

The result obtained is applied to explore basin boundaries of a class of one-dimensional nonlinear sampled-data control systems. Illustrative examples together with numerical experiments show the existence of fractal basin boundaries of the sampled-data control system. These theoretical and numerical results reveal that in order to determine the sampling period, it is necessary to take into account the structure of the basin of final states.

2.2 Preliminaries

This section is devoted to describe the definition and properties of Hausdorff dimension. Furthermore, the invariance of the basin is demonstrated. These items are needed to calculate a lower bound of the Hausdorff dimension of the basin boundary in the next section.

2.2.1 Definition of Hausdorff Dimension

For a subset A of $\mathbf{R}^1$, the diameter of A is defined by

$$|A| = \sup\{|x - y| : x \in A, y \in A\}.$$

If $0 < |U_i| \leq \rho$ for each i and

$$E \subset \bigcup_{i=1}^{\infty} U_i, \quad E \subset \mathbf{R}^1,$$

then the set of subsets $\{U_i\}$ is called the ρ-cover of E. If the case where the number of elements U_i of $\{U_i\}$ is countable, $\{U_i\}$ is called the countable ρ-cover.

Let S be a subset of $\mathbf{R}^1$ and let s be a non-negative number. For a constant $\rho > 0$, define

$$H_\rho^s(S) = \inf \sum_{i=1}^{\infty} |U_i|^s,$$

where the infimum is over all countable ρ-cover $\{U_i\}$ of S. The Hausdorff s-dimensional measure of S is given by

$$H^s(S) = \lim_{\rho \to 0} H_\rho^s(S).$$

Definition 2.1 *(Hausdorff Dimension [Fal85]) For any subset $S \subset \mathbf{R}^1$, there is a unique value $\dim_{\mathrm{H}}(S)$, called the Hausdorff dimension of S, such that*

$$H^s(S) = \begin{cases} \infty, & 0 \leq s < \dim_{\mathrm{H}}(S) \\ 0, & \dim_{\mathrm{H}}(S) < s < \infty. \end{cases}$$

2.2.2 Invariance of Basin

We define the n-hold composition of the function f with itself by

$$f^n(x) = f(f^{n-1}(x)), \quad f^0(x) = x,$$

and furthermore, in order to indicate the initial condition, the state variable x_n starting from an initial condition x_0 is denoted by

$$x_n(x_0) = f^n(x_0).$$

The distance $d(x, E)$ between a point x and a set $E \subset \mathbf{R}^1$ is defined by

$$d(x, E) = \inf\{|x - y| : y \in E\}.$$

The asymptotic behavior of the discrete dynamical system (2.1) with respect to a initial condition $\hat{x}_0$ is given by

$$S_\omega(\hat{x}_0) = \{x : \lim_{n \to \infty} d(x, \bigcup_{k \geq n} x_k(\hat{x}_0)) = 0\}.$$

The basin of the set $S_\omega(\hat{x}_0)$, i.e., the set of initial conditions converging to $S_\omega(\hat{x}_0)$ is defined by

$$\Lambda(S_\omega(\hat{x}_0)) = \{x_0 : \lim_{n\to\infty} d(x_n(x_0), S_\omega(\hat{x}_0)) = 0\} = \{x_0 : \lim_{n\to\infty} d(f^n(x_0), S_\omega(\hat{x}_0)) = 0\}. \tag{2.2}$$

Let S be a set with $S \subset \mathbf{R}^1$. The inverse mapping of S is defined by

$$f^{-1}(S) = \{x : f(x) \in S\}.$$

If a set $S \subset \mathbf{R}^1$ satisfies that

$$f^{-1}(S) = S, \tag{2.3}$$

then the set S is called the invariant set.

The following Lemma gives important properties of the basin Λ:

Lemma 2.1 *The basin Λ, defined by (2.2), satisfies that*

$$f^{-1}(\Lambda) = \Lambda. \tag{2.4}$$

The proof of Lemma 2.1 is shown in Appendix 2A of this chapter.

The Lemma 2.1 indicates that the basin is an invariant set of the system. Hence, from now, our attention is concentrated on a lower bound of the Hausdorff dimension of the boundary of invariant sets and existing conditions of the fractal boundary of invariant sets in the discrete dynamical system (2.1) are clarified. Based on Lemma 2.1, results obtained can be applied to investigate fractal basin boundaries.

2.3 Hausdorff Dimension and Existing Conditions of Fractal Boundaries

Let S be the invariant set of the system (2.1), i.e., $f^{-1}(S) = S$. The boundary of the invariant set S is denoted by ∂S. The goal of this section is to give existing conditions of the fractal boundary ∂S satisfying that $\dim_{\mathrm{H}}(\partial S) > 0$ in the discrete-time system (2.1).

A lower bound of the Hausdorff dimension of the boundary ∂S is calculated and the basic existing conditions for fractal boundaries are demonstrated in the following theorem:

Theorem 2.1 *In the discrete dynamical system (2.1), if there exist two open intervals* $A, B \subset \mathbf{R}^1$ *satisfying that*

(A2.1) $A \cap B = \varnothing$

(A2.2) $f(A) \supset (A \cup B),\ \ f(B) \supset (A \cup B).$

(A2.3) *For any* $u_1, u_2 \in A$ *or* $u_1, u_2 \in B$, *there exists a positive constant* $c < 1$ *satisfying that*

$$|f(u_1) - f(u_2)| \leq \frac{|u_1 - u_2|}{c}.$$

(A2.4) $\partial S \cap (A \cup B) \neq \varnothing.$

then there exists a positive constant $\delta < 1$ *and the Hausdorff dimension of boundaries of the invariant set satisfies that*

$$\dim_{\mathrm{H}}(\partial S) > -\frac{\log 2}{\log c + \log \delta} > 0. \tag{2.5}$$

In order to demonstrate the proof of Theorem 2.1, the following operator is needed: For any set $K \subset (A \cup B)$,

$$f_{AB}^{-1}(K) = \bigcup_{y \in K} \{(f^{-1}(y) \cap A \cap \partial S) \cup (f^{-1}(y) \cap B \cap \partial S)\} \tag{2.6}$$

and

$$f_{AB}^{-(n+1)}(\cdot) = f^{-1}(f_{AB}^{-n}(\cdot)).$$

Furthermore, the following two lemmas are required:

Lemma 2.2 *If assumptions* **(A2.1)** *to* **(A2.3)** *hold, then, for any point* $P \in \partial S \cap (A \cup B)$, *there exists a positive constant* $\delta = \delta(P) < 1$ *such that, for any integer* $n \geq 1$, *in order to cover a set of points*

$$P_n = f_{AB}^{-n}(P), \tag{2.7}$$

at least $2^{n-1} + 1$ *intervals with the length* $c^{n-1}\delta$ *is needed.*

Lemma 2.3 *If, for any countable ρ-cover $\{U_i\}$ of $E \subset \mathbf{R}^1$,*

$$\sum_{i=1}^{\infty} |U_i|^s \geq 1$$

holds, then

$$\dim_{\mathrm{H}}(E) \geq s.$$

The proof of Lemma 2.2 is demonstrated in Appendix 2B, where the invariance of the set S is needed. Namely, in order to obtain Theorem 2.1, the invariance of the set S is needed. Lemma 2.3 is cited from the reference [Fal85].

(Proof of Theorem 2.1) The assumption **(A2.4)** indicates that there exists at least a basin boundary $P \in \{(A \cup B) \cap \partial S\}$. From Lemma 2.2, for any $P \in \{(A \cup B) \cap \partial S\}$ and for any $n \geq 1$, there exists a positive constant $\delta < 1$ such that, in order to cover the set

$$P_n = f_{AB}^{-n}(P),$$

at least $2^{n-1} + 1$ intervals with the length $c^{n-1}\delta$ is needed.

Hence, let $\{V_i\}$ be the $c^{n-1}\delta$-cover of the subset of P_n, i.e.,

$$\{V_i\} = \{V_i : |V_i| = c^{n-1}\delta, P_n \cap V_i \neq \varnothing, 1 \leq i \leq 2^{n-1} + 1\}.$$

On the other hand, let $\{U_j\}$ be the countable ρ-cover of ∂S, i.e.,

$$\{U_j\} = \{U_j : 0 < |U_j| \leq \rho, \partial S \subset \bigcup_{j=1}^{\infty} U_j\}.$$

From the definition (2.7) of P_n and the definition (2.6) of the operator $f_{AB}^{-1}(\cdot)$, it follows that

$$P_n \subset \partial S. \tag{2.8}$$

Furthermore, from the condition $0 < c < 1$ in the assumption **(A2.3)**,

$$\lim_{n \to \infty} c^{n-1}\delta = 0. \tag{2.9}$$

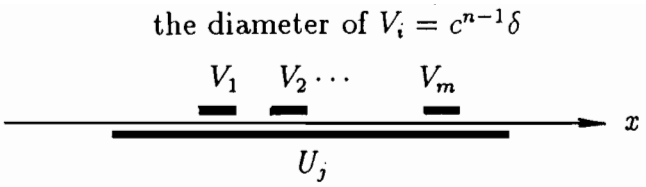

Figure 2.1: Components of $\{V_i\}$ and $\{V_i\}$

Taking into account (2.8) and (2.9), it is derived that, for any countable ρ-cover $\{U_j\}$ of ∂S, we can compose the set $\{V_i\}_{1 \le i \le 2^{n-1}+1}$, with sufficiently large n, satisfying that

$$\bigcup_{j=1}^{\infty} U_j \supset \bigcup_{i=1}^{2^{n-1}+1} V_i \,. \tag{2.10}$$

In this case, as shown in Fig.2.1, if m components of $\{V_i\}$ is included in a component U_j of $\{U_j\}$, then, for any $k > 0$, the inequality

$$|U_j|^k \ge m(c^{n-1}\delta)^k \tag{2.11}$$

holds [Fal85]. From (2.10) and (2.11), we obtain

$$\sum_{j=1}^{\infty} |U_j|^k \ge \sum_{i=1}^{2^{n-1}+1} |V_i|^k = (2^{n-1}+1)(c^{n-1}\delta)^k > 2^{n-1}(c\delta)^{(n-1)k}. \tag{2.12}$$

If a constant k is set as

$$k = -\frac{\log 2}{\log c + \log \delta} > 0, \tag{2.13}$$

then it holds that

$$2^{n-1}(c\delta)^{(n-1)k} = 1.$$

Hence, from (2.12), it is obtained that, if a constant k satisfies Eq.(2.13), then, for any countable ρ-cover $\{U_j\}$ of ∂S, an inequality

$$\sum_{j=1}^{\infty} |U_j|^k > 1 \tag{2.14}$$

holds. This fact and Lemma 2.3 indicate that

$$\dim_{\mathrm{H}}(\partial S) \ge -\frac{\log 2}{\log c + \log \delta} > 0. \tag{2.15}$$

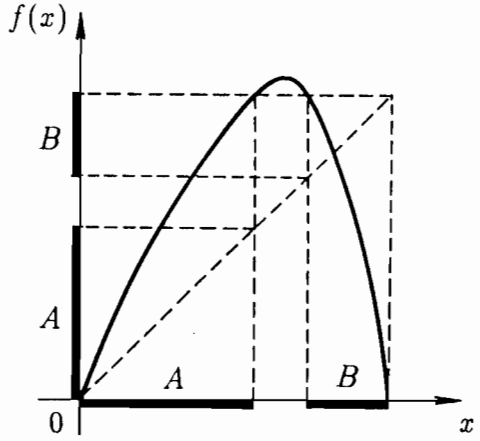

Figure 2.2: A unimodal mapping and open intervals A, B in assumptions **(A2.1)** to **(A2.3)**

(Q.E.D)

A simple example of the nonlinear function satisfying assumptions **(A2.1)** to **(A2.3)** is a unimodal and differentiable one, as plotted in Fig.2.2. However, restrictions for the nonlinear function $f(\cdot)$, described by these assumptions **(A2.1)** to **(A2.3)** of Theorem 2.1, is too strict to apply this result to the sampled-data control system or other engineering systems. Hence, in order to investigate fractal basin boundaries, concerned with engineering systems, it is necessary to modify assumptions of Theorem 2.1. The following Theorem 2.2 presents the relation between periodic point with period three and fractal basin boundaries. In Sec.2.4, by using Theorem 2.2, fractal basin boundaries of a class of sampled-data control system is discussed.

Theorem 2.2 *In the discrete dynamical system (2.1), if there exist points p, q and r satisfying that*

(A2.5) $$f(r) \leq p < f(p) = q < f(q) = r$$

(A2.6) *For any $u_1, u_2 \in]p, r[= \{x : p < x < r\}$, there exists a positive constant $c < 1$ satisfying that*

$$|f(u_1) - f(u_2)| \leq \frac{|u_1 - u_2|}{c}.$$

(A2.7) $$]p, r[\cap \partial S \neq \phi,$$

then the Hausdorff dimension of the boundary ∂S satisfies that

$$\dim_{\mathrm{H}}(\partial S) > 0. \tag{2.16}$$

(Proof) The principal idea for proving Theorem 2.2 is to consider the system

$$\tilde{x}_{n+1} = \tilde{f}(\tilde{x}_n),\ n = 0, 1, 2. \cdots, \tag{2.17}$$

where $\tilde{f}(\cdot) = f(f(\cdot))$. From the definition of the invariant set, the invariant set S of the system (2.1) satisfies that

$$\tilde{f}^{-1}(S) = f^{-1}(f^{-1}(S)) = f^{-1}(S) = S.$$

Namely, the invariant set of the system (2.1) is also the invariant set of the system (2.17). Hence, if the boundary of the invariant set of the system (2.17) is fractal, then that of the system (2.1) is also fractal. Therefore, the remainder of the proof is to show that if **(A2.5)** to **(A2.7)** holds, then the boundary of the invariant set of the system (2.17) is fractal. To do this, in the system (2.17), it is shown that, under assumptions **(A2.5)** to **(A2.7)**, there exist two open intervals satisfying assumptions **(A2.1)** to **(A2.4)** of Theorem 2.1.

If the assumption **(A2.6)** holds, then the nonlinear function $f(\cdot)$ is continuous. Hence, from the assumption **(A2.5)**, we obtain

$$f(]p, q[) \supset]f(p), f(q)[\supset]q, r[\tag{2.18}$$

and

$$f(]q, r[) \supset]f(r), f(q)[\supset]p, r[. \tag{2.19}$$

From the relations presented in (2.18) and (2.19), it follows that

$$\tilde{f}(]p, q[) = f^2(]p, q[) \supset f(]q, r[) \supset]p, r[\tag{2.20}$$

and

$$\tilde{f}(]q, r[) = f^2(]q, r[) \supset f(]p, r[) \supset]p, r[. \tag{2.21}$$

From (2.20) and (2.21), it is shown that, setting $A =]p, q[$, $B =]q, r[$, the nonlinear function $\tilde{f}(\cdot) = f^2(\cdot)$ satisfies the assumption **(A2.2)** in Theorem 2.1. It is clear that sets $A =]p, q[$ and $B =]q, r[$ satisfy the assumption **(A2.1)** in Theorem 2.1.

Furthermore, under the assumption **(A2.6)**, it holds that

$$\begin{aligned} |\tilde{f}(u_1) - \tilde{f}(u_2)| &= |f(f(u_1)) - f(f(u_2))| \\ &< \frac{|f(u_1) - f(u_2)|}{c} \\ &< \frac{|u_1 - u_2|}{c^2}. \end{aligned} \tag{2.22}$$

Therefore, noting that if $0 < c < 1$, then $0 < c^2 < 1$, and replacing c in **(A2.3)** by c^2, it is concluded that the nonlinear function $\tilde{f}(\cdot)$ satisfies the assumption **(A2.3)** of Theorem 2.1.

Finally, noting that **(A2.7)** in Theorem 2.2 is equivalent to **(A2.4)** in Theorem 2.1, it has been shown that in the system (2.17), assumptions **(A2.1)** to **(A2.4)** hold. This complete the proof of Theorem 2.2. **(Q.E.D.)**

Points p, q and r satisfying the condition **(A2.5)** of Theorem 2.2 are called the extended periodic point with period three [LY75]. Theorem 2.2 indicates that *the period three implies fractal boundaries of invariant sets.*

2.4 Fractal Basin Boundaries of a Class of Sampled-Data Control Systems

2.4.1 System Model of Sampled-Data Control Systems

In this section, our attention is focused on the fractal basin boundaries observed in a class of one-dimensional nonlinear sampled-data control systems described by

$$\begin{cases} \dot{x}(t) = ax(t) + bu(t) \\ y(t) = cx(t) \\ u(t) = g(r - y(kT)), \quad kT \le t < (k+1)T, \end{cases} \tag{2.23}$$

where $x \in \mathbf{R}^1$ is the state variable, $y \in \mathbf{R}^1$ is the observation data and $u \in \mathbf{R}^1$ is the control input, r is a constant representing the desired state, a, b and c are constants, T is

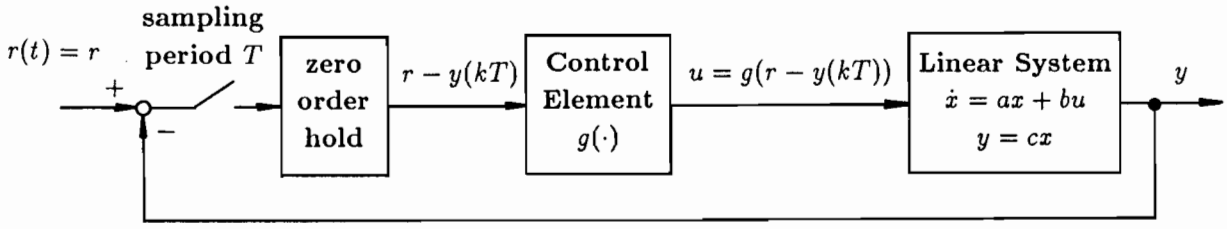

(a) The block diagram

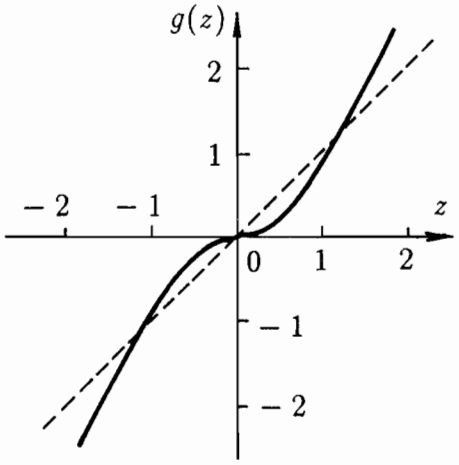

(b) The shape of the nonlinear function $g(\cdot)$

Figure 2.3: The sampled-data control system (2.23)

the sampling period, and $g : \mathbf{R}^1 \to \mathbf{R}^1$ is a nonlinear function representing the nonlinearity of the control element. Figure 2.3(a) shows the block diagram of the sampled-data control system (2.23).

Due to the existence of the nonlinearity of the control element, the asymptotic behavior of the sampled-data control system (2.23) depends on the initial condition. In this example, we consider the case where parameters a, b, c and the desired state r in Eq.(2.23) are set as

$$a = 20,\ b = 5,\ c = 5,\ r = -0.2$$

and the nonlinear function $g(\cdot)$ is given by

$$g(z) = 2z - \frac{3}{\pi}\mathrm{Tan}^{-1}2z.$$

Figure 2.3(b) shows the shape of the nonlinear function $g(\cdot)$. Furthermore the sampling period is set as $T = 0.075$. In this case, the state variable $x(t)$ of the system (2.23) with the initial condition $x(0) = 0.1$ converges to the equilibrium $x_e = -0.04973\cdots$. On the other hand, the state variable $x(t)$ with the initial condition $x(0) = 0.3$ diverges to the infinity. Therefore, in order to indicate the final state of the system from initial conditions, the basin of the equilibrium x_e is needed.

2.4.2 Derivation of Discrete Dynamical Systems

In order to investigate the structure of the basin of the sampled-data control system (2.23) by using theoretical results presented in the section 2.3, we derive the difference equation describing the time evolution of the state variable $x(t)$ of the sampled-data control system (2.23). First, calculating

$$\int_{nT}^{(n+1)T} \dot{x}(t)dt,$$

the following equation is derived from Eq.(2.23):

$$x((n+1)T) = \exp(aT)x(nT) + \exp(aT)\int_0^T \exp(-a\tau)d\tau \cdot bg(r - cx(nT)). \qquad (2.24)$$

The straightforward calculation of the integral included in (2.24) yields

$$x((n+1)T) = \exp(aT)x(nT) + \frac{b}{a}\{\exp(aT) - 1\}g(r - cx(nT)). \tag{2.25}$$

Finally, by using the transformation defined by

$$x_n = r - cx(nT), \tag{2.26}$$

we obtain the following difference equation describing the time evolution of the state variable of the sampled-data control system (2.23):

$$x_{n+1} = f_s(x_n),\ n = 0, 1, 2, \cdots, \tag{2.27}$$

where

$$\begin{aligned} f_s(x) &= \alpha x + \beta g(x) + \gamma, \\ \alpha &= \exp(aT), \\ \beta &= \frac{bc}{a}\{1 - \exp(aT)\}, \\ \gamma &= r\{1 - \exp(aT)\}. \end{aligned} \tag{2.28}$$

2.4.3 Stability of Equilibriums and Structure of Fractal Basin Boundaries

As shown in Eqs.(2.28), parameters α, β and γ include the sampling period T. Hence, the shape of the nonlinear function $f_s(\cdot)$ depends on the sampling period T. Figure 2.4 plots the shape of the nonlinear function $f_s(\cdot)$ with the sampling period $T = 0.075$. From Fig.2.4, it can be seen that the discrete dynamical system (2.27) has the following three equilibriums:

$$x_e^{(1)} = -0.4486\cdots,\ x_e^{(2)} = -0.3222\cdots,\ x_e^{(3)} = 1.0210\cdots.$$

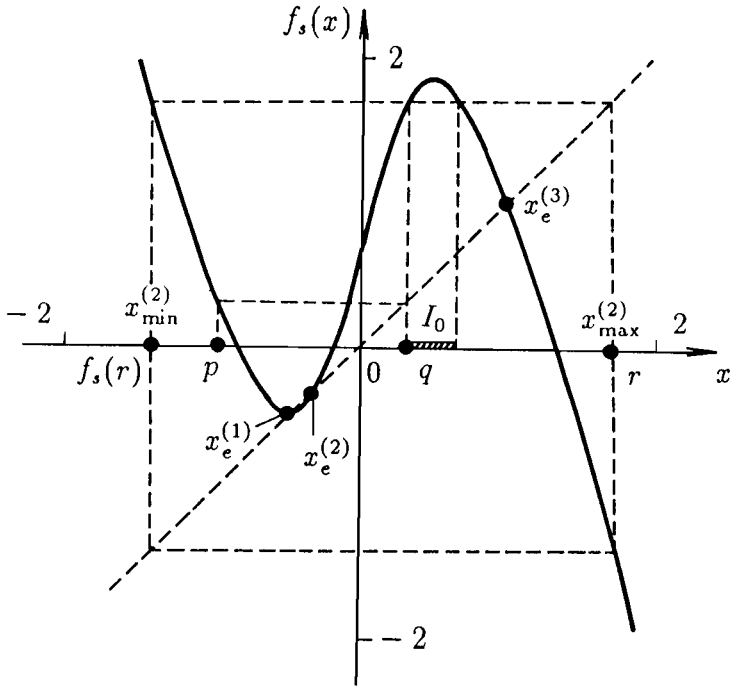

Figure 2.4: The shape of the nonlinear function $f_s(\cdot)$ with $T = 0.075$

The derivatives of the function $f_s(\cdot)$ at these equilibriums are given by

$$\left.\frac{df_s}{dx}\right|_{x=x_e^{(1)}} = 0.3824\cdots,$$

$$\left.\frac{df_s}{dx}\right|_{x=x_e^{(2)}} = 1.6508\cdots,$$

$$\left.\frac{df_s}{dx}\right|_{x=x_e^{(3)}} = -2.6146\cdots.$$

Hence, $x_e^{(1)}$ is an asymptotically stable equilibrium. On the other hand, equilibriums $x_e^{(2)}$ and $x_e^{(3)}$ are unstable. Therefore, in order to predict the asymptotic behavior of the system (2.27), it is needed to obtain the basin of the equilibrium $x_e^{(1)}$ defined by

$$\Lambda(x_e^{(1)}) = \{x_0 : \lim_{n\to\infty} d(x_n(x_0), x_e^{(1)}) = 0\} = \{x_0 : \lim_{n\to\infty} x_n = x_e^{(1)}\}. \tag{2.29}$$

In Fig.2.4, consider an interval I_f on the x-axis, which is given by

$$I_f = [x_{min}^{(2)}, x_{max}^{(2)}], \tag{2.30}$$

where

$$x_{min}^{(2)} = \min\{x : f_s^2(x) = x\}, \quad x_{max}^{(2)} = \max\{x : f_s^2(x) = x\}.$$

It is easy to see that if an initial condition is not included in the interval I_f, then the absolute value of the solution process diverges. For example, the solution process with $x_0 = 2$ exhibits the oscillation and its amplitude infinitely increases as follows:

$$x_0 = 2 < -x_1 = -f(x_0) < x_2 = f^2(x_0) < -x_3 = -f^3(x_0) < \cdots.$$

From this fact, it follows that

$$\Lambda(x_e^{(1)}) \subset I_f.$$

On the other hand, there exists an interval I_0 defined by

$$I_0 = \{x : f(x) > x_{max}^{(2)}\}. \tag{2.31}$$

From the definition of $x_{max}^{(2)}$, it is clear that $I_0 \not\subset \Lambda(x_e^{(1)})$. Hence, $]p, r[\not\subset \Lambda(x_e^{(1)})$.

In the sequel, from the above two facts such that

- an equilibrium $x_e^{(1)} \in]p, r[$ is asymptotically stable.
- an interval $I_0 \subset]p, r[$ is not included in the basin of the equilibrium $x_e^{(1)}$,

it is shown that the assumption **(A2.7)** in Theorem 2.2 holds.

The nonlinear function $f_s(\cdot)$ is continuous and differentiable. Furthermore, as shown in Fig.2.4, there exist extended periodic points p, q, r with period three. Hence, it is shown that, in the case where $T = 0.075$, the nonlinear function $f_s(\cdot)$ satisfies assumptions **(A2.5)** to **(A2.7)** in Theorem 2.2, and fractal basin boundaries appear. In order to show the shape of fractal basin boundaries, numerical calculations have been carried out, which are demonstrated in the following subsection.

2.4.4 Numerical Experiments

(a) Shape of Fractal Basin Boundaries

In numerical calculations for demonstrating the shape of fractal basin boundaries, the following procedures are carried out:

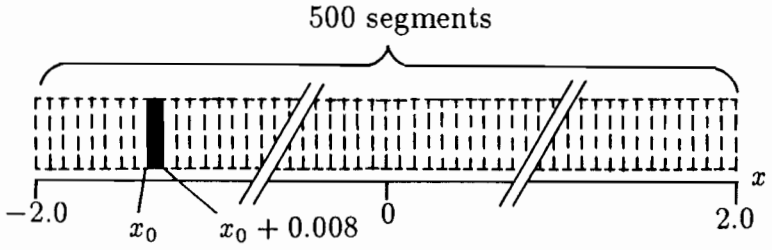

Figure 2.5: Dividing points of an interval

1. An interval $[-2, 2]$ is divided into 500 segments and each dividing point is selected as an initial condition of the difference equation (2.27). (See Fig.2.5.)

2. For an initial condition, the solution process x_n is calculated by using Eq.(2.27).

3. After 400 times iterations, if $|x_e^{(1)} - x_{400}| < 10^{-5}$, then we conclude that the initial condition is included in the basin of the equilibrium $x_e^{(1)}$ and the segment

$$\{x : x_0 \leq x < x_0 + 0.008\}$$

is blackened. (See Fig.2.5.)

In Fig.2.6, the basin of the equilibrium $x_e^{(1)}$ is plotted by black stripes. For example, in Fig.2.6(a), the initial condition x_0, located under a black stripe, converges to the equilibrium $x_e^{(1)}$. On the other hand, the solution process with the initial condition x_0', located in the blank region, diverges to the infinity. Namely, black stripes in Fig.2.6 demonstrate the shape of the basin of the equilibrium $x_e^{(1)}$.

Figure 2.6(b) is a magnification of Fig.2.6(a) and furthermore Fig.2.6(c) is a magnification of Fig.2.6(b). These magnification reveals that the basin of the equilibrium $x_e^{(1)}$ has extremely complicated structure and the magnification does not decrease the complexity of the fractal structure of the basin. Hence, in the neighborhood of the basin boundaries, it is difficult to decide whether an initial condition is included in the basin or not, and it is impossible to preassign the final state of the system.

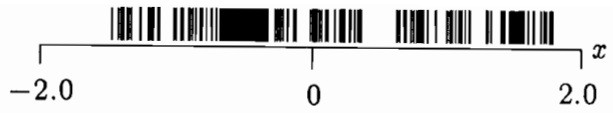

(a) The basin of the equilibrium $x_e^{(1)}$

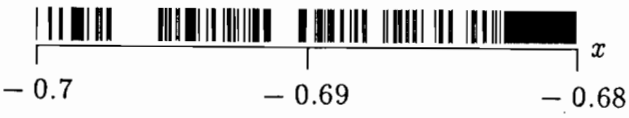

(b) A magnificaton of an interval $[-0.7, -0.68]$

(c) A magnificaton of an interval $[-0.684, -0.682]$

Figure 2.6: Fractal basin boundaries of a sampled-data control system (2.23)

(b) Onset of Fractal Basin Boundaries and its Disappearance in Numerical Experiments

For various values of the sampling period T, solution processes and the basin of the sampled-data control system (2.23) are numerically calculated by using the difference equation (2.27). Figure 2.7(a) plots the relation between the sampling period T and the asymptotic behavior of the system. For example, if the sampling period T is set as $T = 0.075$, the solution processes starting from the basin Λ of the equilibrium $x_e^{(1)} = -0.4486\cdots$ converge to the equilibrium $x_e^{(1)}$, then the position $(T, x) = (0.075, -0.4486\cdots)$ is marked with a black point. The relation between the basin and the sampling period T is shown in Fig.2.7(b). From these numerical experiments, we obtain the following facts:

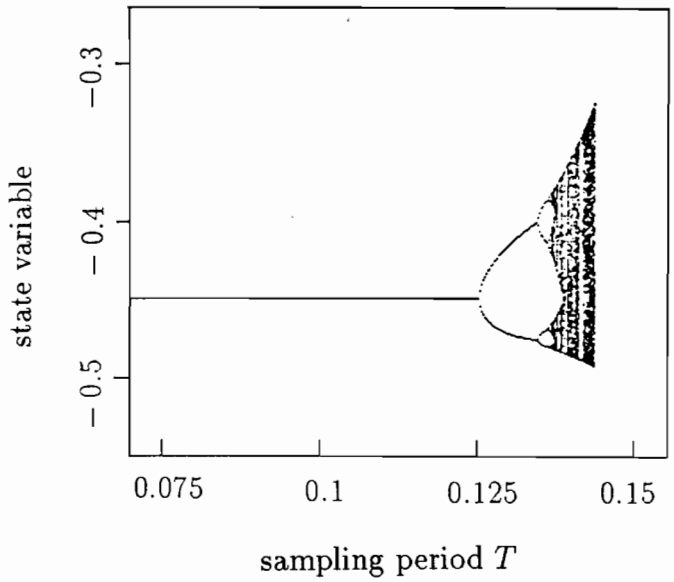

(a) Asymptotic behavior of the system vs sampling period T

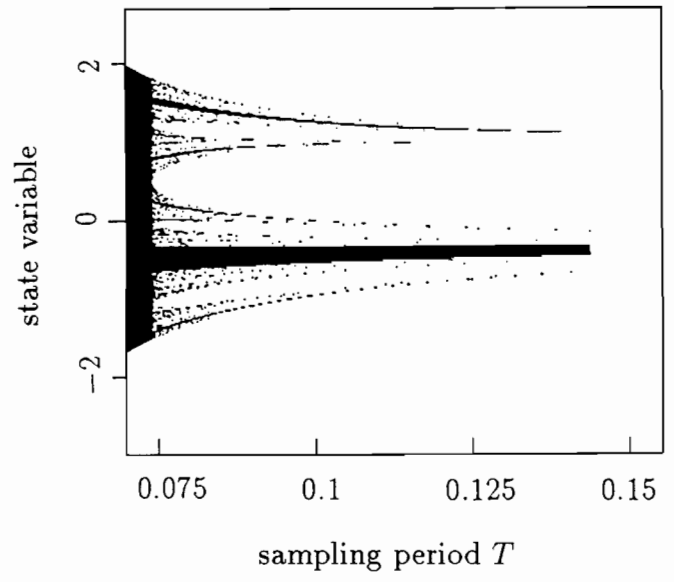

(b) Basin vs sampling period T

Figure 2.7: Bifurcation diagram and fractal basin boundaries of a sampled-data control system (2.23) with $A = 20,\ B = 5,\ C = 5$ and $r = -0.2$

1. From Fig.2.7(a),

   (a) For $T < 0.1253\cdots$, there exists an asymptotically stable equilibrium $x_e^{(1)} = -0.4486\cdots$ and solution processes starting from its basin converge to the equilibrium $x_e^{(1)}$.

   (b) For $T > 0.1253\cdots$, the period doubling bifurcation is observed. Furthermore if the sampling period T increases, then the solution process exhibits chaotic behavior.

2. From Fig.2.7(b),

   (a) For the sampling period $T = 0.07$, the interval I_0 defined by (2.31) does not exist and numerical calculations do not exhibit fractal basin boundaries. More exactly, the closure of the basin is an interval I_f defined by (2.30).

   (b) In the case where $T > 0.0742\cdots$, the interval I_0 appears and the basin boundary exhibits fractal structure. These basin have the positive Lebesgue measure.

   (c) For $T > 0.1439\cdots$, the basin with positive Lebesgue measure can not be observed. For almost all initial conditions, solution processes to Eq.(2.27) diverge to infinity.

2.5 Coexisting Final States and Fractal Basin Boundaries of a Class of Sampled-Data Control Systems

2.5.1 Coexisting Phenomenon of Final States

Recently, it has been shown that different final states coexist and a slightly different initial conditions yield quite different final states of the system [HH87],[HA88],[Hir90].

In this section, existing conditions of fractal basin boundaries, shown in Theorem 2.2 of Sec.2.3, are applied to explore the coexistence phenomenon of final states with fractal basin boundaries, in a class of nonlinear sampled-data control systems (2.23), where it is

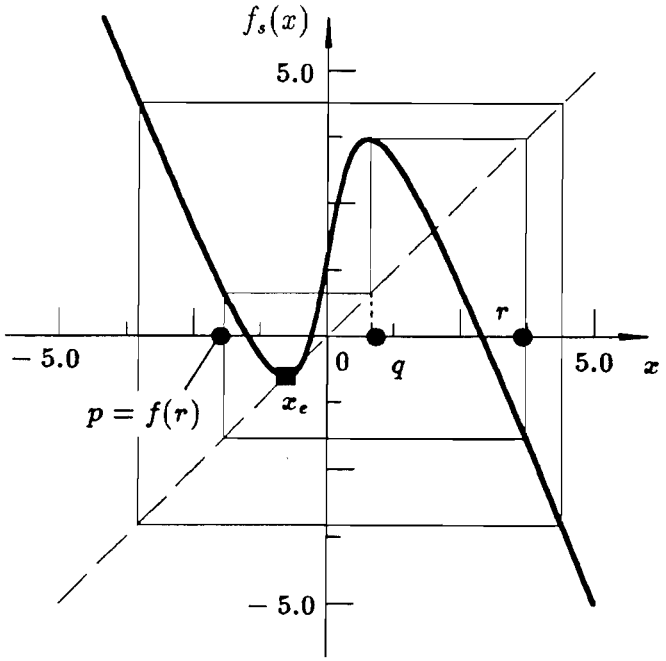

Figure 2.8: The shape of the nonlinear function $f_s(\cdot)$ with $T = 0.0614$

assumed that parameters a, b, c and the desired state r are set as

$$a = 30,\ b = 5,\ c = 5,\ r = -0.28.$$

Under these assumptions, the nonlinear function $f_s(\cdot)$, included in the difference equation (2.27), is plotted in Fig.2.8, where the sampling period is set as $T = 0.0614$. As shown in Fig.2.8, the discrete-time system (2.27) has a stable equilibrium

$$x_e = -0.7615\cdots$$

and stable periodic points with period three

$$p = -1.9164\cdots,\ q = -0.7950\cdots,\ r = 3.7322\cdots.$$

For example, the solution process with the initial condition $x_0 = 1.0985$ converges to the equilibrium $x_e = -0.7615\cdots$. On the other hand, the solution process with the slightly different initial condition $x_0 = 1.09851$ exhibits the periodic behavior with period three. (See Figs.2.9(a) and (b).)

Therefore, in order to predict the asymptotic behavior of the system (2.27), we need the basin of the equilibrium $x_e = -0.7615\cdots$:

$$\Lambda(x_e) = \{x_0 : \lim_{n\to\infty} f^n(x_0) = x_e\}. \tag{2.32}$$

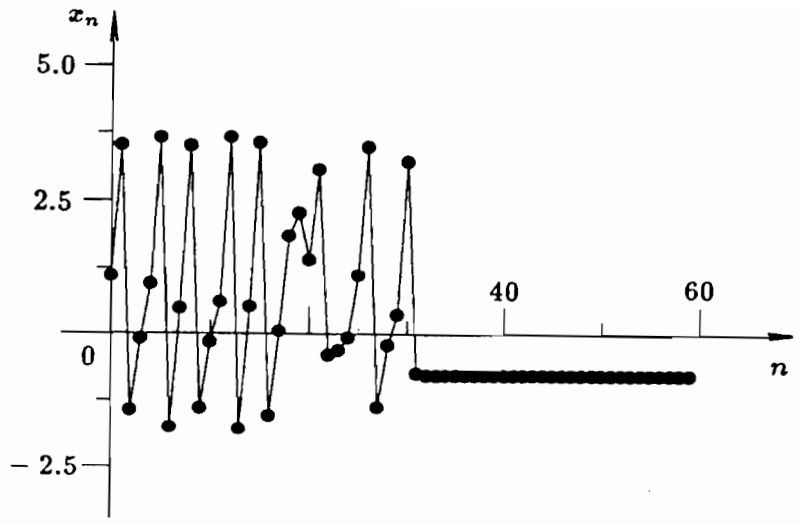

(a) $x_0 = 1.0985$

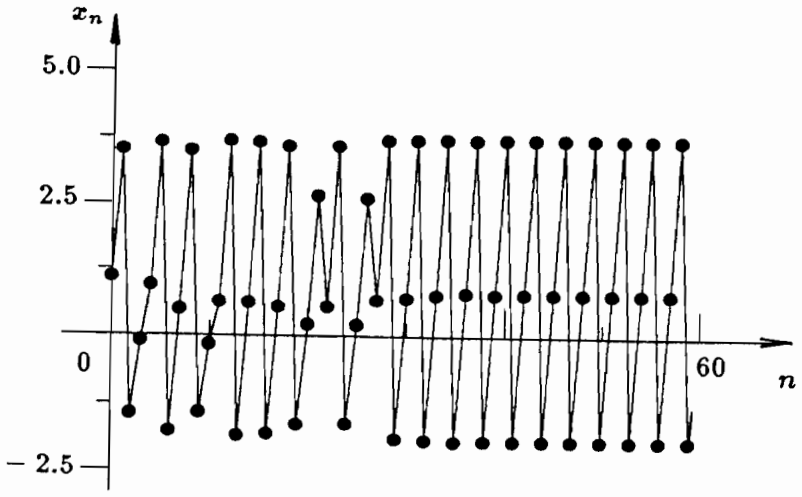

(b) $x_0 = 1.09851$

Figure 2.9: The solution processes of the discrete dynamical system (2.27)

2.5.2 Shape of Basin with Fractal Boundaries

The nonlinear function $f_s(\cdot)$ is continuous and there exist periodic points p, q, r with period three, as shown in Fig.2.8. Furthermore, taking into account that, as mentioned in Subsec.2.5.1, a stable equilibrium x_e and stable periodic point with period three coexist, we obtain

$$]p, r[\cap \partial\Lambda(x_e) \neq \varnothing.$$

From these discussions, in the case where $T = 0.0614$, it is clear that the nonlinear function $f_s(\cdot)$ satisfies conditions **(A2.5)** to **(A2.7)** of Theorem 2.2. Hence, the basin $\Lambda(x_e)$

(a) The basin $\Lambda(x_e)$

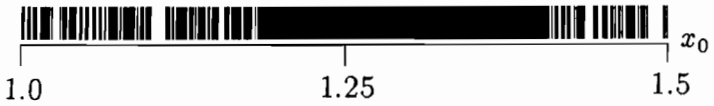

(b) A magnification of (a)

(c) A magnification of (b)

Figure 2.10: The fractal basin boundary of a discrete dynamical system (2.27)

exhibits fractal boundaries.

In Fig.2.10, the basin of the equilibrium x_e is plotted by black stripes. The solution processes starting from the black region of Fig.2.10 converge to the equilibrium x_e. On the other hand, if the initial condition is included in the white region of Fig.2.10, then the solution process exhibits periodic behavior with period three.

Figure 2.10(b) and (c) are respectively a magnification of Fig.2.10(a) and (b). Figures 2.10 reveal that the magnification does not decrease the complexity of the fractal structure of the basin. Hence, it is extremely difficult to decide whether an initial condition is included in the basin of the equilibrium x_e or not, namely, to predict whether the solution process converges to the equilibrium x_e or not.

2.5.3 Bifurcation Diagram of Attractors

For various values of the sampling period T, final states and the basin of the sampled-data control system (2.23) are calculated by using the difference equation (2.27). The relation between the sampling period T and final states of the system is plotted in Fig.2.11(a), which shows that, in the case where the sampling period T satisfies $0.06133\cdots < T < 0.06154\cdots$, attractors A and B coexist, namely, final states coexist. The relation between the sampling period T and the basin of the attractor B is demonstrated in Fig.2.11(b).

2.6 Concluding Remarks

In this investigation, it has been demonstrated that the existence of the periodic point with period three implies the existence of fractal basin boundaries, concerned with a class of one-dimensional discrete dynamical systems. Furthermore, by using the results obtained by theoretical analyses, fractal basin boundaries of a class of sampled-data control systems were investigated. In illustrative examples, it was shown that if the sampling period is long, then fractal basin boundaries appear. Hence, it is difficult to predict the asymptotic behavior of the system. Approaches for detecting fractal basin boundaries, demonstrated in this chapter, are useful for preventing the existence of fractal basin boundaries, when we determine the sampling period of the sampled-data control system.

The fractal set generated by the contraction mapping was already investigated and the excellent results were obtained [Huc81]. However, in the previous results [Huc81], the set itself is fractal, hence the Lebesgue measure of the fractal set is zero. In engineering dynamical systems, including control systems, this fact means that the fractal basin of an equilibrium has the zero Lebesgue measure and for almost all initial conditions, state variables do not converge to the equilibrium. Therefore, in engineering systems, the existing conditions of fractal basin boundaries are valuable, rather than those of the fractal set.

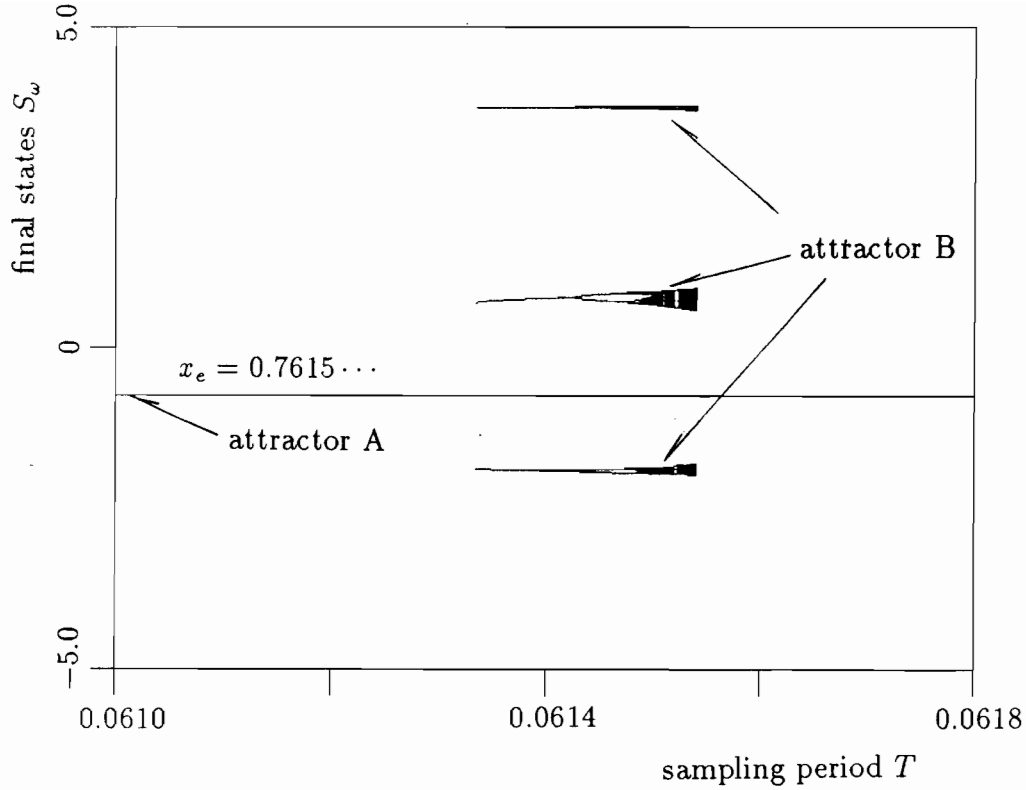

(a) Final states vs sampling period T

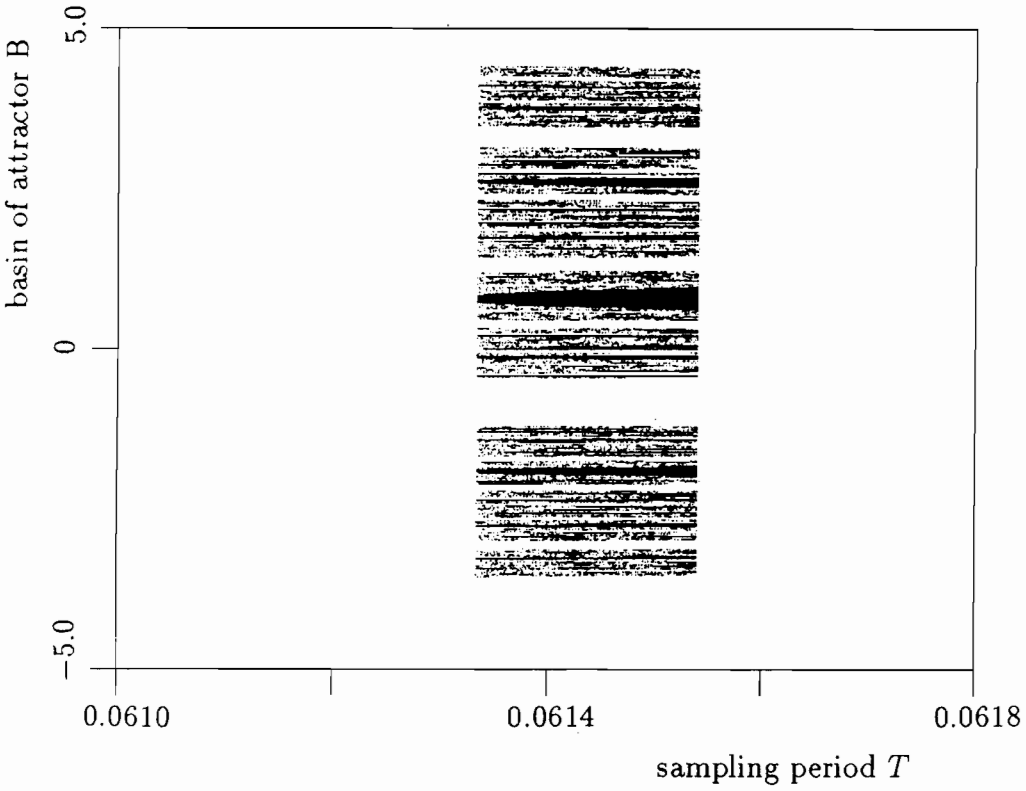

(b) Basin of attractor B vs sampling period T

Figure 2.11: Bifurcation diagram and fractal basin boundaries of a sampled-data control system (2.23) with $A = 30$, $B = 5$, $C = 5$ and $r = -0.28$

Appendix 2A: Proof of Lemma 2.1

From the definition of the inverse mapping $f^{-1}(\cdot)$, if $x \in f^{-1}(\Lambda(S_\omega))$, then $f(x) \in \Lambda(S_\omega)$. Furthermore, from the definition of the basin $\Lambda(S_\omega)$, if $f(x) \in \Lambda(S_\omega)$, then

$$\lim_{n\to\infty} d(f^n(f(x)), S_\omega) = 0. \tag{2.33}$$

By using Eq.(2.33), we obtain that

$$\lim_{n\to\infty} d(f^n(x), S_\omega) = \lim_{n\to\infty} d(f^{n+1}(x), S_\omega) = \lim_{n\to\infty} d(f^n(f(x)), S_\omega) = 0,$$

which indicates that $x \in \Lambda(S_\omega)$. Based on these discussions, it is concluded that, if $x \in f^{-1}(\Lambda(S_\omega))$, then $x \in \Lambda(S_\omega)$, i.e.,

$$f^{-1}(\Lambda(S_\omega)) \subset \Lambda(S_\omega). \tag{2.34}$$

Next, by using the contradiction, it is shown that $f^{-1}(\Lambda(S_\omega)) \supset \Lambda(S_\omega)$. Assume that $x \in \Lambda(S_\omega)$ and $x \notin f^{-1}(\Lambda(S_\omega))$. Then, from the second condition $x \notin f^{-1}(\Lambda(S_\omega))$, it follows that

$$f(x) \notin \Lambda(S_\omega). \tag{2.35}$$

However, from the first condition $x \in \Lambda(S_\omega)$,

$$\lim_{n\to\infty} d(f^n(f(x)), S_\omega) = \lim_{n\to\infty} d(f^n(x), S_\omega) = 0,$$

which indicates that $f(x) \in \Lambda(S_\omega)$. Hence, the contradiction occurs. Therefore, if $x \in \Lambda(S_\omega)$, then $x \in f^{-1}(\Lambda(S_\omega))$, i.e.,

$$f^{-1}(\Lambda(S_\omega)) \supset \Lambda(S_\omega). \tag{2.36}$$

Combining (2.34) and (2.36), the proof of the Lemma 2.1 has been completed.

Appendix 2B: Proof of Lemma 2.2

First of all, two lemmas, which are needed for the proof of Lemma 2.2, are shown:

Lemma 2.4 *Under assumptions* **(A2.2)** *and* **(A2.3)**, *for any* $Q \in \{\partial S \cap (A \cup B)\}$, *it follows that*

$$f^{-1}(Q) \cap A \cap \partial S \neq \varnothing$$

and

$$f^{-1}(Q) \cap B \cap \partial S \neq \varnothing.$$

(Proof) Let $B_\varepsilon(x)$ be the neighborhood of a point x, defined by

$$B_\varepsilon(x) = \{y : |y - x| < \varepsilon\}.$$

If the assumption **(A2.3)** holds, then the function $f(\cdot)$ is continuous on the interval A. Therefore, from the condition $f(A) \supset (A \cup B)$ in **(A2.2)**, for any boundary $Q \in \{\partial S \cap (A \cup B)\}$ and for any constant $\varepsilon > 0$, there exists a point $x \in (f^{-1}(Q) \cap A)$ satisfying that the image $f(B_\varepsilon(x))$ is the neighborhood of a point $Q = f(x)$.

From the definition (2.3) of the invariant set S, it can be derived that

$$f(S) = S. \tag{2.37}$$

Now assume that $B_\varepsilon(x) \subset S$. Then, from Eq.(2.37),

$$f(B_\varepsilon(x)) \subset f(S) = S. \tag{2.38}$$

However, the condition (2.38) is inconsistent with the fact that $f(B_\varepsilon(x))$ is a neighborhood of a boundary $Q \in \partial S$. Hence, we obtain that, for any ε,

$$B_\varepsilon(x) \not\subset S. \tag{2.39}$$

Next, assume that $B_\varepsilon(x) \cap S = \varnothing$. In this case, for any $z \in B_\varepsilon(x)$, it holds that $f(z) \notin S$. (If $f(z) \in S$, then, from definitions of the inverse mapping f^{-1} and the invariant set S, $z \in f^{-1}(S) = S$, i.e., $B_\varepsilon(x) \cap S \neq \varnothing$.)

Hence, if $B_\varepsilon(x) \cap S = \varnothing$, then

$$f(B_\varepsilon(x)) \cap S = \varnothing. \tag{2.40}$$

However, the condition (2.40) is inconsistent with the fact that $f(B_\varepsilon(x))$ is a neighborhood of $Q \in \partial S$. Therefore, it is derived that

$$B_\varepsilon(x) \cap S \neq \varnothing. \tag{2.41}$$

From (2.39) and (2.41), it is stated that, if $f(B_\varepsilon(x))$ is a neighborhood of the boundary $Q \in \{\partial S \cap (A \cup B)\}$ with $Q = f(x)$, then, for any $\varepsilon > 0$, the set $B_\varepsilon(x)$ usually includes points which are included in the set S and points which are not included in the set S. This fact indicates that a point x is a boundary of the set S. Therefore, it has been concluded that

$$f^{-1}(Q) \cap A \cap \partial S \neq \varnothing.$$

The proof of another proposition that $f^{-1}(Q) \cap B \cap \partial S \neq \varnothing$, in Lemma 2.4, is given by the similar procedures. **(Q.E.D.)**

Lemma 2.5 *If assumptions* **(A2.1)** *to* **(A2.3)** *hold and a set of points* $\{P_i : P_i \in \{\partial S \cap (A \cup B)\},\ 1 \leq i \leq n\}$ *satisfies that*

$$\min_{i,j}\{|P_i - P_j| : i \neq j\} > \delta',$$

then, in order to cover a set $f_{AB}^{-1}(\{P_i\})$, *at least* $2\ n - 1$ *intervals with the length* $c\delta'$ *are needed.*

(Proof) From the assumption **(A2.3)**, for any $v_1, v_2 \in (A \cup B)$,

$$\inf\{|u_1 - u_2| : u_1 \in (f^{-1}(v_1) \cap A), u_2 \in (f^{-1}(v_2) \cap A)\} \geq c|v_1 - v_2| \tag{2.42}$$

holds. Noting the assumption of Lemma 2.5 such that $|P_i - P_j| > \delta'$, $i \neq j$, and furthermore using (2.42), we obtain

$$\inf\{|Q_i - Q_j| : Q_i \in (f^{-1}(P_i) \cap A), Q_j \in (f^{-1}(P_j) \cap A)\} \geq c|P_i - P_j| > c\delta'. \tag{2.43}$$

Taking into account that, from Lemma 2.4,

$$f^{-1}(P_i) \cap A \cap \partial S \neq \varnothing$$

and using (2.43), it is obtained that, for any i and j with $1 \leq i < j \leq n$,

$$\inf\{|x-y| : \ x \in (f^{-1}(P_i) \cap A \cap \partial S), \ y \in (f^{-1}(P_j) \cap A \cap \partial S)\} > c\delta'. \tag{2.44}$$

The condition (2.44) indicates that, in order to cover a set of points

$$\bigcup_{i=1}^{n}\{f^{-1}(P_i) \cap A \cap \partial S\},$$

at least n intervals with the length $c\delta'$ are needed. Similarly, in order to cover a set of points

$$\bigcup_{i=1}^{n}\{f^{-1}(P_i) \cap B \cap \partial S\},$$

at least n intervals with the length $c\delta'$ are needed.

However, since the distance between intervals A and B is not determined, an interval with the length $c\delta'$ may cover a point included in the set $\bigcup_{i=1}^{n}\{f^{-1}(P_i) \cap A \cap \partial S\}$ and a point included in the set $\bigcup_{i=1}^{n}\{f^{-1}(P_i) \cap B \cap \partial S\}$. Therefore, it has been shown that, in order to cover a set of points

$$\bigcup_{i=1}^{n}\{f^{-1}(P_i) \cap A \cap \partial S\} \cup \bigcup_{i=1}^{n}\{f^{-1}(P_i) \cap B \cap \partial S\},$$

at least $2\,n-1$ intervals with the length $c\delta'$ are needed. **(Q.E.D)**

(Proof of Lemma 2.2) Consider the set P_1 defined by

$$P_1 = f_{AB}^{-1}(P),$$

where P is a point satisfying $P \in \{\partial S \cap (A \cup B)\}$. From Lemma 2.4, there always exist points P_A and P_B respectively satisfying

$$P_A \in \{f^{-1}(P) \cap A \cap \partial S\} \subset P_1$$

and

$$P_B \in \{f^{-1}(P) \cap B \cap \partial S\} \subset P_1.$$

Taking into account that $P_A \in A$ and $P_B \in B$, and furthermore, noting that A and B are open set, there exists a positive constant $\delta > 0$ such that

$$|P_A - P_B| > \delta. \tag{2.45}$$

Hence, in order to cover a set P_1, at least $N_1 = 2$ intervals with the length δ are needed.

From the inequality (2.45) and Lemma 2.5, in order to cover a set $f_{AB}^{-1}(\{P_A, P_B\})$, at least $N_2 = 2 \times N_1 - 1 = 3$ intervals with the length $c\delta$ are needed. Now, noting that

$$P_2 = f_{AB}^{-2}(P) = f_{AB}^{-1}(\{P_1\}) \supset f_{AB}^{-1}(\{P_A, P_B\}),$$

it is stated that, in order to cover a set P_2, at least $N_2 = 3$ intervals with the length $c\delta$ are needed.

Selecting a point including each intervals with the length $c\delta$, we can construct a set P_2' including 3 points as follows:

$$P_2' = \{x_i, i = 1, 2, 3 : |x_i - x_j| > c\delta,\ 1 \leq i < j \leq 3\}.$$

From the definition of the set P_2' and Lemma 2.5, in order to cover a set $f_{AB}^{-1}(P_2')$, at least $N_3 = 2 \times N_2 - 1 = 5$ intervals with the length $c^2\delta$ are needed. Noting that

$$P_3 = f_{AB}^{-3}(P) = f_{AB}^{-1}(P_2) \supset f_{AB}^{-1}(P_2'),$$

it is obtained that, in order to cover a set P_3, at least $N_3 = 5$ intervals with the length $c^2\delta$ is needed.

Repeating these procedures, we obtain the following equation:

$$N_{n+1} = 2\ N_n - 1, \quad N_1 = 2, \tag{2.46}$$

where N_n is an infimum of the number which is needed, in order to cover the set $P_n = f_{AB}^{-n}(P), n = 1, 2, 3, \cdots$ by using intervals with the length $c^{n-1}\delta$. From Eq.(2.46), we obtain that

$$N_n = 2^{n-1} + 1.$$

These discussions indicate that, for any integer $n \geq 1$, in order to cover a set

$$P_n = f_{AB}^{-n}(P),$$

at least $2^{n-1} + 1$ intervals with the length $c^{n-1}\delta$ are needed. **(Q.E.D)**

Chapter 3

Mechanisms Yielding Fractal Boundaries of Invariant Sets in One-Dimensional Discrete Dynamical Systems

3.1 Introductory Remarks

In Chap.2, existing conditions of fractal boundaries of the invariant set have been discussed by calculating a lower bound of the Hausdorff dimension of boundaries, in connection with a class of one-dimensional nonlinear discrete dynamical systems described by

$$x_{n+1} = f(x_n), \quad n = 0, 1, 2, \cdots, \tag{3.1}$$

where $x_n \in \mathbf{R}^1$ and $f(\cdot)$ is a nonlinear function $f : \mathbf{R}^1 \to \mathbf{R}^1$. The purpose of this chapter is to investigate mechanisms yielding fractal boundaries of the invariant set, by using the notation of symbolic dynamics [SY89].

For simplicity of discussions, throughout this chapter, it is assumed that, for any $x_0 \notin [0, 1]$,

$$\lim_{n\to\infty} |f^n(x_0)| = \lim_{n\to\infty} |x_n| = \infty$$

and we consider the set Λ defined by

$$\Lambda = \{x_0 : x_n = f^n(x_0) \in]0, 1[, \ n \geq 0\}. \tag{3.2}$$

In this case, without loss of generality, we can consider that the nonlinear function $f(\cdot)$ in Eq.(3.1) is defined on the normalized interval $[0, 1]$. Hence, the nonlinear discrete dynamical system, described by the difference equation (3.1), can be converted into

$$\begin{aligned} x_{n+1} &= f(x_n), \quad n = 0, 1, 2, \cdots, \\ x_n &\in \mathbf{R}^1, \ f : [0, 1] \to \mathbf{R}^1. \end{aligned} \tag{3.3}$$

Definition 3.1 *(Invariant Set) The set $\Lambda_a \subset \mathbf{R}^1$, satisfying*

$$f(\Lambda_a) \subset \Lambda_a, \tag{3.4}$$

is called the invariant set of the nonlinear function $f(\cdot)$ [GH83].

The definition 3.1 of the invariant set is given by modifying the strict definition, provided by Eq.(2.3) in Chap.2. Namely, the invariant set, treated in Chap.2, satisfies the condition (3.4).

Lemma 3.1 *The set Λ, defined by (3.2), satisfies that*

$$f(\Lambda) \subset \Lambda, \tag{3.5}$$

that is, the set Λ is an invariant set of the nonlinear function $f(\cdot)$ describing the discrete dynamical system (3.3).

(Proof) From the definition (3.2) of the set Λ, if $x \in \Lambda$, then, for any $n \geq 1$,

$$f^n(f(x)) = f^{n+1}(x) \in]0, 1[. \tag{3.6}$$

The relation (3.6) indicates that if $x \in \Lambda$, then $f(x) \in \Lambda$, namely, $f(\Lambda) \subset \Lambda$. **(Q.E.D.)**

The motivation of investigations, discussed in this chapter, arises as follows: In engineering systems, it is often required that the state variable of the system is bounded, i.e., for a positive constant $M < \infty$,

$$|x_n| < M, \ n = 0, 1, 2, \cdots.$$

In ecological systems, it is required that the population does not disappear, i.e.,

$$x_n > 0, \ n = 0, 1, 2, \cdots.$$

However, due to the existence of the nonlinearity, the asymptotic behavior of nonlinear dynamical systems depends on the initial condition. Hence, in order to predict the asymptotic behavior, it is necessary to obtain a set of initial conditions,

$$\Lambda_M = \{x_0 : |x_n| < M, n = 0, 1, 2, \cdots\}$$

or

$$\Lambda_0 = \{x_0 : x_n > 0, n = 0, 1, 2, \cdots\}.$$

From the definition of the set Λ_M, if an initial condition of the discrete dynamical system (3.1) is included in the set Λ_M, i.e.,

$$x_0 \in \Lambda_M,$$

then, at any time step n, the state variable of the system is finite, i.e.,

$$x_n = f^n(x_0) \in \Lambda_M, \ n = 1, 2, 3, \cdots.$$

Hence, it follows that

$$f(\Lambda_M) \subset \Lambda_M.$$

Similarly, if an initial condition is included in the set Λ_0, then the population size x_n of the ecological system is larger than 0 at any generation n. Therefore, the set Λ_0 also satisfies

$$f(\Lambda_0) \subset \Lambda_0.$$

Based on these facts, in this chapter, the structure of the invariant set Λ, defined by (3.2), is discussed.

There exist various engineering or ecological systems modeled by the simple difference equation (3.1), and numerous important nonlinear phenomena have been studies, for example, bifurcation phenomena, chaos, fractal and so on [Lor63] [May76] [LY75] [Dev89] [Moo92]. In addition to these phenomena, the structure of the invariant set is also an important subject of the nonlinear dynamical system (3.3)

In Sec.3.2, the notation of the symbolic dynamics [CE80] [Dev89] is introduced and the mechanism yielding the fractal structure of the invariant set is investigated, associated with a class of nonlinear functions possessing periodic points with period three. It has been shown in Chap.2 that fractal boundaries of the invariant set generated by the mechanism, demonstrated in Sec.3.2, has non-integer Hausdorff dimension. In Sec.3.3, under more strict conditions for the nonlinear function describing the system dynamics, mechanisms yielding the fractal invariant set are discussed in detail. In each Secs.3.2 and 3.3, illustrative examples are also demonstrated.

3.2 Mechanism Yielding Fractal Boundaries of Invariant Sets and Periodic Points with Period Three

3.2.1 Notation of Symbolic Dynamics

In this section, the following assumptions, concerned with the nonlinear function $f(\cdot)$ describing the dynamical system (3.3), are accepted:

(A3.1) the nonlinear function $f(\cdot)$ is continuous on $[0, 1]$.

(C) there exist points p, q and r satisfying

$$0 \leq f(r) \leq p < q = f(p) < r = f(q) \leq 1.$$

(A3.2) there exists a set S_0 defined by

$$S_0 = \{x : f(x) \geq 1,\ x \in]0, 1[\} \tag{3.7}$$

and satisfying

$$S_0 \cap]p, r[\neq \varnothing.$$

In order to discuss the yielding mechanism of fractal structures of the invariant set Λ defined by (3.2), first of all, it is necessary to remark that if there exists an integer $k \geq 1$ such that

$$x_0 \in f^{-k}(S_0) = \{x : f^k(x) \in S_0\}, \tag{3.8}$$

then the initial condition x_0 satisfies

$$f^k(x_0) \in S_0,$$

and furthermore, in the next step, it follows that

$$f^{k+1}(x_0) \geq 1.$$

Therefore, sets $f^{-k}(S_0),\ k = 0, 1, 2, \cdots$ are not included in the invariant set Λ and the invariant set Λ is produced by the operation described by

$$\Lambda =]0, 1[- \bigcup_{k=0}^{\infty} f^{-k}(S_0). \tag{3.9}$$

From Eq.(3.9), in order to discuss the yielding mechanism of the fractal structure of the invariant set Λ, it is necessary to clarify the yielding rules of sets $f^{-k}(S_0),\ k = 1, 2, 3, \cdots$. Thus, the following notations of symbolic dynamics are introduced: Inverse images S_{00} and S_{01} of the set S_0 are defined by

$$S_{00} = f^{-1}(S_0) \cap]p, q[,$$

$$S_{01} = f^{-1}(S_0) \cap]q, r[.$$

In general, for any subscript $s_1 s_2 \cdots s_k,\ k \geq 1$ with $s_i \in \{0, 1\},\ 1 \leq i \leq k$, inverse images $S_{s_1 s_2 \cdots s_k 0}$ and $S_{s_1 s_2 \cdots s_k 1}$ of the set $S_{s_1 s_2 \cdots s_k}$ are defined by

$$S_{s_1 s_2 \cdots s_k 0} = f^{-1}(S_{s_1 s_2 \cdots s_k}) \cap]p, q[,$$

$$S_{s_1 s_2 \cdots s_k 1} = f^{-1}(S_{s_1 s_2 \cdots s_k}) \cap]q, s[.$$

Noting that, from the definition of sets $S_{s_1 s_2 \cdots s_k},\ k \geq 1$,

$$\bigcup_{k=0}^{\infty} f^{-k}(S_0) \supset \bigcup_{k=0}^{\infty} \bigcup_{\substack{s_i = 0,1 \\ 1 \leq i \leq k}} S_{s_1 s_2 \cdots s_k},$$

it can be shown that

$$\Lambda =]0, 1[- \bigcup_{k=0}^{\infty} f^{-k}(S_0) \subset]0, 1[- \bigcup_{k=0}^{\infty} \bigcup_{\substack{s_i = 0,1 \\ 1 \leq i \leq k}} S_{s_1 s_2 \cdots s_k}. \tag{3.10}$$

These discussions indicate that, in order to clarify the mechanism yielding the fractal structure of the invariant set Λ, it is valuable to investigate the mechanism yielding sets $S_{s_1 s_2 \cdots s_k}$.

3.2.2 Mechanism Yielding Fractal Boundaries

By using the notation of the symbolic dynamics, defined in the previous subsection, we obtain the following theorem, which gives the mechanism yielding fractal boundaries of the invariant set Λ [YS91b].

Theorem 3.1 *If assumptions* **(A3.1)**, **(A3.2)** *and* **(C)** *hold, then sets* $S_{s_1 s_2 \cdots s_k}$ *are generated under the following rules:*

(R1) *If* $S_0 \cap]p, q[\neq \varnothing$ *and* $S_0 \cap]q, r[= \varnothing$, *then a set* S_{01} *exists. On the other hand, if* $S_0 \cap]q, r[\neq \varnothing$, *then sets* S_{00} *and* S_{01} *exist.*

(R2) *For any* $k \geq 2$, *if* $s_k = 0$, *then a set* $S_{s_1 s_2 \cdots s_k 1}$ *exists.*

(R3) *For any* $k \geq 2$, *if* $s_k = 1$, *then sets* $S_{s_1 s_2 \cdots s_k 0}$ *and* $S_{s_1 s_2 \cdots s_k 1}$ *exist.*

(Proof) The proof is divided into three parts.

(i) Existence of $S_{s_1 s_2 \cdots s_k 1}$: From assumptions **(A3.1)** and **(C)**,

$$f(]q, r[) \supset]f(r), f(q)[\supset]p, r[. \tag{3.11}$$

The relation (3.11) indicates that, for any $S_{s_1 s_2 \cdots s_k} \subset]p, r[$,

$$\{x : f(x) \in S_{s_1 s_2 \cdots s_k},\ x \in]q, r[\} \neq \varnothing. \tag{3.12}$$

From (3.12), it is concluded that there always exists one of the inverse image described by

$$\begin{aligned} S_{s_1 s_2 \cdots s_k 1} &= f^{-1}(S_{s_1 s_2 \cdots s_k}) \cap]q, r[\\ &= \{x : f(x) \in S_{s_1 s_2 \cdots s_k}\} \cap]q, r[\\ &= \{x : f(x) \in S_{s_1 s_2 \cdots s_k}, x \in]q, r[\} \\ &\neq \varnothing. \end{aligned}$$

Thus, the existence of S_{01} in **(R1)** (See Fig.3.1.) and $S_{s_1 s_2 \cdots s_k 1}$ in **(R2)** and **(R3)** is shown.

(ii) Existence of S_{00} in **(R.1)**: From assumptions **(A3.1)** and **(C)**,

$$f(]p, q[) \supset]f(p), f(q)[=]q, r[. \tag{3.13}$$

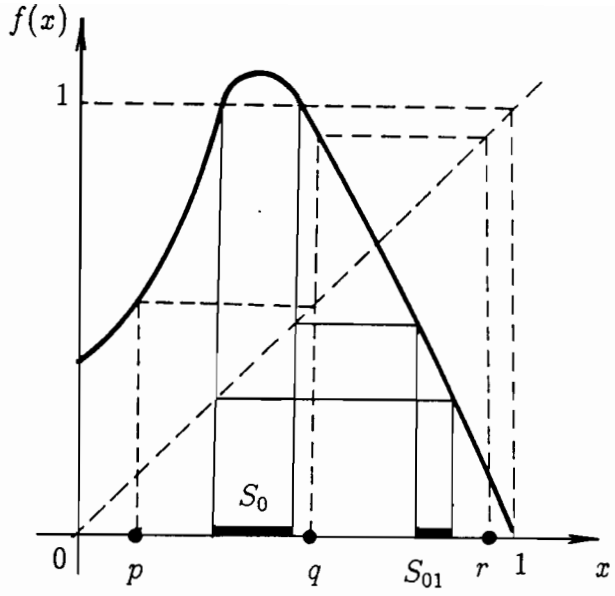

(a) $S_0 \cap]p, q[\neq \varnothing$ and $S_0 \cap]q, r[= \varnothing$

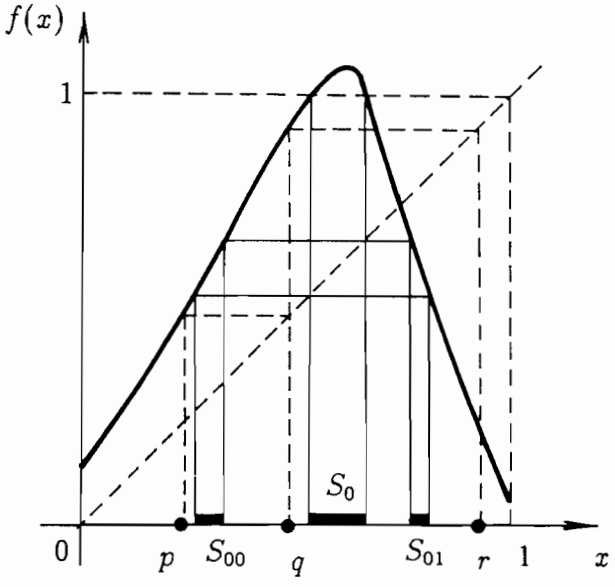

(b) $S_0 \cap]q, r[\neq \varnothing$

Figure 3.1: The existence of S_{00} and S_{01} of the nonlinear function $f(x)$ satisfying conditions **(A3.1)**,**(A3.2)** and **(C)**

Therefore, from (3.13), it is obtained that if $S_0 \cap]q, r[\neq \varnothing$, then, as shown in Fig.3.1(b), there exist

$$S_{00} = f^{-1}(S_0) \cap]p, q[= \{x : f(x) \in S_0, x \in [p, q[\} \neq \varnothing.$$

(iii) the existence of $S_{s_1 s_2 \cdots s_k 0}$ in (**R3**): From the definition of the set $S_{s_1 s_2 \cdots s_k}$, if $s_k = 1$, then

$$S_{s_1 s_2 \cdots s_k} \subset]q, r[. \tag{3.14}$$

Relations (3.13) and (3.14) show that, for any $s_1 s_2 \cdots s_k$ with $s_k = 1$, the inverse image

$$S_{s_1 s_2 \cdots s_k 0} = f^{-1}(S_{s_1 s_2 \cdots s_k}) \cap]p, q[$$

exists. (See Fig.3.2) (**Q.E.D**)

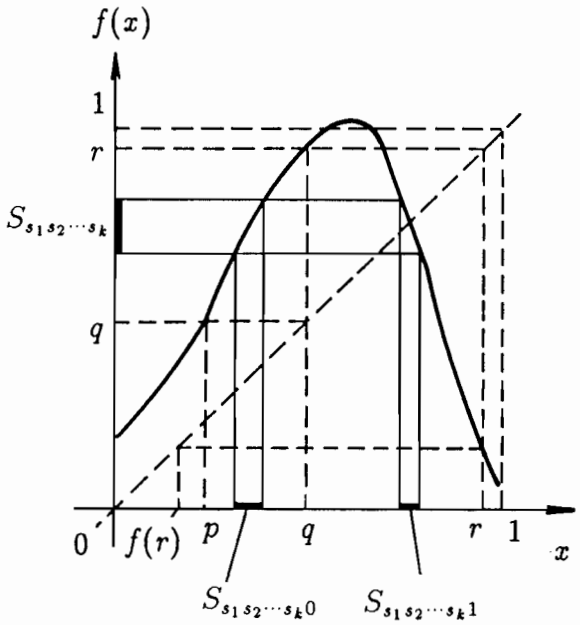

Figure 3.2: The existence of inverse images $S_{s_1 s_2 \cdots s_k 0}$ and $S_{s_1 s_2 \cdots s_k 1}$

Theorem 3.2 *For any* $s_1 s_2 \cdots s_n \neq t_1 t_2 \cdots t_m$,

$$S_{s_1 s_2 \cdots s_n} \cap S_{t_1 t_2 \cdots t_m} = \varnothing. \tag{3.15}$$

(Proof) Theorem 3.2 is proved by using a reduction to absurdity.

(i) Case where $n = m$: First, assume that there exists a point x satisfying that

$$x \in \{S_{s_1 s_2 \cdots s_n} \cap S_{t_1 t_2 \cdots t_m}\} = \{S_{s_1 s_2 \cdots s_n} \cap S_{t_1 t_2 \cdots t_n}\},$$

where, for an integer h with $1 \leq h \leq n$,

$$s_h = 0,\ t_h = 1.$$

From the hypothesis that $x \in S_{s_1 s_2 \cdots s_n}$ with $s_h = 0$,

$$f^{n-h}(x) \in S_{s_1 s_2 \cdots s_h} \subset]p, q[. \tag{3.16}$$

On the other hand, from the hypothesis that $x \in S_{t_1 t_2 \cdots t_n}$ with $t_h = 1$,

$$f^{n-h}(x) \in S_{t_1 t_2 \cdots t_h} \subset]q, r[. \tag{3.17}$$

(3.16) is incompatible with (3.17). Hence, there does not exist a point $x \in \{S_{s_1 s_2 \cdots s_n} \cap S_{t_1 t_2 \cdots t_n}\}$.

(ii) Case where $n < m$: Assume that there exists a point x satisfying

$$x \in \{S_{s_1 s_2 \cdots s_n} \cap S_{t_1 t_2 \cdots t_m}\}.$$

From the hypothesis that $x \in S_{s_1 s_2 \cdots s_n}$,

$$f^n(x) \geq 1. \tag{3.18}$$

However, from the hypothesis that $x \in S_{t_1 t_2 \cdots t_m}$,

$$f^n(x) \in S_{t_1 t_2 \cdots t_{m-n}} \subset]0, 1[. \tag{3.19}$$

(3.18) is incompatible with (3.19). **(Q.E.D)**

Points p, q and r satisfying the condition **(C)** are called the extended periodic point with period three [LY75]. Theorem 3.1 demonstrates the mechanism yielding fractal boundaries of the invariant set, in the case where there exist periodic points with period three of the nonlinear function. Figure 3.3 illustrates the rules described in Theorem 3.1. For example, it can be seen that a set S_{001} yields inverse images S_{0010} and S_{0011}, and that a set S_{010} yields an inverse image S_{0101} only.

Theorems 3.1 and 3.2 reveal that infinite numbers of inverse images $S_{s_1 s_2 \cdots s_k}$ are successively produced through rules **(R1)** to **(R3)** in Theorem 3.1 and are not the empty

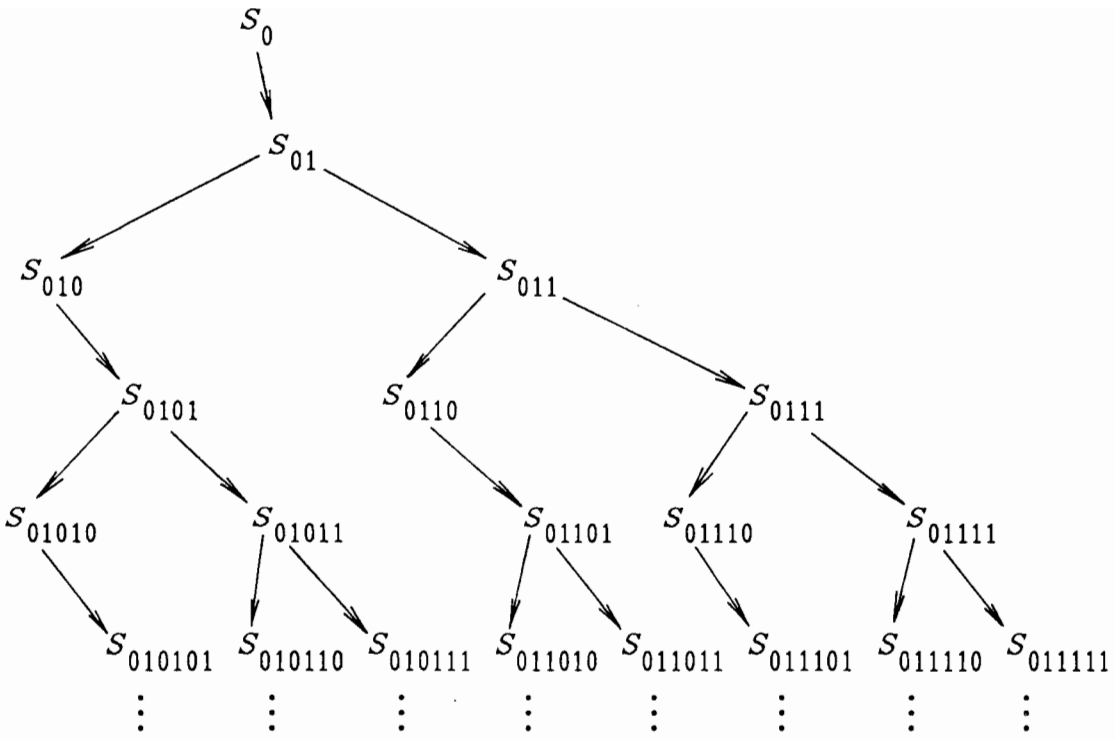

Figure 3.3: Rules described in Theorem 3.1

set. Therefore, the invariant set Λ, satisfying

$$\Lambda =]0,1[- \bigcup_{k=0}^{\infty} f^{-k}(S_0) \subset]0,1[- \bigcup_{k=0}^{\infty} \bigcup_{\substack{s_i=0,1 \\ 1 \le i \le k}} S_{s_1 s_2 \cdots s_k},$$

exhibits the fractal structure of boundaries.

3.2.3 Example

(a) Definition of Capacity Dimension

In this example, a nonlinear discrete dynamical system with the fractal invariant set is demonstrated, where the fractal structure of the invariant set Λ is generated by the mechanism presented in Theorem 3.1 [YS91a]. Furthermore, the fractal dimension, concretely the capacity dimension, of the fractal invariant set is calculated. The capacity dimension, which is one of the fractal dimension, is defined as follows:

Definition 3.2 *(Capacity Dimension) [Fed88] If, for a set S in the one-dimensional*

space, the number $N(\ell)$ of intervals of length ℓ needed to cover the set S increases like

$$N(\ell) \propto \ell^{-D} \text{ for } \ell \to 0, \tag{3.20}$$

then $D \equiv \dim_C(S)$ is called the capacity dimension of the set.

From (3.20), we obtain the equation, which is useful for calculating the capacity dimension $\dim_C(S)$, of the form

$$\dim_C(S) = D = \lim_{\ell \to 0} \frac{\log N(\ell)}{\log \frac{1}{\ell}}. \tag{3.21}$$

(b) System Model

Consider the one-dimensional discrete non-linear system described by

$$x_{n+1} = f_c(x_n), \tag{3.22}$$

where the nonlinear function $f_c : [0, 1] \to \mathbf{R}^1$ is defined by

$$f_c(x) = \begin{cases} 2x + \frac{1}{2}, & 0 \le x \le \frac{3}{8} \\ 2(1 - x), & \frac{3}{8} < x \le 1. \end{cases}$$

Figure 3.4 shows the shape of the nonlinear function $f_c(\cdot)$ describing the system (3.22).

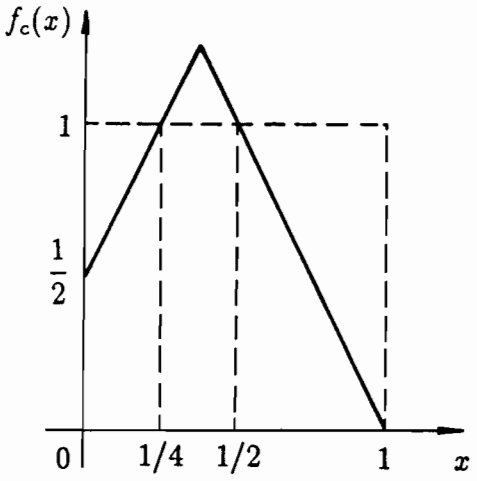

Figure 3.4: The shape of the nonlinear function $f_c(\cdot)$

In the nonlinear system (3.22), points p, q and r in Theorem 3.1 are respectively given by $p = 0, q = 0.5$ and $r = 1$. Furthermore, the set S_0 defined by (3.7) is given by $S_0 = [1/4, 1/2]$. Hence, assumptions of Theorem 3.1 hold and the invariant set Λ, defined by (3.2), exhibits the fractal structure. The generating procedure of the fractal structure of Λ is illustrated in Table 3.1.

(c) Number of Intervals Covering Invariant Set Λ

In order to calculate the capacity dimension of the invariant set Λ, note that the invariant set Λ of the system (3.22) is given by

$$\Lambda =]0,1[- \bigcup_{k=0}^{\infty} f_c^{-k}(S_0) =]0,1[- \bigcup_{k=0}^{\infty} \bigcup_{\substack{s_i=0,1 \\ 1\le i\le k}} S_{s_1 s_2 \cdots s_k}.$$

Now, define

$$\Lambda_0 =]0,1[$$

$$\Lambda_n =]0,1[- \bigcup_{k=0}^{n-1} f_c^{-k}(S_0), \ n = 1, 2, 3, \cdots$$

and consider the number of intervals of length $(1/2)^{n+1}$ needed to cover the set Λ_n, which is denoted by

$$a_n = N\left(\left(\frac{1}{2}\right)^{n+1}\right).$$

As shown in Table 3.1, the series $\{a_n\}$ satisfies that

$$a_{n+2} = a_{n+1} + a_n, \quad a_0 = 2, \ a_1 = 3. \tag{3.23}$$

By introducing the new variable t_n defined by

$$t_n = a_{n+1} + pa_n, \quad p = \frac{\sqrt{5}-1}{2}, \tag{3.24}$$

Equation (3.23) is converted into

$$\begin{aligned} t_{n+1} &= qt_n, \quad q = \frac{\sqrt{5}+1}{2}, \\ t_0 &= a_1 + pa_0 = \frac{\sqrt{5}+3}{2}. \end{aligned} \tag{3.25}$$

Now, we consider the variable S_n defined by

$$S_{n+1} = t_{n+1} + (-p)t_n + (-p)^2 t_{n-1} + \cdots + (-p)^{n+1} t_0. \tag{3.26}$$

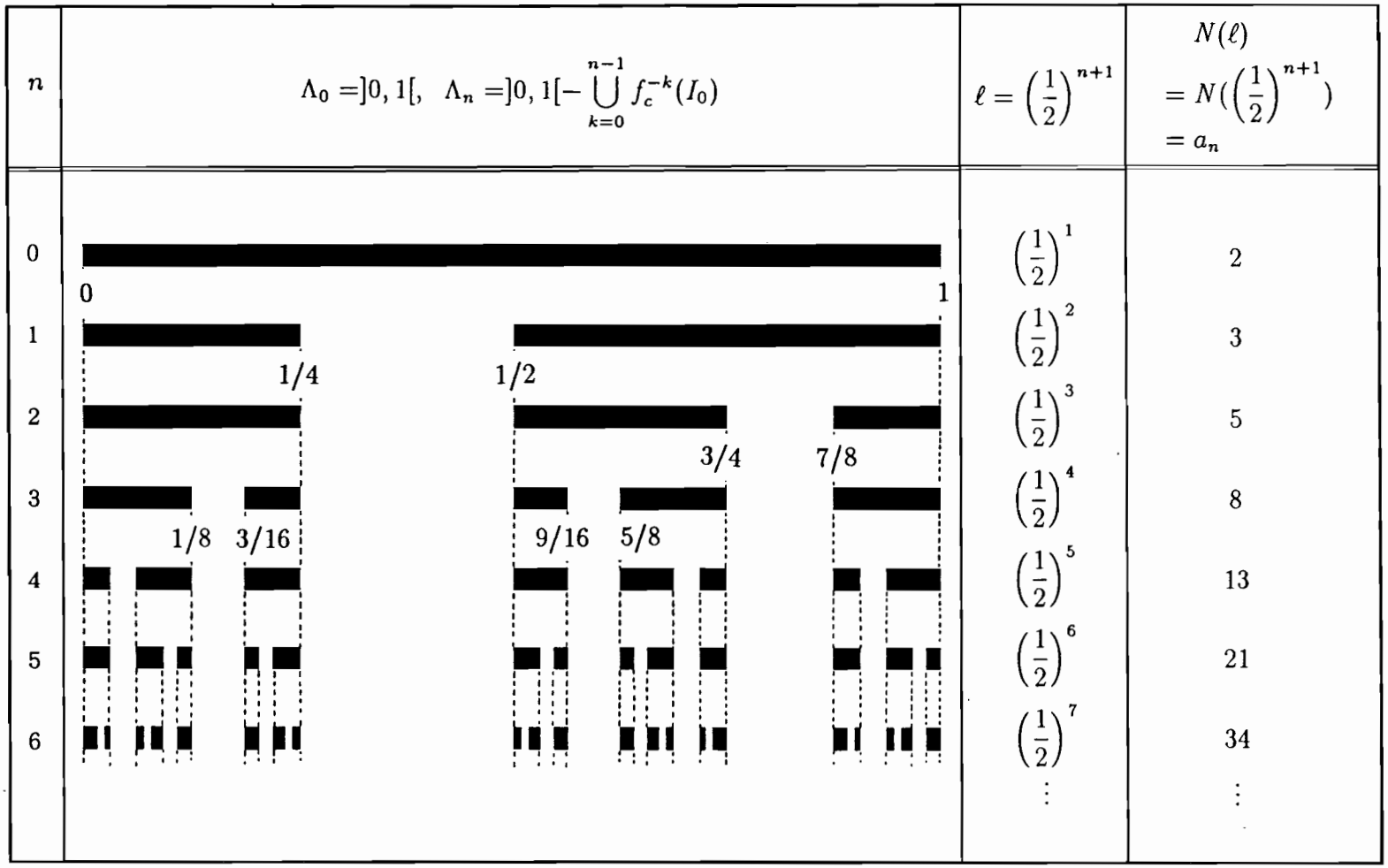

ℓ : the length of intervals covering the set Λ_n

$N(\ell)$: the number of intervals of length ℓ needed to cover the set Λ_n

Table 3.1: The genarating procedure of the invariant set Λ

Substituting (3.24) into (3.26), it is obtained that

$$\begin{aligned} S_{n+1} &= a_{n+2} + pa_{n+1} \\ &\quad + (-p)a_{n+1} + (-p)pa_n \\ &\quad\quad + (-p)^2 a_n + (-p)^2 pa_{n-1} \\ &\quad \cdots \\ &\quad\quad + (-p)^n a_2 + (-p)^n pa_1 \\ &\quad\quad\quad + (-p)^{n+1} a_1 + (-p)^{n+1} pa_0, \end{aligned}$$

hence,

$$S_{n+1} = a_{n+2} - (-p)^{n+2} a_0. \tag{3.27}$$

On the other hand, Equation (3.25) brings us

$$t_n = q^n t_0. \tag{3.28}$$

Substituting (3.28) into (3.26), it follows that

$$S_{n+1} = q^{n+1} t_0 + (-p)q^n t_0 + \cdots + (-p)^{n+1} t_0. \tag{3.29}$$

Furthermore, multiplying both sides of (3.29) by $-p/q$, we obtain

$$-\frac{p}{q} S_{n+1} = (-p)q^n t_0 + (-p)^2 q^{n-1} t_0 + \cdots + (-p)^{n+1} t_0 + \frac{(-p)^{n+2}}{q} t_0. \tag{3.30}$$

Equations (3.29) and (3.30) yield

$$S_{n+1} + \frac{p}{q} S_{n+1} = q^{n+1} t_0 - \frac{(-p)^{n+2}}{q} t_0.$$

Hence,

$$S_{n+1} = \frac{q^{n+2} - (-p)^{n+2}}{q+p} t_0 = \frac{q^{n+2} - (-p)^{n+2}}{q+p} (a_1 + pa_0). \tag{3.31}$$

Comparing Eqs.(3.27) and (3.31), we have

$$a_{n+2} - (-p)^{n+2} a_0 = \frac{q^{n+2} - (-p)^{n+2}}{q+p} (a_1 + pa_0). \tag{3.32}$$

Substituting $a_0 = 2$ and $a_1 = 3$ into (3.32), we obtain

$$a_{n+2} = \frac{2+\sqrt{5}}{\sqrt{5}} q^{n+2} - \frac{2-\sqrt{5}}{\sqrt{5}} (-p)^{n+2},$$

namely,

$$a_n = \frac{2+\sqrt{5}}{\sqrt{5}} q^n - \frac{2-\sqrt{5}}{\sqrt{5}} (-p)^n. \tag{3.33}$$

(d) Capacity Dimension

Noting that

$$\lim_{n\to\infty} \Lambda_n = \Lambda$$

and by using Eq.(3.21), the capacity dimension of the invariant set Λ of the system (3.22) is calculated by

$$\begin{aligned}
\dim_C(\Lambda) = \ D \ &= \lim_{n\to\infty} \frac{\log a_n}{\log 2^n} \\
&= \lim_{n\to\infty} \frac{\log \left[\dfrac{2+\sqrt{5}}{\sqrt{5}} q^n - \dfrac{2-\sqrt{5}}{\sqrt{5}} (-p)^n \right]}{n \log 2} \\
&= \lim_{n\to\infty} \frac{\log \left[\dfrac{2+\sqrt{5}}{\sqrt{5}} q^n \left\{ 1 - \dfrac{2-\sqrt{5}}{2+\sqrt{5}} \left(-\dfrac{p}{q} \right)^n \right\} \right]}{n \log 2}.
\end{aligned}$$

From the fact that

$$\lim_{n\to\infty} \left(-\frac{p}{q} \right)^n = \lim_{n\to\infty} \left(-\frac{\sqrt{5}-1}{\sqrt{5}+1} \right)^n = 0,$$

in the sequel, the capacity dimension of the invariant set Λ of the system (3.22) is calculated as

$$\begin{aligned}
&\dim_C(\Lambda) \\
= \ &\lim_{n\to\infty} \frac{1}{n \log 2} \left[\log \left(\frac{2+\sqrt{5}}{\sqrt{5}} \right) + n \log q + \log \left\{ 1 - \frac{2-\sqrt{5}}{2+\sqrt{5}} \left(-\frac{p}{q} \right)^n \right\} \right] \\
= \ &\frac{\log q}{\log 2} = \frac{\log \dfrac{\sqrt{5}+1}{2}}{\log 2} = 0.6942 \cdots.
\end{aligned}$$

3.3 Mechanisms Yielding Fractal Invariant Sets of Unimodal Mappings

3.3.1 Notation of Symbolic Dynamics

In Sec.3.2, under assumptions **(A3.1)**,**(A3.2)** and **(C)**, a mechanism yielding fractal boundaries of the invariant set has been shown. In this section, more detailed discus-

sions are demonstrated under the following assumptions for the nonlinear function $f(\cdot)$, describing the discrete dynamical system (3.3):

(A3.3) The nonlinear function $f(\cdot)$ is continuous on the closed interval $[0, 1]$.

(A3.4) The nonlinear function $f(\cdot)$ is unimodal on the closed interval $[0, 1]$, i.e., there exists a point $x_m \in]0, 1[$ satisfying that

if $x \in [0, x_m[$, then the function $f(\cdot)$ is uniformly increases,

and

if $x \in [x_m, 1]$, then the function $f(\cdot)$ is uniformly decreases.

(A3.5) The nonlinear function $f : [0, 1] \rightarrow \mathbf{R}^1$ satisfies the following conditions:

(a) $0 \leq f(0) < 1$,
(b) $f(x_m) > 1$,
(c) $f(1) = 0$.

Figure 3.5 plots the nonlinear function satisfying assumptions **(A3.3)** to **(A3.5)**. As

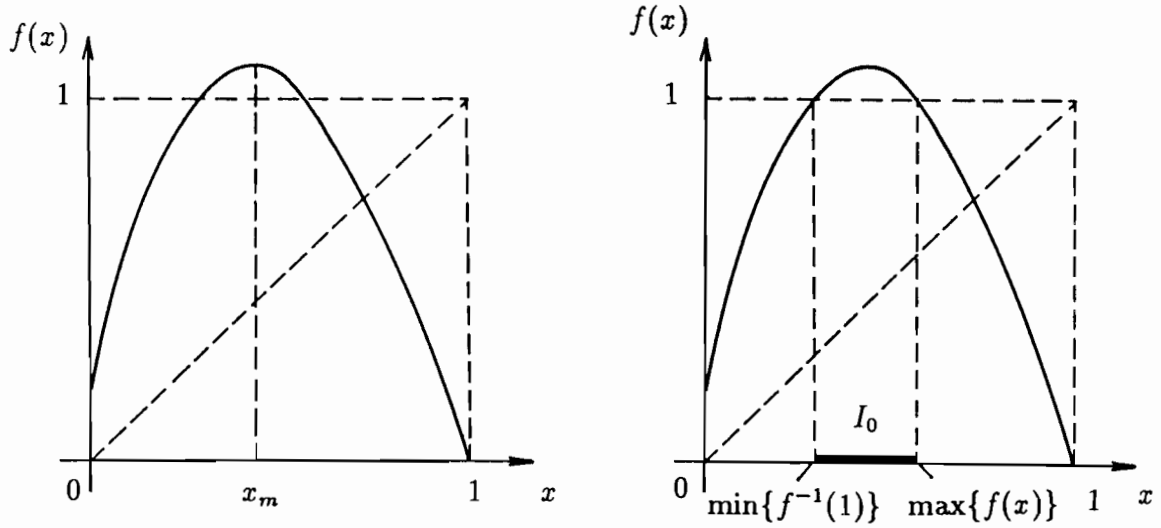

(a) Shape of the nonlinear function (b) Interval I_0

Figure 3.5: The shape of a unimodal function $f(\cdot)$ satisfying assumptions **(A3.3)**,**(A3.4)** and **(A3.5)**

shown in Fig.3.5(b), under assumptions **(A3.3)** to **(A3.5)**, there exists an interval I_0 defined by

$$I_0 = \{x \in]0,1[: f(x) \geq 1\} \tag{3.34}$$

and the invariant set Λ is given by

$$\Lambda =]0,1[- \bigcup_{k=0}^{\infty} f^{-k}(I_0). \tag{3.35}$$

The principal technique used in this section is also provided by the notation of the symbolic dynamics, which is introduced as follows: First of all, noting that the interval I_0 defined by Eq.(3.34) is given by

$$I_0 = [\min\{f^{-1}(1)\}, \max\{f^{-1}(1)\}],$$

two open intervals J_0 and J_1 are introduced by

$$J_0 =]0, \min\{f^{-1}(1)\}[, \quad J_1 =]\max\{f^{-1}(1)\}, 1[.$$

(See Fig.3.6(a).) Secondly, inverse images of the interval I_0 is defined by

$$I_{00} = f^{-1}(I_0) \cap J_0, \quad I_{01} = f^{-1}(I_0) \cap J_1.$$

In general, inverse images $I_{s_1 s_2 \cdots s_k s_{k+1}}$ of the interval $I_{s_1 s_2 \cdots s_k}$ are defined by

$$I_{s_1 s_2 \cdots s_k s_{k+1}} = f^{-1}(I_{s_1 s_2 \cdots s_k}) \cap J_{s_{k+1}}. \tag{3.36}$$

(See Fig.3.6.)

By using the notation defined by Eq.(3.36), it becomes that

$$\bigcup_{k=0}^{\infty} f^{-k}(I_0) = \bigcup_{k=0}^{\infty} \bigcup_{\substack{s_i=0,1 \\ 1 \leq i \leq k}} I_{s_1 s_2 \cdots s_k},$$

and the invariant set Λ, defined by (3.2), is given by

$$\Lambda =]0,1[- \bigcup_{k=0}^{\infty} \bigcup_{\substack{s_i=0,1 \\ 1 \leq i \leq k}} I_{s_1 s_2 \cdots s_k}.$$

Hence, in order to clarify the mechanism yielding fractal boundaries of the invariant set Λ, we investigate the mechanism yielding intervals $I_{s_1 s_2 \cdots s_k}$.

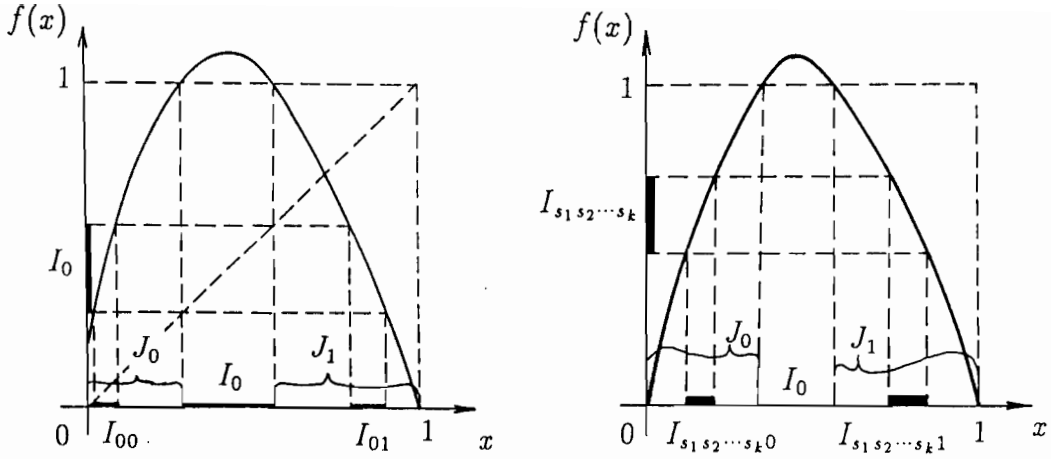

(a) I_{00} and I_{01} (b) $I_{s_1 s_2 \cdots s_k 0}$ and $I_{s_1 s_2 \cdots s_k 1}$

Figure 3.6: Inverse images $I_{s_1 s_2 \cdots s_k 0}$ and $I_{s_1 s_2 \cdots s_k 1}$ of an interval $I_{s_1 s_2 \cdots s_k}$

3.3.2 Mechanisms Yielding Fractal Boundaries

It is already well-known that if $f(0) = 0$, then intervals $I_{s_1 s_2 \cdots s_k}$ are generated under the following rule [Dev89]:

(R0) For any s_k with $k \geq 1$, intervals $I_{s_1 s_2 \cdots s_k 0}$ and $I_{s_1 s_2 \cdots s_k 1}$ always exist.

It is well-known that the Cantor middle third set is a typical example of the invariant set with the fractal structure [Dev89], generated under the rule **(R0)**. Figure 3.7 illustrates the rule **(R0)**.

The following Theorems 3.3a to 3.3d newly demonstrate mechanisms yielding fractal boundaries of the invariant set Λ, which are different from that yielding the Cantor middle third set.

Theorem 3.3a *If assumptions* **(A3.3)** *to* **(A3.5)** *and*

(Ca) $$\max\{f^{-1}(\min\{f^{-1}(1)\})\} > f(0) \geq \max\{f^{-1}(\max\{f^{-1}(1)\})\}$$

hold, then intervals $I_{s_1 s_2 \cdots s_k}$ *are generated under the following rules:*

(R1a) *For any* $k \geq 1$, *if* $s_k = 0$, *then an interval* $I_{s_1 s_2 \cdots s_k 1}$ *exists and an interval* $I_{s_1 s_2 \cdots s_k 0}$ *does not exist.*

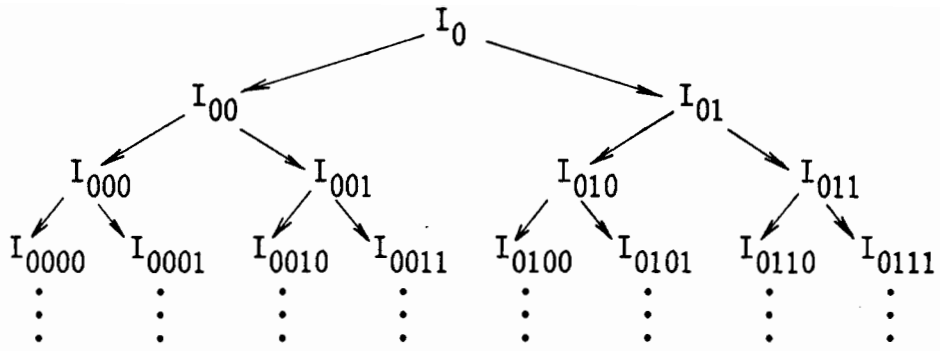

Figure 3.7: The Rule generating the Cantor middle third set described in (**R0**)

(R2a) *For any* $k \geq 1$, *if* $s_k = 0$ *and* $s_{k+1} = 1$, *then intervals* $I_{s_1 s_2 \cdots s_{k+1} 0}$ *and* $I_{s_1 s_2 \cdots s_{k+1} 1}$ *exist.*

(R3a) *For any* $k \geq 1$, *if* $s_k = 1$ *and* $s_{k+1} = 1$, *then an interval* $I_{s_1 s_2 \cdots s_{k+1} 1}$ *exists and an interval* $I_{s_1 s_2 \cdots s_{k+1} 0}$ *does not exist.*

The proof of Theorem 3.3a is demonstrated in Appendix 3A. Similarly, proofs of the following Theorems 3.3b to 3.3d are also demonstrated in Appendix 3B to 3D respectively.

Theorem 3.3b *If assumptions* (**A3.3**) *to* (**A3.5**) *and*

(Cb) $$\max\{f^{-1}(\max\{f^{-1}(1)\})\} > f(0) \geq \max\{f^{-1}(1)\}$$

hold, then intervals $I_{s_1 s_2 \cdots s_k}$ *are generated under the following rules:*

(R1b) *For any* $k \geq 1$, *if* $s_k = 0$, *then an interval* $I_{s_1 s_2 \cdots s_k 1}$ *exists and an interval* $I_{s_1 s_2 \cdots s_k 0}$ *does not exist.*

(R2b) *For any* $k \geq 1$, *if* $s_k = 0$ *and* $s_{k+1} = 1$, *then intervals* $I_{s_1 s_2 \cdots s_{k+1} 0}$ *and* $I_{s_1 s_2 \cdots s_{k+1} 1}$ *exist.*

(R3c) *For any* $k \geq 1$, *if* $s_k = 1$ *and* $s_{k+1} = 1$, *then an interval* $I_{s_1 s_2 \cdots s_{k+1} 1}$ *always exists and an interval* $I_{s_1 s_2 \cdots s_{k+1} 0}$ *does not always exist.*

Theorem 3.3c *If assumptions* **(A3.3)** *to* **(A3.5)** *and*

(Cc) $$\max\{f^{-1}(1)\} > f(0) \geq \min\{f^{-1}(1)\}$$

hold, then intervals $I_{s_1 s_2 \cdots s_k}$ *are generated under the following rules:*

(R1c) *There exist intervals* I_{00} *and* I_{01}.

(R2c) *For any* $k \geq 2$, *if* $s_k = 0$, *then an interval* $I_{s_1 s_2 \cdots s_k 1}$ *exists and* $I_{s_1 s_2 \cdots s_k 0}$ *does not exist.*

(R3c) *For any* $k \geq 2$, *if* $s_k = 1$, *then intervals* $I_{s_1 s_2 \cdots s_k 0}$ *and* $I_{s_1 s_2 \cdots s_k 1}$ *exist.*

Theorem 3.3d *If assumptions* **(A3.3)** *to* **(A3.5)** *and*

(Cd) $$\min\{f^{-1}(1)\} \geq f(0)$$

hold, then intervals $I_{s_1 s_2 \cdots s_k}$ *are generated under the following rules:*

(R1d) *There exist intervals* I_{00} *and* I_{01}.

(R2d) *For any* $k \geq 2$, *if* $s_k = 0$, *then an interval* $I_{s_1 s_2 \cdots s_k 1}$ *always exists and an interval* $I_{s_1 s_2 \cdots s_k 0}$ *does not always exist.*

(R3d) *For any* $k \geq 2$, *if* $s_k = 1$, *then intervals* $I_{s_1 s_2 \cdots s_k 0}$ *and* $I_{s_1 s_2 \cdots s_k 1}$ *exist.*

Figures 3.8 show rules described in Theorems 3.3a and 3.3c. For example, in Fig.3.8(a), it can be seen that an interval I_{001} yields inverse images I_{0010} and I_{0011}, and that an interval I_{010} yields an inverse image I_{0101} only. Furthermore, the self-similarity of the generating mechanism is observed as follows: the generating mechanism of inverse images of an interval I_{01} is similar to that of inverse images of an interval I_{001} or I_{0101} and so on.

Theorem 3.4 *For any* $s_1 s_2 \cdots s_n \neq t_1 t_2 \cdots t_m$,

$$I_{s_1 s_2 \cdots s_n} \cap I_{t_1 t_2 \cdots t_m} = \varnothing.$$

(Proof) The proof of Theorem 3.4 is similar to that of Theorem 3.2, hence, is omitted.

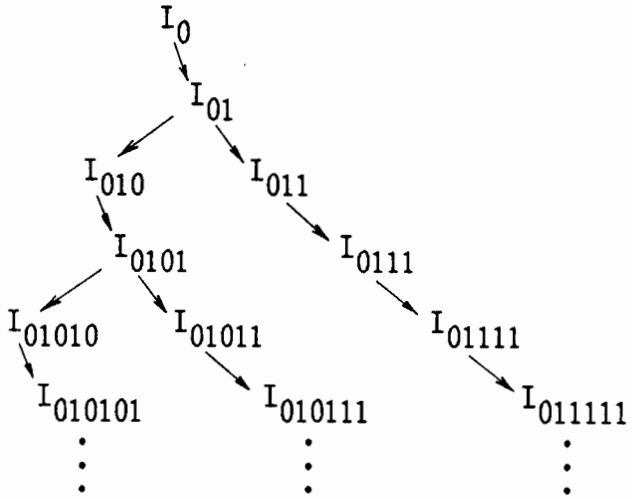

(a) Rules in Theorem 3.3a

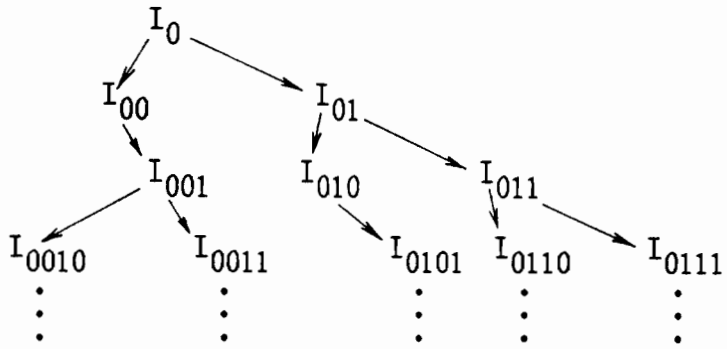

(b) Rules in Theorem 3.3c

Figure 3.8: Rules yielding inverse images $I_{s_1 s_2 \cdots s_k}$ in Theorems 3.3a and 3.3c

3.3.3 Example

In this subsection, results, presented in the subsection 3.3.2, are applied to the logistic system, which is well studied as the mathematical model exhibiting the population dynamics in ecology:

$$\begin{aligned} x_{n+1} &= f_A(x_n),\ n = 0, 1, 2, \cdots, \\ f_A(x) &= Ax(1-x), \end{aligned} \tag{3.37}$$

where x_n represents the population density of the n–th generation and A is a constant representing the growth rate of the species.

Consider a set of initial conditions, under which, for any generation $n \geq 0$, the population density is larger than a preassigned lower bound C, that is,

$$\Lambda_C = \{x_0 : x_n = f_A^n(x_0) > C,\ n \geq 0\}. \tag{3.38}$$

From the shape of the nonlinear function $f_A(\cdot)$ plotted in Fig.3.9, if $x_n \geq \max\{f_A^{-1}(C)\}$, then, in the next generation, $x_{n+1} \leq C$. Hence, in order to satisfy the condition that

$$x_n > C,\ n = 0, 1, 2, \cdots,$$

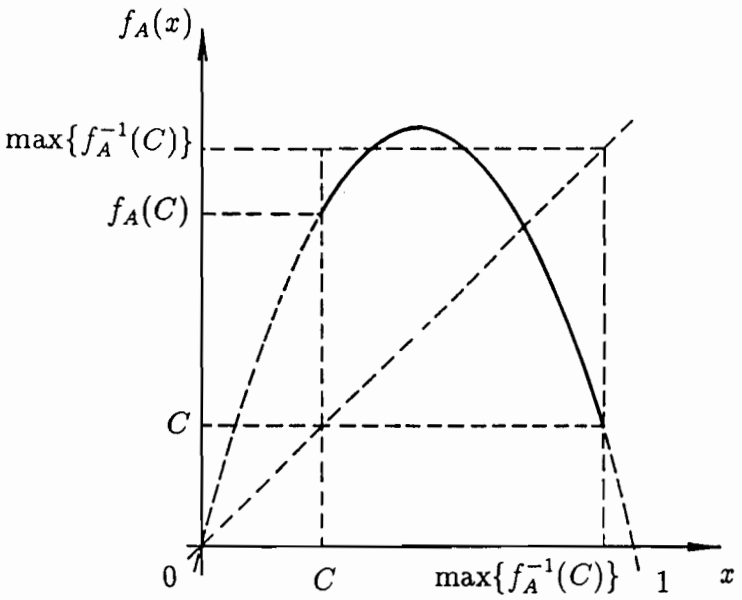

Figure 3.9: The shape of the nonlinear function $f_A(\cdot)$

it is necessary that

$$C < x_n < \max\{f_A^{-1}(C)\},\ n \geq 0.$$

From this fact, the set of initial conditions Λ_C, defined by Eq.(3.38), is converted into

$$\Lambda_C = \{x_0 : x_n = f_A^n(x_0) \in]C, \max\{f_A^{-1}(C)[,\ n \geq 0\}.$$

By regarding an interval $]C, \max\{f_A^{-1}(C)[$ as a unit interval $]0, 1[$, theoretical results, presented in subsection 3.3.2, can be applied to the generating mechanism of fractal structures of the set Λ_C. It is clear that the function $f_A(\cdot)$ satisfies the assumption **(A3.3)**. Furthermore, if inequalities

$$C < f_A(C) < \max\{f_A^{-1}(C)\} < f_A(0.5)$$

hold, then a function $f_A(\cdot)$ is a unimodal mapping on a closed interval $[C, \max\{f_A^{-1}(C)\}]$, satisfying the assumption **(A3.5)**. An interval I_0, defined by Eq.(3.34), is converted into

$$I_C = \{x : f_A(x) \geq \max\{f_A^{-1}(C)\}\}$$

and the generating mechanism of the invariant set Λ is also converted into

$$\Lambda_C =]C, \max\{f_A^{-1}(C)\}[- \bigcup_{k=0}^{\infty} f_A^{-k}(I_C).$$

For example, the assumption **(Ca)** in Theorem 3.3a is rewritten by

$$\begin{aligned} &\max\{f_A^{-1}(\min\{f_A^{-1}(\max\{f_A^{-1}(C)\})\})\} \\ &\quad > f_A(C) \\ &\quad\quad \geq \max\{f_A^{-1}(\max\{f_A^{-1}(\max\{f_A^{-1}(C)\})\})\}. \end{aligned}$$

Hence, in the case where the growth rate A is assigned, we can obtain conditions for a constant C, under which Theorems 3.3a to 3.3d are respectively hold. For example, in the case where the growth rate A is set as $A = 3.9$, the following results are obtained:

(a) If $0.359\cdots > C \geq 0.289\cdots$, then Theorem 3.3a holds.

(b) If $0.289\cdots > C \geq 0.181\cdots$, then Theorem 3.3b holds.

(c) If $0.181\cdots > C \geq 0.133\cdots$, then Theorem 3.3c holds.

(d) If $0.133\cdots > C > 0.052\cdots$, then Theorem 3.3d holds.

In Fig.3.10, conditions of Theorems 3.3 are summarized on the A–C parameter space, by the aid of numerical calculations.

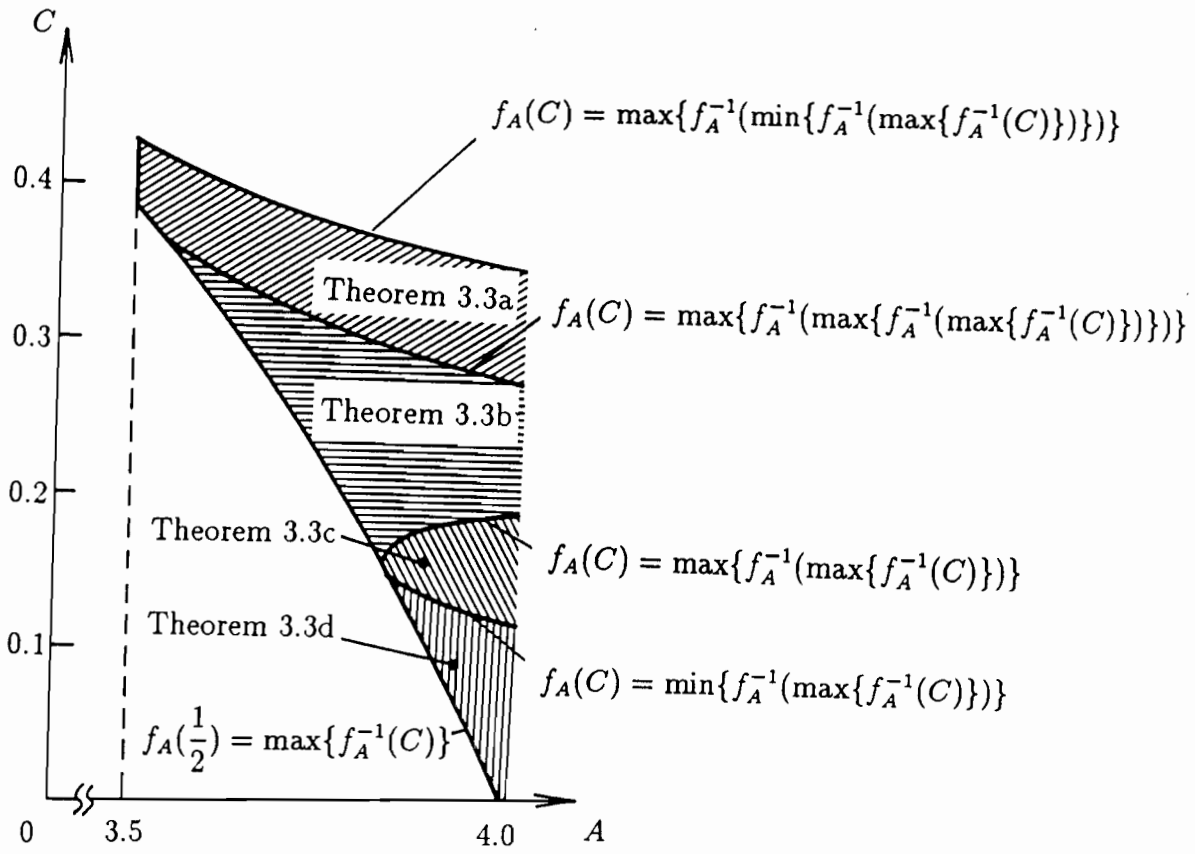

Figure 3.10: The A–C parameter space for conditions of Theorems 3.3a to 3.3d associated with the logistic mapping

(Remark) The Lebesgue measure of the set Λ_C is zero. Hence, for almost all initial conditions $x_0 \in]C, \max\{f_A^{-1}(C)\}[$, there exists n such that $x_n \leq C$. However, in practical point of view, the Lebesgue measure of the set

$$\Lambda_{C,N} = \{x_0 : x_n = f_A^n(x_0) > C,\ 0 \leq n \leq N\}$$

is not zero. Hence, in view of Theorems 3.3a to 3.3d, it is concluded that, for a large N,

the structure of the set $\Lambda_{C,N}$ is extremely complicated and it is difficult to predict whether the population density x_n is larger than C for any n with $0 \leq n \leq N$.

3.4 Concluding Remarks

In this chapter, mechanisms yielding fractal boundaries of the invariant set of nonlinear functions were investigated by using the notation of the symbolic dynamics, concerned with a class of one-dimensional discrete dynamical systems.

First, the mechanism yielding the fractal structure of the invariant set has been clarified, concerned with the nonlinear function possessing periodic points with period three and a typical example of the fractal invariant set with non-integer capacity dimension has been shown.

Furthermore, associated with a class of one-dimensional nonlinear discrete dynamical systems described by the unimodal mapping, it has been shown that mechanisms yielding fractal boundaries of the invariant set are classified to the five different mechanisms by using the notation of the symbolic dynamics.

In the next chapter, by applying results obtained in this chapter, mechanisms yielding fractal boundaries of the invariant domain will be discussed, concerned with a class of two-dimensional dynamical system, and the usefulness of results of this chapter will be shown again.

Appendix 3A: Proof of Theorem 3.3a

(i) Existence of the inverse image $I_{s_1 s_2 \cdots s_k 1}$: Noting that, under assumptions **(A3.3)** to **(A3.5)**,

$$f(J_1) = f(]\max\{f^{-1}(1)\}, 1[) =]0, 1[,$$

it can be obtained that, for any interval $I_{s_1 s_2 \cdots s_k} \subset]0, 1[$, $k \geq 1$,

$$\{x : f(x) \in I_{s_1 s_2 \cdots s_k},\ x \in J_1\} \neq \varnothing.$$

This fact shows that, for any $s_1 s_2 \cdots s_k$, one of the inverse image of the interval $I_{s_1 s_2 \cdots s_k}$, defined by

$$I_{s_1 s_2 \cdots s_k 1} = f^{-1}(I_{s_1 s_2 \cdots s_k}) \cap J_1 = \{x : f(x) \in I_{s_1 s_2 \cdots s_k}\} \cap J_1,$$

always exists. Hence, in the remainder of proofs demonstrated in Appendix 3A to 3D, our attention is concentrated on the existence of the other inverse image

$$I_{s_1 s_2 \cdots s_k 0} = f^{-1}(I_{s_1 s_2 \cdots s_k}) \cap J_0.$$

Before proceeding proofs, note that, as shown in Fig.3.11, under assumptions **(A3.3)** to **(A3.5)**, the following inequality holds:

$$\begin{aligned} & \max\{f^{-1}(\min\{f^{-1}(1)\})\} \\ > \ & \max\{f^{-1}(\max\{f^{-1}(1)\})\} \\ > \ & \max\{f^{-1}(1)\} \\ > \ & \min\{f^{-1}(1)\}. \end{aligned} \tag{3.39}$$

(ii) Proof of **(R1a)**: First, as shown in Fig.3.12 which plots the shape of the function $f(\cdot)$ satisfying the conditions **(A3.3)** to **(A3.5)** and **(Ca)** in Theorem 3.3a,

$$f(J_0) \cap I_0 = f(]0, \min\{f^{-1}(1)\}[) \cap I_0 =]f(0), 1[\cap[\min\{f^{-1}(1)\}, \max\{f^{-1}(1)\}] = \varnothing.$$

Hence, it is obtained that the inverse image $I_{00} = f^{-1}(I_0) \cap J_0$ does not exist.

Secondly, the inverse image of the interval $I_{s_1 s_2 \cdots s_k}, k \geq 2$ is considered. From the definition of the interval $I_{s_1 s_2 \cdots s_k}$, if $s_k = 0$, then

$$I_{s_1 s_2 \cdots s_k} \subset J_0. \tag{3.40}$$

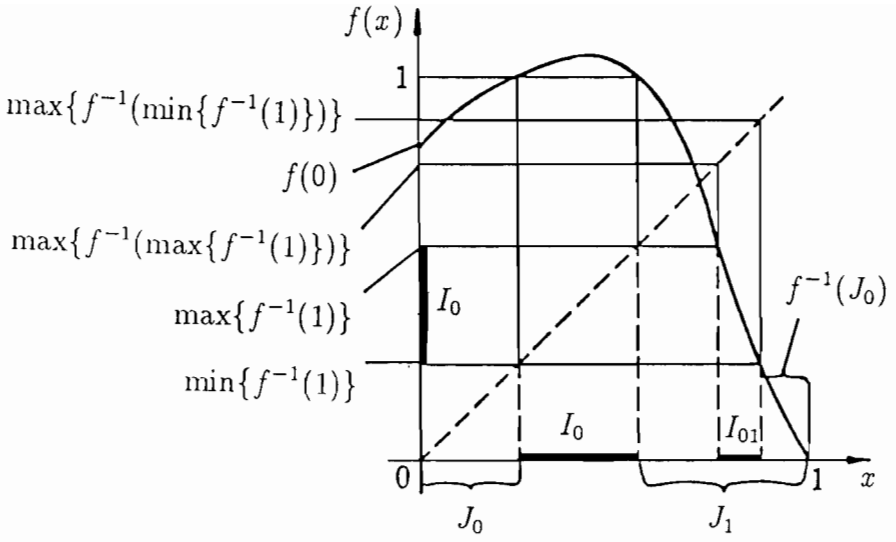

Figure 3.11: The shape of the nonlinear function $f(x)$ satisfying conditions **(A3.3)** to **(A3.5)**

Under the condition **(Ca)**, as shown in Fig.3.11,

$$f^{-1}(J_0) = f^{-1}(]0, \min\{f^{-1}(1)\}[) =]\max\{f^{-1}(\min\{f^{-1}(1)\})\}, 1[. \tag{3.41}$$

From the inequality (3.39),

$$]\max\{f^{-1}(\min\{f^{-1}(1)\})\}, 1[\subset]\max\{f^{-1}(1)\}, 1[= J_1. \tag{3.42}$$

From (3.41) and (3.42), it follows that

$$f^{-1}(J_0) \subset J_1. \tag{3.43}$$

The relation (3.43) indicates that, if $I_{s_1 s_2 \cdots s_k} \subset J_0$, then

$$f^{-1}(I_{s_1 s_2 \cdots s_k}) \subset J_1. \tag{3.44}$$

The relation (3.44) shows that if $s_k = 0$, then the inverse image $I_{s_1 s_2 \cdots s_k 1}$ exists and however the inverse image $I_{s_1 s_2 \cdots s_k 0}$ does not exist.

(iii) Existence of $I_{s_1 s_2 \cdots s_{k+1} 0}$ in **(R2a)**: From the definition of the interval $I_{s_1 s_2 \cdots s_{k+1}}$,

$$f(I_{s_1 s_2 \cdots s_{k+1}}) = I_{s_1 s_2 \cdots s_k}. \tag{3.45}$$

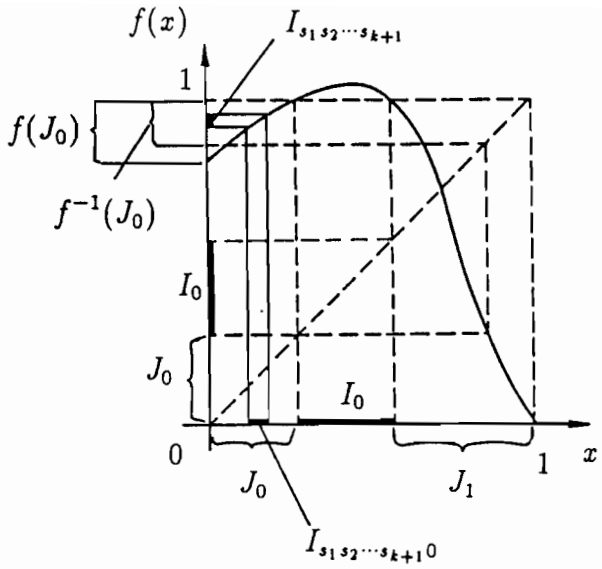

Figure 3.12: The shape of the nonlinear function $f(x)$ satisfying conditions **(Ca)**

Therefore, noting that if $s_k = 0$, then $I_{s_1 s_2 \cdots s_k} \subset J_0$, we obtain that

$$f(I_{s_1 s_2 \cdots s_{k+1}}) = I_{s_1 s_2 \cdots s_k} \subset J_0. \tag{3.46}$$

Considering the inverse image of both side of (3.46), it follows that

$$I_{s_1 s_2 \cdots s_{k+1}} \subset f^{-1}(J_0). \tag{3.47}$$

On the other hand, by using the assumption **(Ca)** and (3.41), we obtain that

$$f(J_0) = f(]0, \min\{f^{-1}(1)\}[) =]f(0), 1[\supset]\max\{f^{-1}(\min\{f^{-1}(1)\})\}, 1[= f^{-1}(J_0)$$

i.e.,

$$f(J_0) \supset f^{-1}(J_0). \tag{3.48}$$

Relations (3.47) and (3.48) show that, if $s_k = 0$, then

$$f(J_0) \supset I_{s_1 s_2 \cdots s_{k+1}}. \tag{3.49}$$

From (3.49), it is concluded that, if $s_k = 0$, then there exists an interval $I_{s_1 s_2 \cdots s_{k+1}0} = f^{-1}(I_{s_1 s_2 \cdots s_k}) \cap J_0$. (See Fig.3.12.)

(iv) Existence of $I_{s_1 s_2 \cdots s_{k+1} 0}$ in **(R3a)**: In the case where $s_{k+1} = 1$,

$$I_{s_1 s_2 \cdots s_{k+1}} \subset J_1. \tag{3.50}$$

From the definition of the interval $I_{s_1 s_2 \cdots s_{k+1}}$,

$$f(I_{s_1 s_2 \cdots s_{k+1}}) = I_{s_1 s_2 \cdots s_k}. \tag{3.51}$$

Now, noting that if $s_k = 1$, then $I_{s_1 s_2 \cdots s_k} \subset J_1$, we obtain

$$f(I_{s_1 s_2 \cdots s_{k+1}}) = I_{s_1 s_2 \cdots s_k} \subset J_1. \tag{3.52}$$

Considering the inverse image of both side of (3.52), it follows that

$$I_{s_1 s_2 \cdots s_{k+1}} \subset f^{-1}(J_1). \tag{3.53}$$

Combining (3.50) and (3.53), we obtain that

$$I_{s_1 s_2 \cdots s_{k+1}} \subset \{J_1 \cap f^{-1}(J_1)\}. \tag{3.54}$$

Under the assumption **(Ca)**,

$$\begin{aligned} & J_1 \cap f^{-1}(J_1) \\ = \; &]\max\{f^{-1}(1)\}, 1[\cap f^{-1}(]\max\{f^{-1}(1)\}, 1[) \\ = \; &]\max\{f^{-1}(1)\}, 1[\cap\{]0, \min\{f^{-1}(1)\}[\cup]\max\{f^{-1}(1)\}, \max\{f^{-1}(\max\{f^{-1}(1)\})\}[\} \\ = \; &]\max\{f^{-1}(1)\}, \max\{f^{-1}(\max\{f^{-1}(1)\})\}[\end{aligned} \tag{3.55}$$

Hence, under the assumption **(Ca)**,

$$f(J_0) \cap \{J_1 \cap f^{-1}(J_1)\} =]f(0), 1[\cap]\max\{f^{-1}(1)\}, \max\{f^{-1}(\max\{f^{-1}(1)\})\}[= \varnothing. \tag{3.56}$$

From (3.54) and (3.56), it can be obtained that, if $s_k = 1$ and $s_{k+1} = 1$, then the interval $I_{s_1 s_2 \cdots s_{k+1} 0}$ does not exist. **(Q.E.D.)**

Appendix 3B: Proof of Theorem 3.3b

Proofs of rules (**R1b**) and (**R2b**) are similar to that of rules (**R1a**) and (**R2a**). The existence of an interval $I_{s_1 s_2 \cdots s_{k+1} 1}$ in the rule (**R3c**) is also proved by the same discussions as shown in the first part of Appendix 3A. Hence, in this Appendix 3B, the existence of an interval $I_{s_1 s_2 \cdots s_{k+1} 0}$ in the rule (**R3c**) is discussed.

If $s_k = 1$ and $s_{k+1} = 1$, then

$$I_{s_1 s_2 \cdots s_{k+1}} \subset \{J_1 \cap f^{-1}(J_1)\} =]\max\{f^{-1}(1)\}, \max\{f^{-1}(\max\{f^{-1}(1)\})\}[.$$

Noting that $f(J_0) =]f(0), 1[$, it can be obtained that, under the assumption (**Cb**),

$$f(J_0) \cap \{J_1 \cap f^{-1}(J_1)\} =]f(0), 1[\cap]\max\{f^{-1}(1)\}, \max\{f^{-1}(\max\{f^{-1}(1)\})\}[\neq \varnothing$$

and

$$f(J_0) \not\supset \{J_1 \cap f^{-1}(J_1)\}.$$

Hence, if

$$I_{s_1 s_2 \cdots s_{k+1}} \cap \{f(J_0) \cap \{J_1 \cap f^{-1}(J_1)\}\} \neq \varnothing,$$

then there exists an interval $I_{s_1 s_2 \cdots s_{k+1} 0} = f^{-1}(I_{s_1 s_2 \cdots s_{k+1}}) \cap J_0$. On the other hand, if

$$I_{s_1 s_2 \cdots s_{k+1}} \cap \{f(J_0) \cap \{J_1 \cap f^{-1}(J_1)\}\} = \varnothing,$$

then an interval $I_{s_1 s_2 \cdots s_{k+1} 0}$ does not exist. (**Q.E.D.**)

Appendix 3C: Proof of Theorem 3.3c

(i) Existence of I_{00} in **(R1c)**: From the assumption **(Cc)**,

$$\begin{aligned} & f(J_0) \cap I_0 \\ = \; & f(]0, \min\{f^{-1}(1)\}[) \cap [\min\{f^{-1}(1)\}, \max\{f^{-1}(1)\}] \\ = \; &]f(0), 1[\cap[\min\{f^{-1}(1)\}, \max\{f^{-1}(1)\}] \\ = \; &]f(0), \max\{f^{-1}(1)\}] \\ \neq \; & \varnothing \end{aligned} \tag{3.57}$$

Hence, there exist an interval I_{00} defined by $f^{-1}(I_0) \cap J_0$.

(ii) Existence of $I_{s_1 s_2 \cdots s_k 0}$ in **(R2c)**: Note that, in the case where $s_k = 0$,

$$I_{s_1 s_2 \cdots s_k} \subset J_0. \tag{3.58}$$

Under the assumption **(Cc)**,

$$f^{-1}(J_0) \cap J_0 =]\max\{\min\{f^{-1}(1)\}\}, 1[\cap]0, \min\{f^{-1}(1)\}[= \varnothing. \tag{3.59}$$

From relations (3.58) and (3.59), for any interval $I_{s_1 s_2 \cdots s_k} \subset J_0$ with $s_k = 0$, we obtain

$$f^{-1}(I_{s_1 s_2 \cdots s_k}) \cap J_0 = \varnothing, \tag{3.60}$$

which shows that an inverse image $I_{s_1 s_2 \cdots s_k 0}$ does not exist.

(iii) Proof of **(R3c)**: Note that, in the case where $s_k = 1$,

$$I_{s_1 s_2 \cdots s_k} \subset J_1. \tag{3.61}$$

Noting that $f(J_0) =]f(0), 1[$, it is obtained that, under the assumption **(Cc)**,

$$f(J_0) =]f(0), 1[\supset]\max\{f^{-1}(1)\}, 1[= J_1 \tag{3.62}$$

Hence, from relations (3.61) and (3.62), it is concluded that, for any interval $I_{s_1 s_2 \cdots s_k} \subset J_1$, there exists an inverse image $I_{s_1 s_2 \cdots s_k 0} \subset J_0$. **(Q.E.D.)**

Appendix 3D: Proof of Theorem 3.3d

Proofs of rules (**R1d**) and (**R3d**) are omitted, since discussions for these proofs are similar to those of (**R1c**) and (**R3c**) presented in Appendix 3C. Hence, in this appendix, the existence of an interval $I_{s_1 s_2 \cdots s_k 0}$ in the rule (**R2d**) is discussed.

Noting that

$$f(J_0) =]f(0), 1[$$

and

$$J_0 =]0, \min\{f^{-1}(1)\}[,$$

it is obtained that, under the assumption (**Cd**),

$$\begin{aligned} & f(J_0)) \cap J_0 \\ = \; &]f(0), 1[\cap]0, \min\{f^{-1}(1)\}[\\ = \; &]f(0), \min\{f^{-1}(1)\}[\\ \neq \; & \varnothing. \end{aligned}$$

Hence, if

$$I_{s_1 s_2 \cdots s_k} \cap \{f(J_0) \cap J_0\} \neq \varnothing,$$

then there exists an inverse image $I_{s_1 s_2 \cdots s_k 0}$. On the other hand, if

$$I_{s_1 s_2 \cdots s_k} \cap \{f(J_0) \cap J_0\} = \varnothing,$$

then an inverse image $I_{s_1 s_2 \cdots s_k 0}$ does not exist. (**Q.E.D.**)

Chapter 4

Fractal Boundaries of the Invariant Domain of a Discrete Predator-Prey System

4.1 Introductory Remarks

Theoretical and numerical investigations, demonstrated in Chaps.2 and 3, clarify existing conditions and yielding mechanisms of fractal boundaries of the invariant set, concerned with a class of one-dimensional discrete nonlinear dynamical systems. In this chapter, these results are applied to discuss fractal boundaries of the invariant domain, concerned with a class of two-dimensional dynamical systems [YS90], [YS91c], [Yas91].

The mathematical model, treated in this chapter, is described by a class of two-dimensional difference equations of the form

$$\begin{cases} x_{n+1} = Ax_n(1 - x_n - y_n) \\ y_{n+1} = By_n\left(-1 + \dfrac{x_n}{C}\right), \end{cases} \tag{4.1}$$

which gives a model describing the population dynamics of predator-prey systems. In the system (4.1), x_n and y_n represent respectively the population densities of preys and predators at the n-th generation, A and B are positive constants representing the growth rates of the prey and predator respectively, and C is a positive constant representing the interconnected rate between two species. The derivation of the mathematical model (4.1) is demonstrated in Appendix 4A.

The predator-prey system (4.1) exhibits a rich variety of asymptotic behavior, conver-

gence to stable equilibriums, periodic oscillations, limit cycles, chaotic behavior and so on. However, due to the nonlinearity of the system, the asymptotic behavior of solution processes depends on the initial condition. Furthermore, noting that x_n and y_n represent the population density, if either x_n or y_n reaches zero or negative value, then populations are considered to have been wiped out and the ecological system to have collapsed. Hence, in order to conserve the ecological system, it is important to find the set of initial conditions, which eventually approach a final state without leaving from the first quadrant of the phase space $\mathbf{R^2}$, described by

$$\mathcal{D} = \{(x_0, y_0) : x_n > 0,\ y_n > 0,\ n = 0, 1, 2, \cdots\}. \tag{4.2}$$

In this chapter, it will be shown that the set $\mathcal{D}$, defined by (4.2), often exhibits complicated boundaries, as shown in Figs.4.1. Initial conditions in the dark region of Figs.4.1 generate orbits which asymptotically approach an equilibrium, without leaving from the first quadrant of the phase space $\mathbf{R}^2$. On the other hand, solution processes with

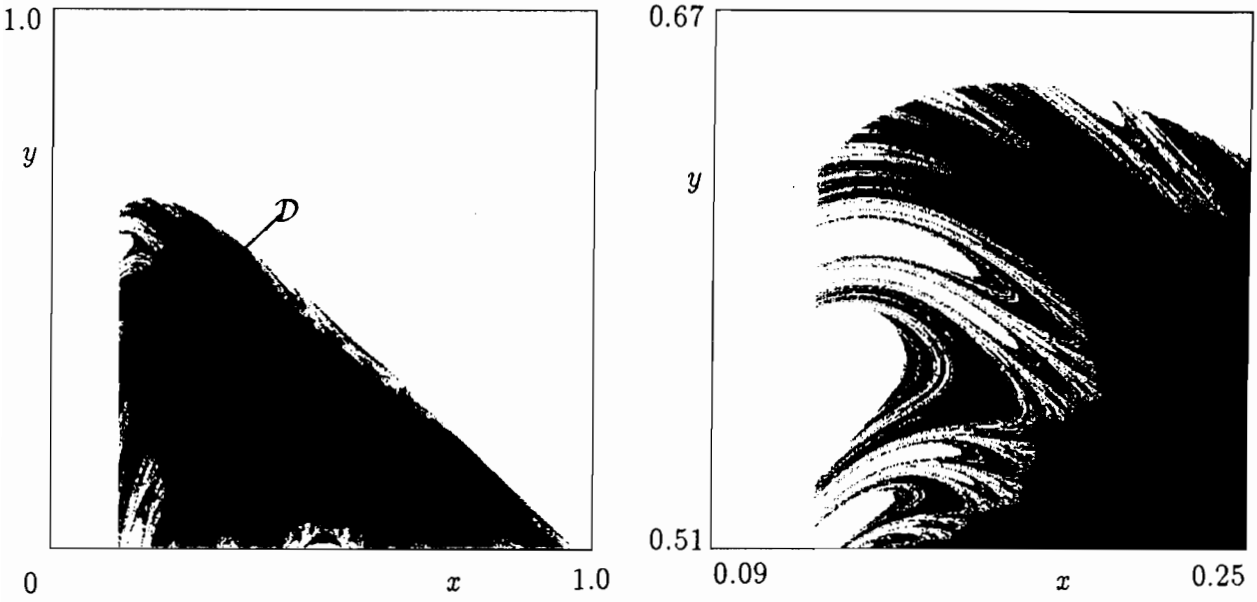

(a) The set $\mathcal{D}$ (b) A magnification of (a)

Figure 4.1: Complicated boundaries of the set $\mathcal{D}$ observed in the system (4.1) with $A = 3.89$, $B = 0.45$ and $C = 0.12$

the initial condition included in the white region escape from the first quadrant of the phase space $\mathbf{R}^2$. Figure 4.2 (a) shows a magnification of Fig.4.1 (b). Figure 4.2 (b) and (c) show respectively magnifications of square regions in Fig.4.2 (a). These magnifications reveal that boundaries have the self-similarity property and the complexity of boundaries does not decrease by any magnification. Hence, it is difficult to predict the asymptotic behavior of the solution whose initial condition is the neighborhood of boundaries.

The purpose of this chapter is to clarify mechanisms yielding complicated boundaries and to find conditions under which complicated boundaries appear, associated with a class of discrete predator-prey systems (4.1), by applying results demonstrated in Chaps.2 and 3. In order to examine results of this chapter, obtained by theoretical analysis, numerical experiments are carried out. Through theoretical investigations and numerical experiments, fractal properties of complicated boundaries in Figs.4.1 and 4.2 are clarified.

4.2 Nonlinear Mapping and Invariant Domain

First of all, concerned with the system (4.1), the definition of the invariant domain is shown and a candidate for the invariant domain is derived. For convenience of discussions, a nonlinear function $F : \mathbf{R}^2 \to \mathbf{R}^2$ defined by

$$F(x, y) = \left(Ax(1 - x - y), \;\; By\left(-1 + \frac{x}{C}\right)\right) \tag{4.3}$$

is introduced.

Definition 4.1 *A subset $\mathcal{D}_a \subset \mathbf{R}^2$ is called the invariant domain of the nonlinear function $F : \mathbf{R}^2 \to \mathbf{R}^2$, if the following condition holds:*

$$F(\mathcal{D}_a) \subset \mathcal{D}_a. \tag{4.4}$$

Now, note that

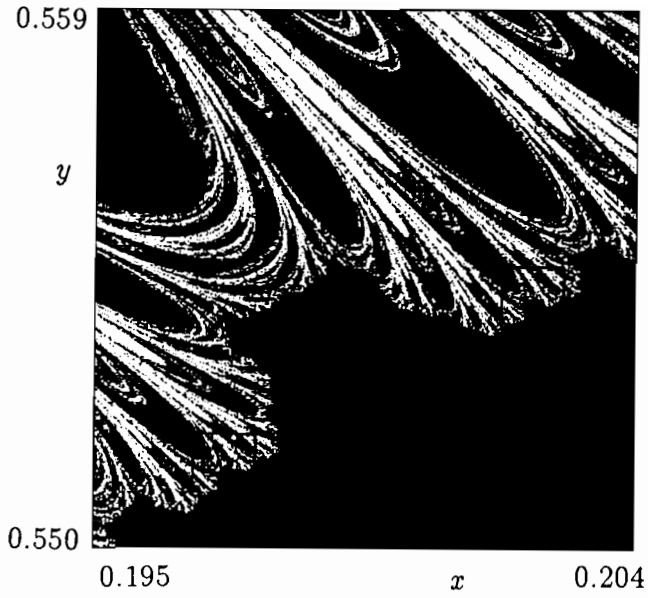

(a) A magnification of Fig.4.1(b)

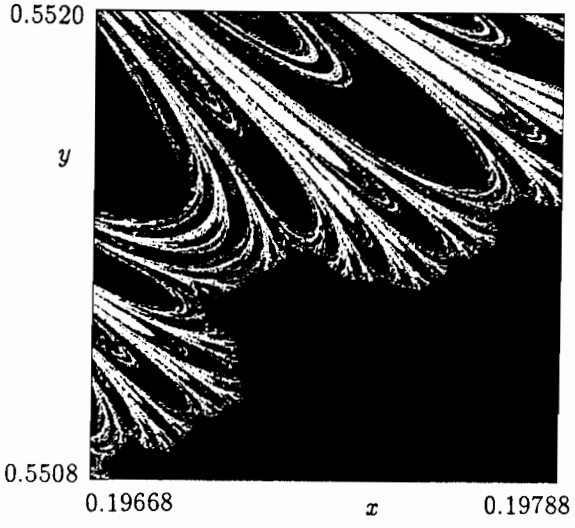

(b) A magnification of a left square of (a)

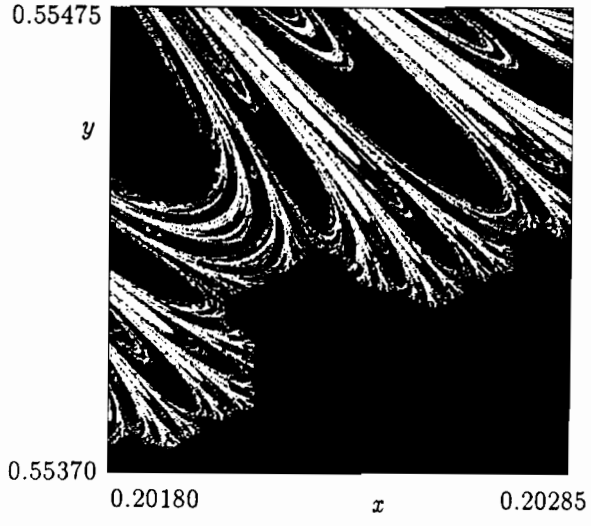

(c) A magnification of a right square of (a)

Figure 4.2: The self similarity observed in complicated boundaries in Figs.4.1

(i) From the definition (4.2) of the set $\mathcal{D}$, if $(x_0, y_0) \in \mathcal{D}$, then, for any $n \geq 1$, $x_{n+1} > 0$ and $y_{n+1} > 0$ which are given by $F^{n+1}(x_0, y_0) = F^n(F(x_0, y_0))$. Namely, if $(x_0, y_0) \in \mathcal{D}$, then $F(x_0, y_0) \in \mathcal{D}$. This fact indicate that the set $\mathcal{D}$ satisfies

$$F(\mathcal{D}) \subset \mathcal{D},$$

that is, the set $\mathcal{D}$ is a invariant domain of the nonlinear function $F : \mathbf{R}^2 \to \mathbf{R}^2$.

(ii) Furthermore, if a set $\mathcal{D}_s$ is an invariant domain, included in the first quadrant of the phase space $\mathbf{R}^2$, then, from the definition of the invariant domain,

$$F(\mathcal{D}_s) \subset \mathcal{D}_s.$$

Hence, $F(\mathcal{D}_s)$ is included in the first quadrant of the phase space. Namely, if $(x_0, y_0) \in \mathcal{D}_s$, then solution processes satisfy that $x_n > 0$ and $y_n > 0$. This fact indicates that

$$\mathcal{D}_s \subset \mathcal{D}.$$

In view of these discussions (i) and (ii), it is obtained that our target set $\mathcal{D}$ is the largest invariant domain of the function F, included in the first quadrant of $\mathbf{R}^2$.

A candidate for the invariant domain $\mathcal{D}$ is obtained as follows: First, assume that

$$x_n > 0, \; y_n > 0. \tag{4.5}$$

From Eq.(4.1), under the condition (4.5), if and only if conditions

$$1 - x_n - y_n > 0 \tag{4.6}$$

and

$$x_n > C \tag{4.7}$$

hold, then $x_{n+1} > 0$ and $y_{n+1} > 0$. Furthermore, if $x_{n+1} < C$, then $y_{n+2} < 0$. In order to satisfy the condition

$$x_{n+1} > C,$$

the following condition is needed:

$$x_{n+1} = Ax_n(1 - x_n - y_n) > C. \tag{4.8}$$

From conditions (4.5), (4.7) and (4.8), a candidate for the invariant domain $\mathcal{D}$ is obtained by

$$\mathcal{D}_- = \{(x, y) : x > C, y > 0, Ax(1 - x - y) > C\}. \tag{4.9}$$

Figure 4.3 shows the shape of the candidate $\mathcal{D}_-$.

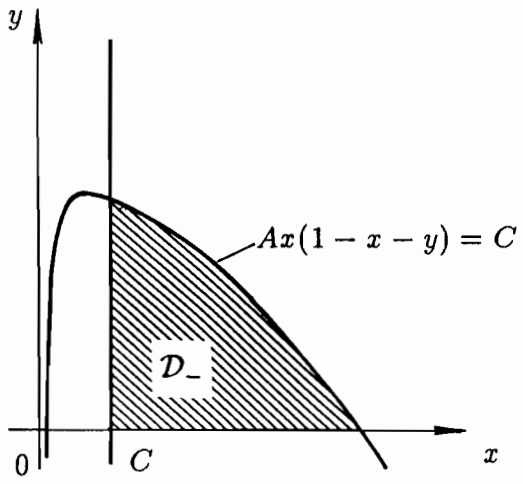

Figure 4.3: A candidate $\mathcal{D}_-$ for the invariant domain $\mathcal{D}$

4.3 Existing Conditions of Fractal Boundaries

In this section, necessary conditions, under which fractal boundaries of the invariant domain $\mathcal{D}$ shown in Figs.4.1 and 4.2, are shown.

4.3.1 Images of Candidate for Invariant Domain

First of all, our attention is concentrated on the image $F(\mathcal{D}_-)$ of the candidate $\mathcal{D}_-$, generated by the two-dimensional noninvertible smooth mapping $F : \mathbf{R}^2 \to \mathbf{R}^2$ in Eq.(4.3).

Let $DF(x, y)$ be Jacobian of the function $F(x, y)$ and consider a curve L defined by

$$L = \{(x, y) : |DF(x, y)| = 0\} = \left\{(x, y) : y = \frac{2}{C}(x - C)\left(x - \frac{1}{2}\right)\right\}. \tag{4.10}$$

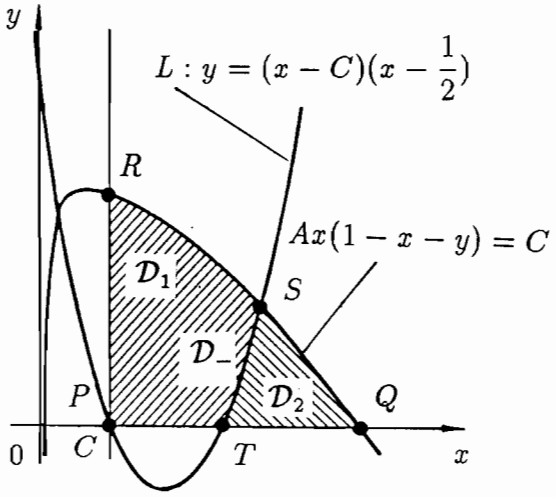

Figure 4.4: A curve defined by $|DF(x, y)| = 0$

As shown in Fig.4.4, the candidate $\mathcal{D}_-$ is divided into two parts $\mathcal{D}_1$ and $\mathcal{D}_2$ by a curve L defined by (4.10). Points P, Q, R, S and T are set as shown in Fig.4.4. A line with a starting point P and an ending point Q is denoted by $\overline{PQ}$ or a curve with a starting point S and an ending point T is also denoted by $\widetilde{ST}$. Furthermore, the image of the point P is denoted by $F(P)$.

Using these notions, we obtain

(i) A common image of a segment $\overline{TQ}$ and a broken line $\overline{RPT}$ are given by the nonlinear function F on x-axis and

$$\overline{F(R)F(P)F(T)} = \overline{F(Q)F(T)}.$$

(ii) A common image of curves $\widetilde{SR}$ and $\widetilde{SQ}$ are given by the nonlinear function F on a line $x = C$ and

$$\overline{F(S)F(R)} = \overline{F(S)F(Q)}.$$

(iii) A image $F(\widetilde{S)F(T)}$ of a curve $\widetilde{ST}$ also construct boundaries of the image $F(\mathcal{D}_-)$.

Therefore, the image $F(\mathcal{D}_-)$ of the candidate $\mathcal{D}_-$, generated by the nonlinear function F,

satisfies that

$$F(\mathcal{D}_1) = F(\mathcal{D}_2) = F(\mathcal{D}_-).$$

Boundaries of the image $F(\mathcal{D}_-)$ consist of lines $\overline{F(S)F(R)}$, $\overline{F(R)F(T)}$ and a curve $F(\widetilde{S)F}(T)$, as shown in Fig.4.5. Hence,

$$F(\mathcal{D}_-) \subset \mathcal{D}_-$$

holds and a candidate $\mathcal{D}_-$ with smooth boundaries is the invariant domain of F, if and only if a curve $F(\widetilde{S)F}(T)$ is included in $\mathcal{D}_-$.

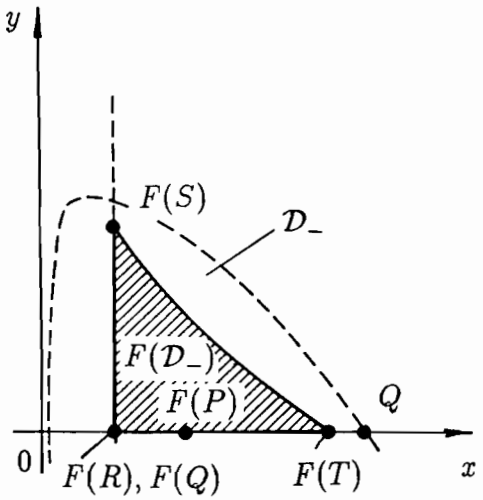

Figure 4.5: Image $F(\mathcal{D}_-)$

4.3.2 Necessary Condition for Existing Fractal Boundaries

In this subsection, it is shown that if $F(T) \notin \mathcal{D}_-$, then the invariant domain with fractal boundaries appears. If $F(T) \notin \mathcal{D}_-$, then the image $F(\mathcal{D}_-)$ has a cross-hatched region

$$\mathcal{A} = \{(x, y) : (x, y) \in F(\mathcal{D}_-), (x, y) \notin \mathcal{D}_-\},$$

which is not included in $\mathcal{D}_-$, as shown in Fig.4.6.

Consider inverse images $F^{-k}(\mathcal{A})$, $k = 1, 2, 3, \cdots$ of $\mathcal{A}$.

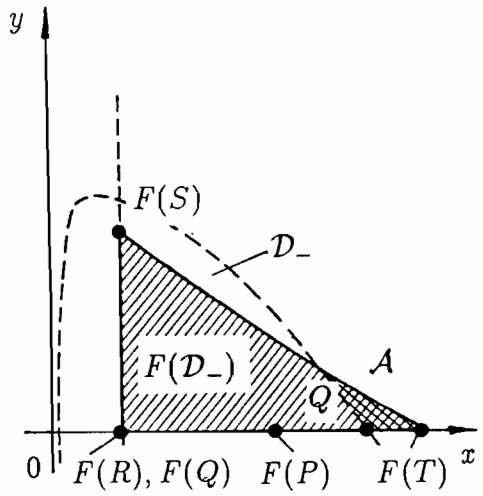

Figure 4.6: Image $F(\mathcal{D}_-)$ with region $\mathcal{A}$

(step 1) Noting that $\mathcal{A}$ is in the neighborhood of $F(T)$, it can be shown that the inverse image $F^{-1}(\mathcal{A})$ is in the neighborhood of the point T, as shown in Fig.4.7(a).

(step 2) Taking into account that $F^{-1}(\mathcal{A})$ exists on the segment

$$\overline{F(R)F(P)F(T)} = \overline{F(Q)F(T)},$$

it is obtained that one of the inverse images $F^{-1}(F^{-1}(\mathcal{A})) = F^{-2}(\mathcal{A})$ of $F^{-1}(\mathcal{A})$ exists on the segment $\overline{RP}$ or $\overline{PT}$ and another inverse image exists on the segment $\overline{QT}$. (See Fig.4.7(b))

(step 3) Similar procedures are repeated infinitely and inverse images $F^{-k}(\mathcal{A})$, $k = 3, 4, 5, \cdots$ appear successively on the segments $\overline{RP}$, $\overline{PT}$ and $\overline{QT}$.

(step 4) Noting that

$$\overline{F(S)F(R)} = \overline{F(S)F(Q)} \subset \overline{RP},$$

it is easy to see that $F^{-k}(\mathcal{A})$ also appears on the curve $\widetilde{RQ}$.

Now, note that if $(x_n, y_n) \in \mathcal{A}$, then $x_{n+1} < C$ and furthermore $y_{n+2} < 0$. If $(x_n, y_n) \in F^{-k}(\mathcal{A})$, then $(x_{n+k}, y_{n+k}) = F^k(x_k, y_k) \in \mathcal{A}$. Furthermore, if $(x_{n+k}, y_{n+k}) \in \mathcal{A}$, then

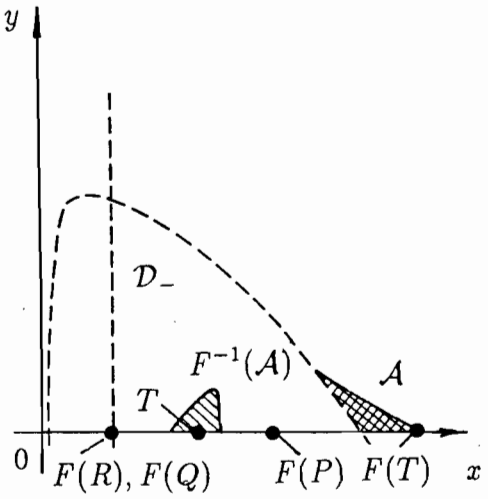

(a) $F^{-1}(\mathcal{A})$

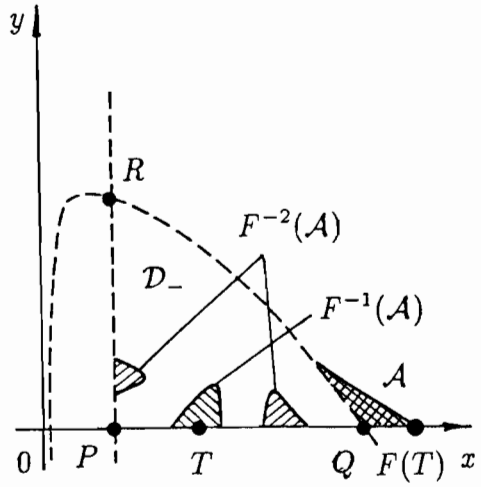

(b) $F^{-2}(\mathcal{A})$

Figure 4.7: Inverse images $F^{-k}(\mathcal{A})$

$y_{n+k+2} < 0$. Namely, solution processes starting from $F^{-k}(\mathcal{A})$, $k = 1, 2, 3, \cdots$ eventually escape from the first quadrant of the x-y plane. Hence, sets $F^{-k}(\mathcal{A})$ are not included in the invariant domain $\mathcal{D}$. Therefore, the invariant domain $\mathcal{D}$ is produced by the mechanism described by

$$\mathcal{D} = \mathcal{D}_- - \bigcup_{n=1}^{\infty} F^{-n}(\mathcal{A}). \tag{4.11}$$

From the definition (4.10) of the line L, the coordinates of the point T is given by

$$T = (\frac{1}{2}, 0). \tag{4.12}$$

Substituting (4.12) into (4.3), we obtain

$$F(T) = (\frac{A}{4}, 0). \tag{4.13}$$

From the definition of the candidate $\mathcal{D}_-$, the coordinates of the point Q is given by

$$Q = \left(\frac{1}{2} + \sqrt{\frac{1}{4} - \frac{C}{A}}, 0\right).$$

Comparing the x coordinates of points $F(T)$ and Q, it is concluded that the region $\mathcal{A}$ in Fig.4.6 exists, if the condition

$$\frac{A}{4} > \frac{1}{2} + \sqrt{\frac{1}{4} - \frac{C}{A}} \tag{4.14}$$

holds. These discussions and the straightforward calculation of (4.14) brings us the following result:

Theorem 4.1 *The necessary conditions for the existence of fractal boundaries of the invariant domain $\mathcal{D}$ is given by*

$$A^3 - 4A^2 - 16C > 0, \quad A > 4C. \tag{4.15}$$

4.4 Fractal Boundaries and Symbolic Dynamics

As shown in Fig.4.6, if $F(T) \notin \mathcal{D}_-$, then

$$F(\overline{PQ}) = \overline{F(Q)F(T)} \supset \overline{PQ}.$$

Therefore, a subset $\mathcal{S}$ on the segment $\overline{PQ}$ has its inverse images $F^{-1}(\mathcal{S})$ on the segment $\overline{PQ}$. On the other hand, the inverse image of a subset on the segment $\overline{RP}$ does not exist on segments $\overline{RP}$ and $\overline{PQ}$. Hence, our attention is concentrated to inverse images $F^{-k}(\mathcal{A})$ on the segment $\overline{PQ}$.

The symbolic dynamics are often used for characterizing chaotic behavior [CE80]. In this study, in order to discuss generating mechanisms of fractal boundaries, the following

notation associated with the symbolic dynamics is introduced:

(i) Let $\mathcal{A}_0$ be defined by

$$\mathcal{A}_0 = F^{-1}(\mathcal{A}), \tag{4.16}$$

where $\mathcal{A}$ is a cross hatched area depicted in Fig.4.6.

(ii) Let $\mathcal{A}_{00}$ be a subset of the inverse image $F^{-1}(\mathcal{A}_0)$ on the segment $\overline{PT}$ and $\mathcal{A}_{01}$ be also a subset of $F^{-1}(\mathcal{A}_0)$ on segment $\overline{TQ}$. (See Fig.4.8(a))

(iii) Similarly, sets $\mathcal{A}_{s_1 s_2 \cdots s_k 0}$ and $\mathcal{A}_{s_1 s_2 \cdots s_k 1}$ are subsets of $F^{-1}(\mathcal{A}_{s_1 s_2 \cdots s_k})$ on segments $\overline{PT}$ and $\overline{TQ}$ respectively. (See Fig.4.8(b))

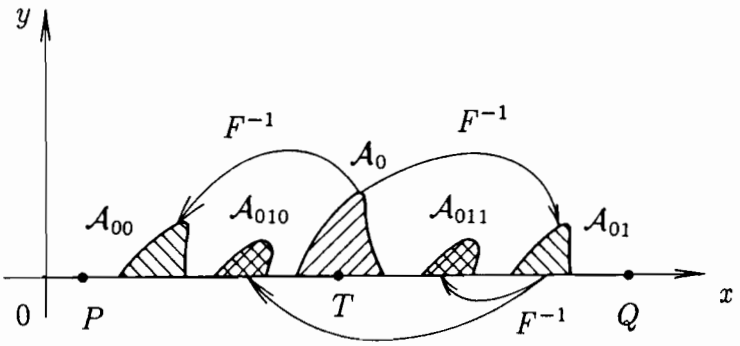

(a) $\mathcal{A}_{00}$ and $\mathcal{A}_{01}$

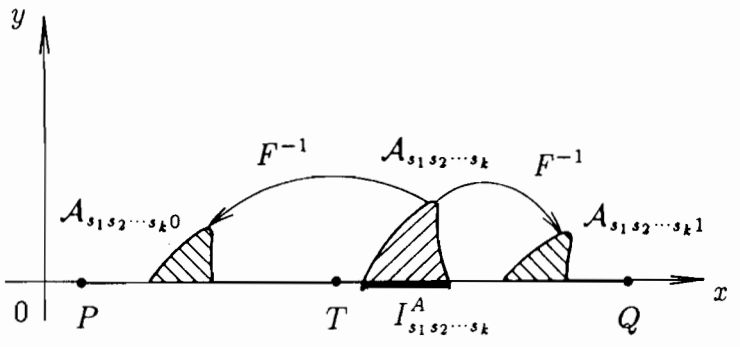

(b) $\mathcal{A}_{s_1 s_2 \cdots s_k 0}$ and $\mathcal{A}_{s_1 s_2 \cdots s_k 1}$

Figure 4.8: Inverse images $F^{-k}(\mathcal{A})$ with the notation of the symbolic dynamics

Now intervals $I^A_{s_1 s_2 \cdots s_k}$, $k = 0, 1,\ k \geq 1$ on the x axis are defined by

$$I^A_{s_1 s_2 \cdots s_k} = \overline{\mathcal{A}_{s_1 s_2 \cdots s_k}} \cap \{(x, y) :\ x \geq C,\ y = 0\},$$

where $\overline{\mathcal{A}_{s_1 s_2 \cdots s_k}}$ is the closure of the set $\mathcal{A}_{s_1 s_2 \cdots s_k}$ (See Fig.4.8.(b).). From the definition of the interval $I^A_{s_1 s_2 \cdots s_k}$ and the set $A_{s_1 s_2 \cdots s_k}$, it can be shown that

$$\begin{aligned} \bigcup_{s_{k+1}=0,1} I^A_{s_1 s_2 \cdots s_k s_{k+1}} &= \overline{F^{-1}(\mathcal{A}_{s_1 s_2 \cdots s_k})} \cap \{(x, y) :\ x \geq C,\ y = 0\} \\ &= f_A^{-1}(I^A_{s_1 s_2 \cdots s_k}) \cap \{x :\ x \geq C\}, \end{aligned}$$

where the function $f_A(\cdot)$ defined by

$$f_A(x) = Ax(1 - x - y)|_{y=0} = Ax(1 - x). \tag{4.17}$$

As shown in Fig.4.9, if conditions

$$f_A(C) < \max\{f_A^{-1}(C)\} < f(\frac{1}{2})$$

hold, then the function $f_A(\cdot)$ satisfies conditions **(A3.3)** and **(A3.5)** of Theorems 3.3a to 3.3d in Chap.3, where the closed unit interval $[0, 1]$ is converted into a closed interval $[C, \max\{f_A^{-1}(C)\}]$. Hence, by applying Theorems 3.3a to 3.3d, we can obtain the generating mechanism of intervals $I^A_{s_1 s_2 \cdots s_k}$, namely the generating mechanism of sets $\mathcal{A}_{s_1 s_2 \cdots s_k}$.

Theorem 4.3a *If conditions*

(U) $$f_A(C) < \max\{f_A^{-1}(C)\} < f_A(0.5)$$

and

$$\begin{aligned} & \max\{f_A^{-1}(\min\{f_A^{-1}(\max\{f_A^{-1}(C)\})\})\} \\ > \ & f_A(C) \\ \geq \ & \max\{f_A^{-1}(\max\{f_A^{-1}(\max\{f_A^{-1}(C)\})\})\} \end{aligned} \tag{4.18}$$

hold, then sets $\mathcal{A}_{s_1 s_2 \cdots s_k}$ are generated under the following rules:

(R4.1a) *For any $k \geq 1$, if $s_k = 0$, then a set $\mathcal{A}_{s_1 s_2 \cdots s_k 1}$ exists and a set $\mathcal{A}_{s_1 s_2 \cdots s_k 0}$ does not exist.*

(R4.2a) *For any $k \geq 2$, if $s_{k-1} = 0$ and $s_k = 1$, then sets $\mathcal{A}_{s_1 s_2 \cdots s_k 1}$ and $\mathcal{A}_{s_1 s_2 \cdots s_k 0}$ exist.*

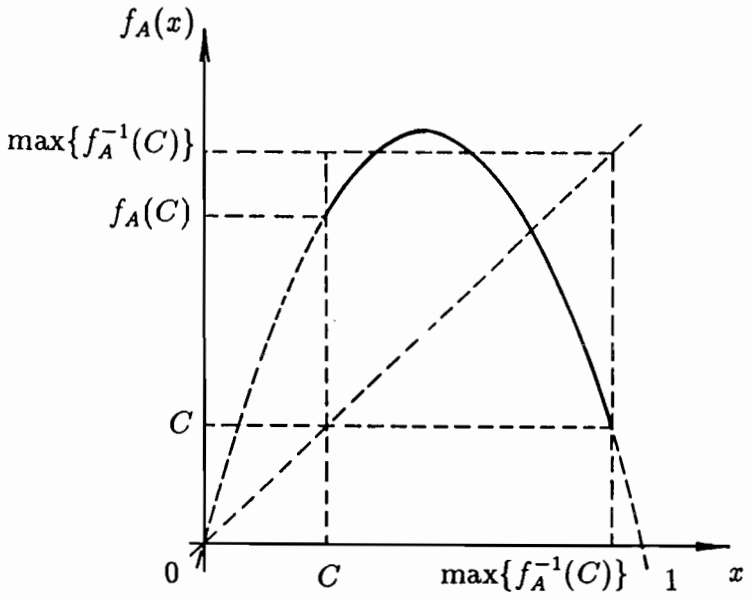

Figure 4.9: The logistic mapping $f_A(x)$

(R4.3a) *For any $k \geq 2$, if $s_{k-1} = 1$ and $s_k = 1$, then a set $\mathcal{A}_{s_1 s_2 \cdots s_k 1}$ exists and a set $\mathcal{A}_{s_1 s_2 \cdots s_k 0}$ does not exist.*

Theorem 4.3b *If conditions* **(U)** *and*

$$\begin{aligned} & \max\{f_A^{-1}(\max\{f_A^{-1}(\max\{f_A^{-1}(C)\})\})\} \\ > \; & f_A(C) \\ \geq \; & \max\{f_A^{-1}(\max\{f_A^{-1}(C)\})\} \end{aligned} \tag{4.19}$$

hold, then sets $\mathcal{A}_{s_1 s_2 \cdots s_k}$ are generated under the following rules:

(R4.1b) *For any $k \geq 1$, if $s_k = 0$, then a set $\mathcal{A}_{s_1 s_2 \cdots s_k 1}$ exists and a set $\mathcal{A}_{s_1 s_2 \cdots s_k 0}$ does not exist.*

(R4.2b) *For any $k \geq 2$, if $s_{k-1} = 0$ and $s_k = 1$, then sets $\mathcal{A}_{s_1 s_2 \cdots s_k 1}$ and $\mathcal{A}_{s_1 s_2 \cdots s_k 0}$ exist.*

(R4.3b) *For any $k \geq 2$, if $s_{k-1} = 1$ and $s_k = 1$, then a set $\mathcal{A}_{s_1 s_2 \cdots s_k 1}$ exists and a set $\mathcal{A}_{s_1 s_2 \cdots s_k 0}$ does not always exist.*

Theorem 4.3c *If conditions* **(U)** *and*

$$\begin{aligned} & \max\{f_A^{-1}(\max\{f_A^{-1}(C)\})\} \\ > \; & f_A(C) \\ \geq \; & \min\{f_A^{-1}(\max\{f_A^{-1}(C)\})\} \end{aligned} \tag{4.20}$$

hold, then sets $\mathcal{A}_{s_1 s_2 \cdots s_k}$ *are generated under the following rules:*

(R4.1c) *Sets* $\mathcal{A}_{00}$ *and* $\mathcal{A}_{01}$ *exist.*

(R4.2c) *For any* $k \geq 2$, *if* $s_{k-1} = 0$, *then a set* $\mathcal{A}_{s_1 s_2 \cdots s_k 1}$ *exists and a set* $\mathcal{A}_{s_1 s_2 \cdots s_k 0}$ *does not exist.*

(R4.3c) *For any* $k \geq 2$, *if* $s_{k-1} = 1$, *then sets* $\mathcal{A}_{s_1 s_2 \cdots s_k 0}$ *and* $\mathcal{A}_{s_1 s_2 \cdots s_k 1}$ *exist.*

Theorem 4.3d *If conditions* **(U)** *and*

$$\min\{f_A^{-1}(\max\{f_A^{-1}(C)\})\} > f_A(C) \tag{4.21}$$

hold, then sets $\mathcal{A}_{s_1 s_2 \cdots s_k}$ *are generated under the following rules:*

(R4.1d) *Sets* $\mathcal{A}_{00}$ *and* $\mathcal{A}_{01}$ *exist.*

(R4.2d) *For any* $k \geq 2$, *if* $s_{k-1} = 0$, *then a set* $\mathcal{A}_{s_1 s_2 \cdots s_k 1}$ *exists and a set* $\mathcal{A}_{s_1 s_2 \cdots s_k 0}$ *does not always exist.*

(R4.3d) *For any* $k \geq 2$, *if* $s_{k-1} = 1$, *then sets* $\mathcal{A}_{s_1 s_2 \cdots s_k 0}$ *and* $\mathcal{A}_{s_1 s_2 \cdots s_k 1}$ *exist.*

Furthermore, we obtain the following result:

Theorem 4.4 *If* $s_1 s_2 \cdots s_i \neq t_1 t_2 \cdots t_j$, $i \leq j$, *then*

$$\mathcal{A}_{s_1 s_2 \cdots s_i} \cap \mathcal{A}_{t_1 t_2 \cdots t_j} = \varnothing. \tag{4.22}$$

Figure 4.10 shows the rules described in Theorem 4.3a. For example, it can be seen that a set $\mathcal{A}_{001}$ yields inverse images $\mathcal{A}_{0010}$ and $\mathcal{A}_{0011}$, and that a set $\mathcal{A}_{010}$ yields an inverse image $\mathcal{A}_{0101}$ only.

As shown in Fig.4.10, the procedure yielding inverse images $F^{-k}(\mathcal{A}_{01})$, $k = 1, 2, 3, \cdots$ is similar to that yielding inverse images $F^{-k}(\mathcal{A}_{001})$, $k = 1, 2, 3, \cdots$ or inverse images $F^{-k}(\mathcal{A}_{0101})$, $k = 1, 2, 3, \cdots$ and so on. Namely, the mechanism yielding inverse images has the self-similarity. Therefore, complicated boundaries, shown in Figs.4.1 and 4.2, exhibit the self-similarity. In this sense, it can be concluded that *complicated boundaries, generated by mechanism in Theorems 4.3a to 4.3d, is fractal.*

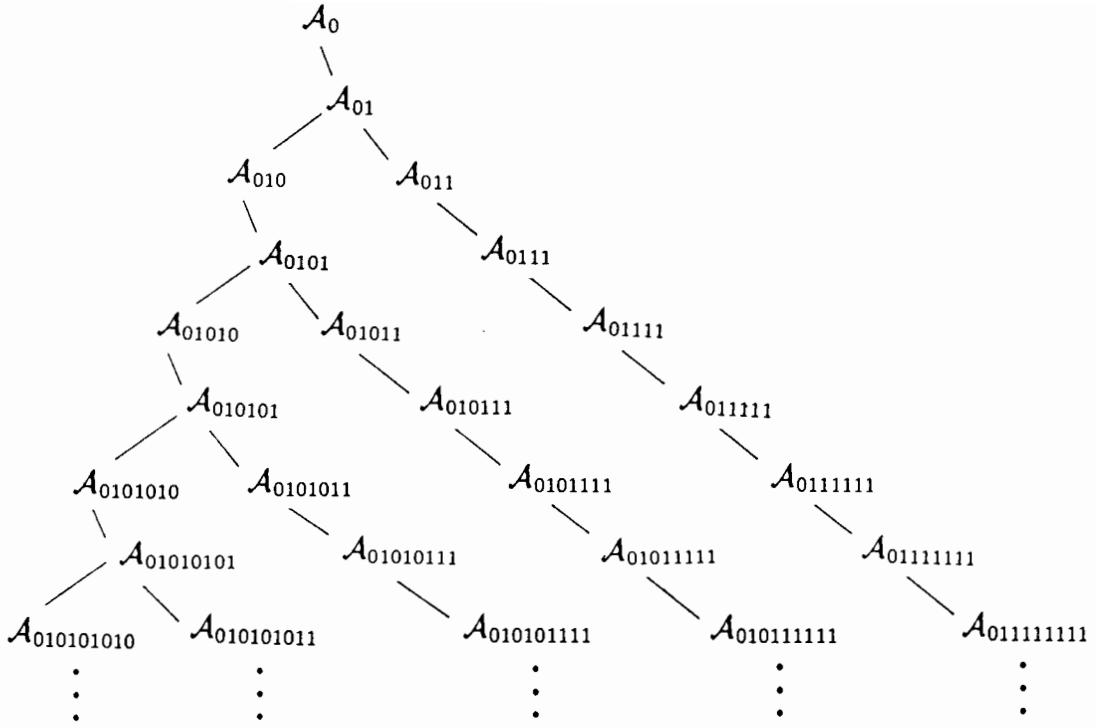

Figure 4.10: The mechanism yielding fractal boundaries in Theorem 4.3a

4.5 Numerical Experiments

Numerical experiments are demonstrated to show the validity of results in sections 4.3 and 4.4.

4.5.1 Numerical Technique for Calculating the Invariant Domain

In order to obtain the shape of the invariant domain $\mathcal{D}$ by using numerical calculations, the following procedures are carried out:

(step 1) Interval $[0, 1]$ in both the x and y axes are divided equally into 500 segments. By drawing the vertical and horizontal lines through dividing points, a mesh is constructed in the $x - y$ plane. Intersections between vertical and horizontal lines are selected as initial condition (x_0, y_0). (See Fig.4.11.)

(step 2) Each initial condition is iterated 400 times through the difference equation (4.1).

(step 3) If, for any n, $0 < n < 400$, the solution (x_n, y_n) is included in the first quadrant of the $x-y$ plane, then this initial condition (x_0, y_0) is regarded as an element of the invariant domain and the region $\{(x, y) : x_0 \leq x \leq x_0 + 0.002,\ y_0 \leq y \leq y_0 + 0.002\}$ is blackened.

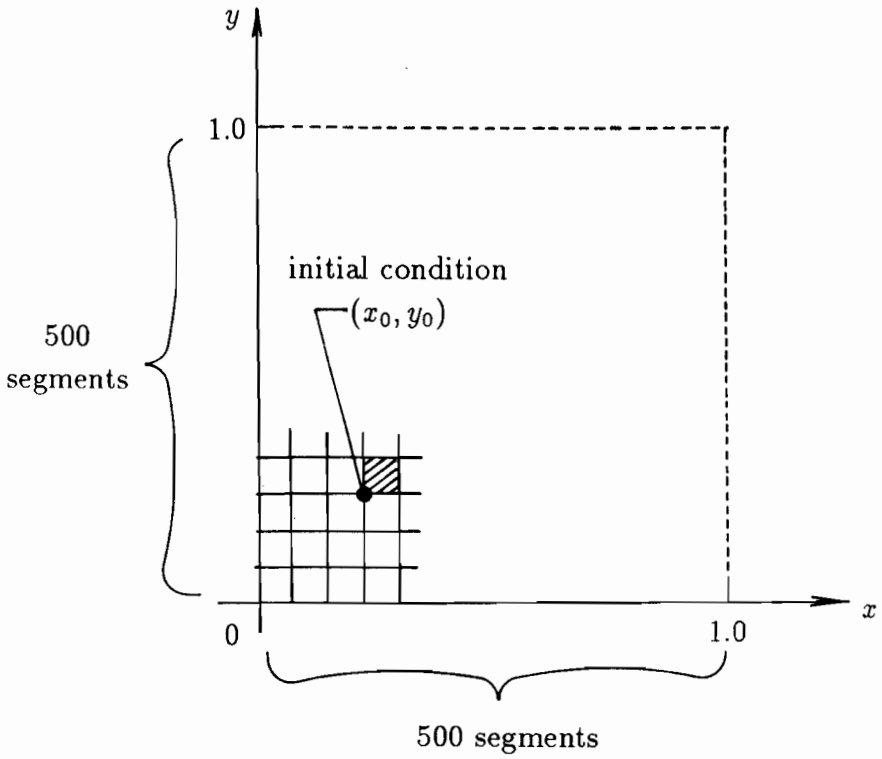

Figure 4.11: Numerical technique for calculating the shape of fractal boundaries

4.5.2 Onset of Fractal Boundaries of the Invariant Domain

In this example, the transition from the smooth boundary to the fractal one is discussed by using Theorem 4.1 in subsection 4.3.2 and computer experiments. Numerical calculations are carried out for fixed parameters $B = 0.45$ and $C = 0.12$. Figure 4.12(a) and (b) depict the invariant domain of the system (4.1), where the parameter A is set as $A = 3.85$ and $A = 3.9$ respectively.

In the case where $A = 3.85, B = 0.45$ and $C = 0.12$, from Theorem 4.1, the condition (4.15) does not hold and the invariant domain is the set $\mathcal{D}_-$ defined by Eq.(4.9) with smooth boundaries, which is shown in Fig.4.12(a).

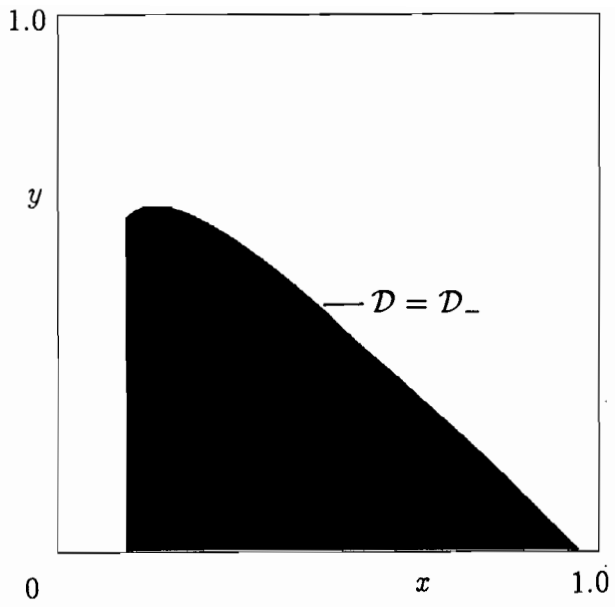

(a) $A = 3.85$

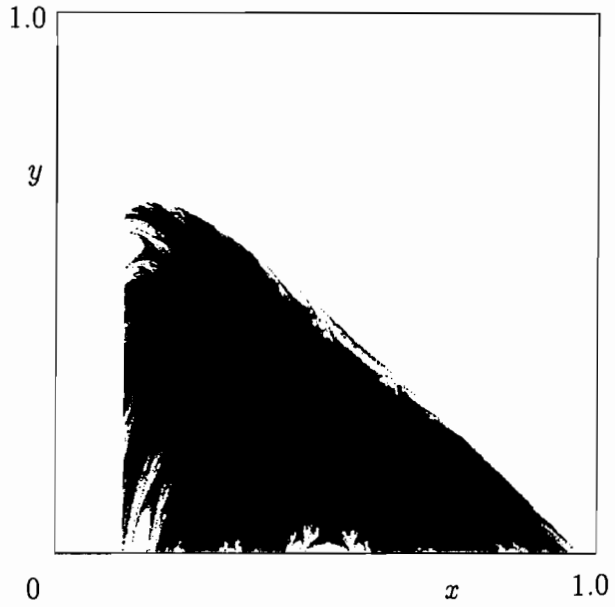

(b) $A = 3.89$

Figure 4.12: Onset of Fractal Boundaries of the Invariant Domain observed in the system (4.1) with $B = 0.45$ and $C = 0.12$

From Theorem 4.1, if the parameter A is larger than $3.87193\cdots$, then the condition (4.15) holds and the invariant domain possesses fractal boundaries. In the case where $A = 3.89$ which is slightly larger than the critical value $3.87193\cdots$, the invariant domain of the system (4.1) is depicted in Fig.4.12(b), where $A = 3.9$, $B = 0.45$ and $C = 0.12$. The boundary is fractal and the onset of fractal boundaries are confirmed. Results presented above show the validity of analyses demonstrated in this chapter.

4.6 Concluding Remarks

In this chapter, associated with a class of predator-prey systems, it has been shown that mechanisms yielding complicated boundaries of the invariant domain are discussed by considering the inverse mapping of the nonlinear function. From the condition, under which fractal boundaries appear, it has been obtained that complicated boundaries appear as the growth rate of preys increases.

Furthermore, by using the notation of the symbolic dynamics, mechanisms yielding complicated boundaries are classified to the four different mechanisms and the self-similarity of the yielding mechanisms are clarified.

Throughout these discussions, it was concluded that complicated boundaries observed in this chapter are fractal.

Appendix 4A: Derivation of Predator-Prey Systems Modeled by Difference Equations

Some biological populations with overlapping generations take the growth rate as a continuous process, and the appropriate mathematical description involves nonlinear differential equations. There are other biological systems whose populations consist of non-overlapping generations, where the growth rate takes place of discrete intervals of time and is described in terms of nonlinear difference equations [May73].

Although we have two methods stated above for modeling the system behaviors of biological population, it is well-known that simple nonlinear difference equation

$$x_{n+1} = \alpha x_n(1 - x_n) \tag{4.23}$$

was derived from the continuous-time logistic equation

$$\frac{dx(t)}{dt} = \alpha x(t) - \beta x^2(t), \tag{4.24}$$

through Euler's method, and that the solution x_n in Eq.(4.23) exhibits a wide variety of solution behaviors such as convergence, periodicity with any period and chaotic property (non-periodicity), while $x(t)$ in Eq.(4.24) only shows a convergent property [May74],[May76]. It was observed that some kinds of insects oscillate unperiodically, and a discrete model can explain such oscillation better than continuous one. Chaotic behaviors can also be observed in discrete systems such as sampled-data control systems and PWM control systems in engineering field even if the low dimensional case, while, in general, continuous systems also exhibit chaotic behaviors in higher dimensional case.

In an ecosystem, Volterra considered a continuous-time, predator-prey system which is an extension of a continuous-time logistic equation to the two-dimensional one. The discrete version of Volterra-Lotka type predator-prey systems is derived as follows [Hay80]:

Consider a continuous predator-prey system [May73] modeled by

$$\begin{cases} \dfrac{dx(t)}{dt} = ax(t) - bx^2(t) - cx(t)y(t) \\ \dfrac{dy(t)}{dt} = -ey(t) + c'x(t)y(t), \end{cases} \tag{4.25}$$

where $x(t)$ and $y(t)$ denote respectively the size of the prey population and that of the predator's at time t, and where parameters a, b, c, c' and e are positive constants.

Letting Δt denote the time step, then Eq.(4.25) can be transformed into the following difference equations by Euler's method:

$$\begin{cases} \dfrac{x((n+1)\Delta t) - x(n\Delta t)}{\Delta t} = ax(n\Delta t) - bx^2(n\Delta t) - cx(n\Delta t)y(n\Delta t) \\ \dfrac{y((n+1)\Delta t) - y(n\Delta t)}{\Delta t} = -ey(n\Delta t) + c'x(n\Delta t)y(n\Delta t). \end{cases} \tag{4.26}$$

Defining

$$x_n = \frac{b\Delta t}{1 + a\Delta t} x(n\Delta t) \tag{4.27}$$

and

$$y_n = \frac{c\Delta t}{1 + a\Delta t} y(n\Delta t), \tag{4.28}$$

for $\Delta t > 1/e$, Eq.(4.26) is converted into a set of difference equations:

$$\begin{cases} x_{n+1} = Ax_n(1 - x_n - y_n) \\ y_{n+1} = By_n(-1 + \dfrac{x_n}{C}), \end{cases} \tag{4.29}$$

where A, B and C are positive constants defined by

$$A = 1 + a\Delta t,\ B = e\Delta t - 1,\ C = \frac{b(e\Delta t - 1)}{c'(1 + a\Delta t)}.$$

On the other hand, for $0 < \Delta t < 1/e$, Eq.(4.26) is converted into a set of difference equations:

$$\begin{cases} x_{n+1} = Ax_n(1 - x_n - y_n) \\ y_{n+1} = By_n(1 + \dfrac{x_n}{C}), \end{cases} \tag{4.30}$$

where A, B and C are positive constants defined by

$$A = 1 + a\Delta t,\ B = 1 - e\Delta t,\ C = \frac{b(1 - e\Delta t)}{c'(1 + a\Delta t)}.$$

Chapter 5

Chaotic Behavior and Fractal Boundaries of a Discrete Predator-Prey System with a Constant Control

5.1 Introductory Remarks

Motivated by the fact that discrete predator-prey systems often exhibit chaotic behavior [May76],[BFL75],[Hay80], in this chapter and next one, stabilization problems of a class of discrete predator-prey systems are studied [SMYN87],[SMYH87],[YS90],[Yas91].

The first aim of chapters 5 and 6 is to find the control scheme which prevents the oscillation of populations observed in uncontrolled discrete predator-prey systems of the form:

$$\Sigma_I \begin{cases} x_{n+1} = Ax_n(1 - x_n - y_n) \\ y_{n+1} = By_n\left(1 + \dfrac{x_n}{C}\right) \end{cases} \tag{5.1}$$

and

$$\Sigma_{II} \begin{cases} x_{n+1} = Ax_n(1 - x_n - y_n) \\ y_{n+1} = By_n\left(-1 + \dfrac{x_n}{C}\right), \end{cases} \tag{5.2}$$

where, in both systems, x_n and y_n respectively denote the population (density) of the prey and the predator at the n-th generation, and where A and B are positive constants associated with a growth rate of the prey and the predator respectively, and C is a positive constant associated with a dependence of the predator on the prey, namely, the more C

decreases, the more the behavior of the number of predators depends on the number of preys. From the assumption that if the number of preys is zero, then the predator dies out, the parameter B satisfies that $B < 1$. These models have been already derived in Appendix 4A in Chap.4 and the fractal structure of the invariant domain, observed in the system Σ_{II}, has been already discussed in Chap.4.

The predator-prey systems Σ_I and Σ_{II} often exhibit the oscillation of populations, for example, periodic solutions, limit cycles, chaotic behavior and so on. These oscillations are not desirable from viewpoints of conservation of ecosystems, because these oscillation often drive the population into such a small number that the population dies out due to unexpected small perturbing effects, for example, a sudden change of the environment. On the other hand, if populations converge to an equilibrium with large populations, then the small perturbation does not collapse the ecosystem. Therefore, it is important to find the stabilization scheme which converts the system with oscillating behavior into the system whose solutions converge to an equilibrium.

In this thesis, it is assumed that predator-prey systems are controlled by the harvesting or supplying of predators. Furthermore, in this chapter, it is assumed that the amount of harvesting and supplying at the n-th generation is constant. Under these assumptions, the following mathematical models of controlled predator-prey systems are derived through the stock-recruitment model approach [Cla76]:

$$\Sigma_{IH} \begin{cases} x_{n+1} = Ax_n(1 - x_n - y_n) \\ y_{n+1} = By_n\left(1 + \dfrac{x_n}{C}\right) + H \end{cases} \tag{5.3}$$

and

$$\Sigma_{IIH} \begin{cases} x_{n+1} = Ax_n(1 - x_n - y_n) \\ y_{n+1} = By_n\left(-1 + \dfrac{x_n}{C}\right) + H, \end{cases} \tag{5.4}$$

where H is a constant representing the amount of the harvesting ($H < 0$) or supplying ($H > 0$) at the n-th generation. The derivation of these mathematical models are shown in Appendix 5A of this chapter.

First, in order to stabilize oscillations of populations observed in systems (5.1) and (5.2), the relation between the stability of equilibriums and the control input H are dis-

cussed in controlled systems (5.3) and (5.4). Furthermore, our investigations are extended to explore the shape of the invariant domain in controlled predator-prey systems and effects of the constant harvesting of predators on fractal boundaries are discussed.

5.2 Stabilization of Type I Predator-Prey Systems

In this section, the nonlinear dynamics of the controlled system Σ_{IH}, described by Eq.(5.3), are discussed [SMYN87].

5.2.1 Existence of Equilibriums

Dynamical properties of the solution process to Eq.(5.3) are closely related to the stability of equilibriums of the system (5.3). In order to find the control scheme which prevents the oscillation of populations, the stability of equilibriums are investigated.

Equilibriums of (5.3) are defined by

$$\begin{cases} x_{n+1} = x_n \\ y_{n+1} = y_n. \end{cases}$$

From Eq.(5.3), if the condition

$$x_n = 0 \tag{5.5}$$

or

$$y_n = 1 - \frac{1}{A} - x_n \tag{5.6}$$

holds, then $x_{n+1} = x_n$. Equations (5.5) and (5.6) give prey isoclines:

$$\ell_1 : \ x = 0 \tag{5.7}$$

and

$$\ell_2 : \ y = 1 - \frac{1}{A} - x, \tag{5.8}$$

depicted in Fig.5.1, where the axis of abscissa is the number of preys and the axis of ordinate is the number of predators. Similarly, from Eq.(5.3), the predator isocline is determined as follows:

$$\ell_3 : \ y = By\left(1 + \frac{x}{C}\right) + H. \tag{5.9}$$

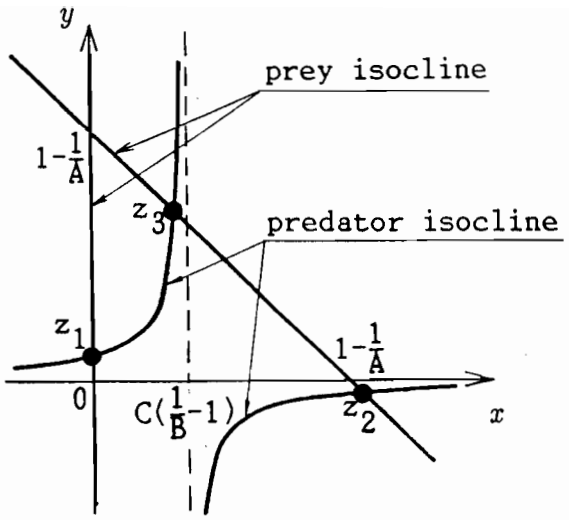

(a) $H > 0$

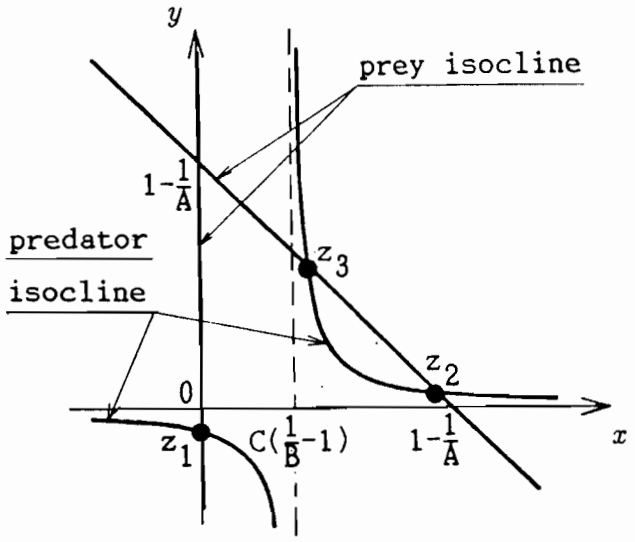

(b) $H < 0$

Figure 5.1: Predator and prey isoclines and equilibriums

Equilibriums of the system (5.3) are determined by intersections of prey isoclines and predator one. Hence, three equilibriums of (5.3) are given by

$$z_1 = \left(0, \frac{H}{1-B}\right), \tag{5.10}$$

$$z_2 = \left(\frac{1}{2}\left\{\alpha + \sqrt{\beta^2 + \frac{4CH}{B}}\right\}, \frac{1}{2}\left\{\beta - \sqrt{\beta^2 + \frac{4CH}{B}}\right\}\right) \tag{5.11}$$

$$z_3 = \left(\frac{1}{2}\left\{\alpha - \sqrt{\beta^2 + \frac{4CH}{B}}\right\}, \frac{1}{2}\left\{\beta + \sqrt{\beta^2 + \frac{4CH}{B}}\right\}\right) \tag{5.12}$$

where

$$\alpha = 1 - \frac{1}{A} + C\left(\frac{1}{B} - 1\right), \quad \beta = 1 - \frac{1}{A} - C\left(\frac{1}{B} - 1\right). \tag{5.13}$$

The predator isocline, prey isoclines and equilibriums are illustrated in Fig.5.1.

Noting that x_n and y_n present the population, our attention is concentrated on equilibriums included in the first quadrant of the x-y plane. In order that each equilibrium is included in the first quadrant of the x-y plane, it is necessary to impose the following conditions on parameters A, B, C and H:

Lemma 5.1 (E1) *The equilibrium z_1 is in the first quadrant of the x-y plane under the following conditions:*

$$0 < B < 1,\ 0 \leq H. \tag{5.14}$$

(E2) *The equilibrium z_2 is in the first quadrant of the x-y plane under the following conditions:*

$$\begin{gathered} A^* \leq A, \\ \frac{C}{1+C} < B \leq 1, \\ \frac{-B}{4C}\left\{1 - \frac{1}{A} - C\left(\frac{1}{B} - 1\right)\right\}^2 \leq H \leq 0, \end{gathered} \tag{5.15}$$

where

$$A^* = \frac{1}{1 - C\left(\frac{1}{B} - 1\right)}.$$

(E3) *The equilibrium z_3 is in the first quadrant of the x-y plane under the following conditions:*

(i) *for* $1 \leq A \leq A^*$,

$$\begin{aligned} 0 < B \leq 1, \\ 0 < H \leq \left(1 - \frac{1}{A}\right)(1 - B). \end{aligned} \tag{5.16}$$

(ii) *for* $A^* < A$,

$$\begin{aligned} \frac{C}{1+C} < B \leq 1, \\ \frac{-B}{4C}\left\{1 - \frac{1}{A} - C\left(\frac{1}{B} - 1\right)\right\}^2 \leq H \leq \left(1 - \frac{1}{A}\right)(1 - B). \end{aligned} \tag{5.17}$$

Lemma 5.1 is derived from coordinates of equilibriums z_1, z_2 and z_3 given by Eqs.(5.10) to (5.13). Straightforward calculations are omitted to write here.

5.2.2 Stability of Equilibriums

For simplicity of notations, Eq.(5.3) is rewritten by using a mapping $F_{IH} : \mathbf{R}^2 \to \mathbf{R}^2$:

$$(x_{n+1}, y_{n+1}) = F_{IH}(x_n, y_n), \tag{5.18}$$

where

$$F_{IH}(x, y) = \left(Ax(1 - x - y),\ By\left(1 + \frac{x}{C}\right) + H\right). \tag{5.19}$$

If every solutions starting from the neighborhood of the equilibrium z_i converge to z_i, then the equilibrium z_i is said to be locally asymptotically stable. An equilibrium is locally asymptotically stable, if both eigenvalues of Jacobian $DF_{IH}(x, y)$ at the equilibrium is less than 1 in the absolute value. By solving the equation for eigenvalues λ given by

$$\begin{aligned} & |DF_{IH}(x, y) - \lambda I| \\ = & \begin{vmatrix} A(1 - 2x - y) - \lambda & \frac{B}{C}y \\ -Ax & B\left(1 + \frac{x}{C}\right) - \lambda \end{vmatrix} \\ = & \lambda^2 - \left\{A(1 - 2x - y) + B\left(1 + \frac{x}{C}\right)\right\}\lambda + A(1 - 2x - y)B\left(1 + \frac{x}{C}\right) + \frac{AB}{C}xy \\ = & 0, \end{aligned}$$

it can be obtained that

$$\begin{aligned}\lambda_{\pm} &= \frac{1}{2}\left[A(1-2x-y)+B\left(1+\frac{x}{C}\right)\right. \\ &\left.\pm\sqrt{\left\{A(1-2x-y)-B\left(1+\frac{x}{C}\right)\right\}^2-\frac{4AB}{C}xy}\right].\end{aligned} \tag{5.20}$$

The stability of each equilibrium is determined by studying the condition $|\lambda_{\pm}(z_i)| < 1,\ i = 1,2,3$ under constraints (5.14) to (5.17). By carrying out calculations, results are shown below:

Theorem 5.1 (S-1) *The equilibrium z_1 is locally asymptotically stable if and only if*

$$0 < B < 1,\ \left(1-\frac{1}{A}\right)(1-B) < H < \left(1+\frac{1}{A}\right)(1-B). \tag{5.21}$$

(S-2) *The equilibrium z_2 is always unstable.*

(S-3) *The equilibrium z_3 is locally asymptotically stable if and only if*

(i) *for $AC \geq B$,*

$$0 \leq p_3 \leq \frac{C(B+3)}{AC-B}, \tag{5.22}$$

$$\begin{aligned}&\max\left\{p_3 - C\left(\frac{1}{B}-1\right),\ \left(1-\frac{2}{Ap_3}\right)\left\{p_3 - C\left(\frac{1}{B}-1\right)\right\}\right\} \\ &< q_3 < p_3 + \left(C-\frac{1}{A}\right) + \frac{C}{Ap_3}\left(\frac{1}{B}-1\right).\end{aligned} \tag{5.23}$$

(ii) *for $AC < B$,*

$$0 \leq p_3 \leq \frac{C(B-1)}{AC-B}, \tag{5.24}$$

$$p_3 - C\left(\frac{1}{B}-1\right) < q_3 < p_3 + \left(C-\frac{1}{A}\right) + \frac{C}{Ap_3}\left(\frac{1}{B}-1\right), \tag{5.25}$$

where p_3 and q_3 are the x and y coordinate of the equilibrium z_3 respectively.

5.2.3 Stabilizability

No use is made for stabilizing equilibriums z_1 or z_2, because, in the uncontrolled system (5.1), the convergence to the equilibrium solution z_1 or z_2 means the extinction of preys or predators. Hence, the useful stabilization of the system (5.1) is realized by stabilizing the equilibrium z_3.

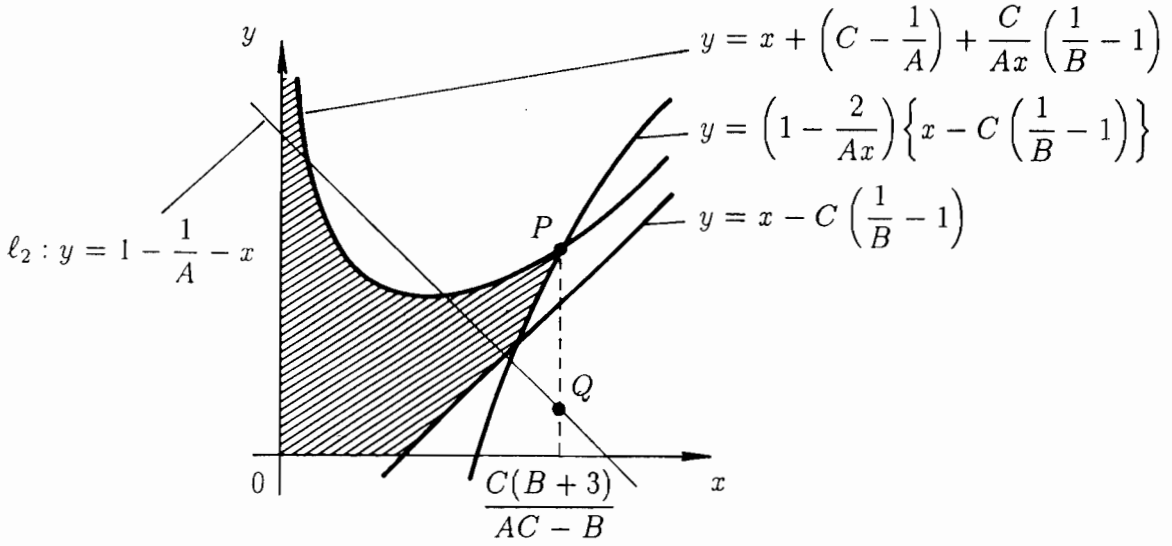

(a) $AC \geq B$

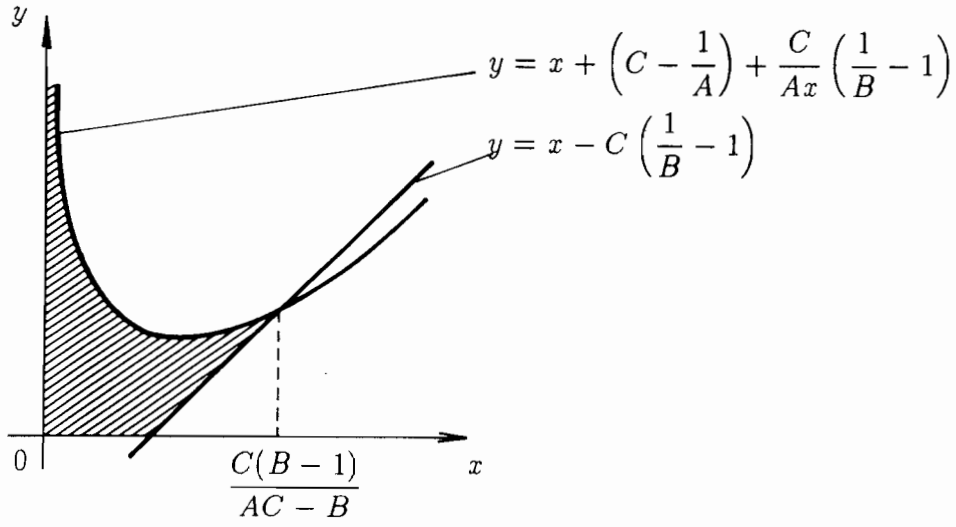

(b) $AC < B$

Figure 5.2: The stable area of the equilibrium z_3

By using conditions (5.22) to (5.25), the stable area of the equilibrium z_3 is presented in Fig.5.2. Namely, if the equilibrium z_3 is included in the hatched region of Fig.5.2, then the equilibrium z_3 is asymptotically stable.

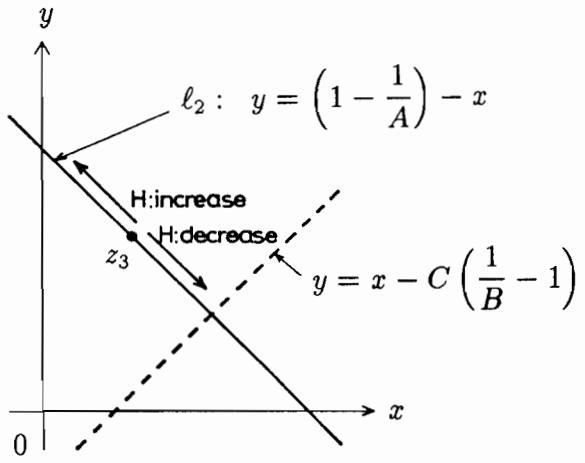

Figure 5.3: The relation between the position of z_3 and H

Note that the equilibrium z_3 is always on the prey isocline

$$\ell_2: \ y = \left(1 - \frac{1}{A}\right) - x$$

and the position of z_3 depends on the value of the control input H. As the control input H increases, the position of z_3 moves toward the y axis. In the case where

$$H = (1 - B)\left(1 - \frac{1}{A}\right),$$

the equilibrium z_3 is on the y axis (See Fig.5.3). On the other hand, as the control input H decreases, the position of the equilibrium z_3 moves toward the intersection of the prey isocline

$$\ell_2: \ y = \left(1 - \frac{1}{A}\right) - x$$

and a line

$$y = x - C\left(\frac{1}{B} - 1\right).$$

In the case where

$$H = -\frac{B}{4C}\left\{\left(1-\frac{1}{A}\right) - C\left(\frac{1}{B}-1\right)\right\}^2,$$

the equilibrium reaches the intersection. If H decreases further and

$$H < -\frac{B}{4C}\left\{\left(1-\frac{1}{A}\right) - C\left(\frac{1}{B}-1\right)\right\}^2$$

holds, then the equilibrium z_3 does not exist.

From these discussions and Fig.5.2, it is clear that if H increases, then, under appropriate $H > 0$, the equilibrium z_3 is always included in the stable area. Furthermore, if, as shown in Fig.5.2(a), the condition

the y coordinate of the point $P >$ the y coordinate of the point Q,

namely,

$$\left(1-\frac{2}{Ax}\right)\left\{x - C\left(\frac{1}{B}+1\right)\right\}\Big|_{x=\frac{C(B+3)}{AC-B}} > 1-\frac{1}{A}-x\Big|_{x=\frac{C(B+3)}{AC-B}}$$

holds, then there exists $H < 0$ such that the equilibrium z_3 is included in the stable area. In the sequel, the following theorem is obtained:

Theorem 5.2 *(i) The unstable equilibrium z_3 of the uncontrolled system (5.1) is always converted into the stable one by the supplying of predators.*
(ii) The unstable equilibrium z_3 of the uncontrolled system (5.1) is converted into the stable one by the harvesting of predators, if the following conditions hold:
(a) for $AC \geq B$,

$$\frac{2C(B+3)}{AC-B} + (C-1) + \frac{(1-B)(AC-B)}{AB(B+3)} > 0. \tag{5.26}$$

(b) for $AC < B$,

$$\frac{2C(B-1)}{AC-B} + \left(1-\frac{1}{A}\right) + C\left(\frac{1}{B}-1\right) > 0. \tag{5.27}$$

5.2.4 Invariant Domain

Noting that variables x_n and y_n are regarded as population sizes, if either x_n or y_n takes negative value, then the population is considered to have been wiped out and the system

is considered to have collapsed. Furthermore, due to the existence of the nonlinearity of the system, the asymptotic behavior of solution processes depends on the initial condition. Hence, in order to obtain conditions, under which the solution process (x_n, y_n) remains in the first quadrant of the x-y plane for all $n \geq 0$, it is necessary to find the set of initial conditions of the form:

$$\mathcal{D} = \{(x_0, y_0) : \ x_n > 0, \ y_n > 0, \ n = 0, 1, 2, \cdots\}. \tag{5.28}$$

To proceed discussions, the concept of the invariant domain is introduced:

Definition 5.1 *A subset $\mathcal{S} \subset \mathbf{R}^2$ is called the invariant domain of the function $G : \mathbf{R}^2 \to \mathbf{R}^2$, if the set $\mathcal{S}$ satisfies that*

$$G(\mathcal{S}) \subset \mathcal{S}.$$

From the definition of the invariant domain, the solution process with an initial condition included in the invariant domain does not leave from the invariant domain. Hence, it is concluded that the target set $\mathcal{D}$ is the largest invariant domain of the function F_{IH} included in the first quadrant of the x-y plane.

(a) the case where $H \geq 0$: (Supplying of predators)

Note that, from Eq.(5.3), if

$$1 - x_n - y_n < 0,$$

then $x_{n+1} < 0$. Hence, a candidate of the invariant domain $\mathcal{D}$ is given by

$$\mathcal{D}_+ = \{(x, y) : \ x > 0, \ y > 0, \ 1 - x - y > 0\}. \tag{5.29}$$

Figure 5.4 shows the shape of the candidate $\mathcal{D}_+$.

Theorem 5.3 (i) *In the case where $0 < C \leq 1$, if conditions*

$$0 < A < 4, \ \ 0 < B < \frac{4C}{(1+C)^2},$$
$$0 \leq H < \min\left\{1 - \frac{A}{4}, 1 - \frac{B(1+C)^2}{4C}\right\}$$

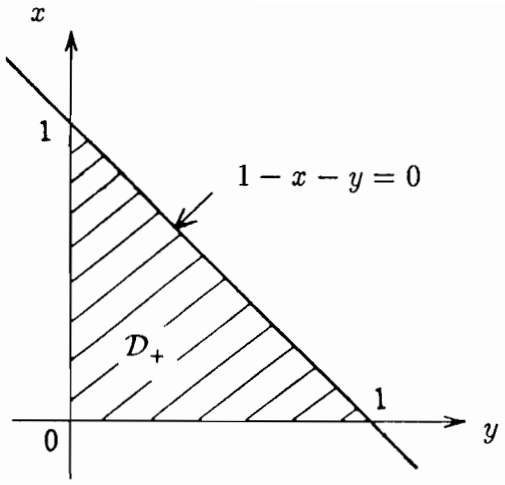

Figure 5.4: A candidate $\mathcal{D}_+$

hold, then the domain $\mathcal{D}_+$ *is the invariant domain of the function* F_{IH}.

(ii) In the case where $1 < C$, *if conditions*

$$0 < A < 4, \quad 0 < B < 1,$$
$$0 \leq H < \min\left\{1 - \frac{A}{4}, 1 - B\right\}$$

hold, then the domain $\mathcal{D}_+$ *is the invariant domain of the function* F_{IH}.

(Proof) The determinant of Jacobian of the function $F_{IH}(x, y)$ is given by

$$|DF_{IH}(x, y)| = -AB\left\{\frac{1}{C}(2x - 1)(x + C) + y\right\}.$$

(i) In the case where $0 < C \leq 1$, as shown in Fig.5.5, the candidate $\mathcal{D}_+$ is divided into two parts $\mathcal{D}_1$ and $\mathcal{D}_2$ by a curve L, defined by

$$\begin{aligned} L &= \{(x, y) : |DF_{IH}(x, y)| = 0\} \\ &= \left\{(x, y) : y = -\frac{1}{C}(2x - 1)(x + C)\right\}. \end{aligned}$$

Figure 5.6 shows the image $F_{IH}(\mathcal{D}_+)$, which satisfies

$$F_{IH}(\mathcal{D}_+) = F_{IH}(\mathcal{D}_1) = F_{IH}(\mathcal{D}_2).$$

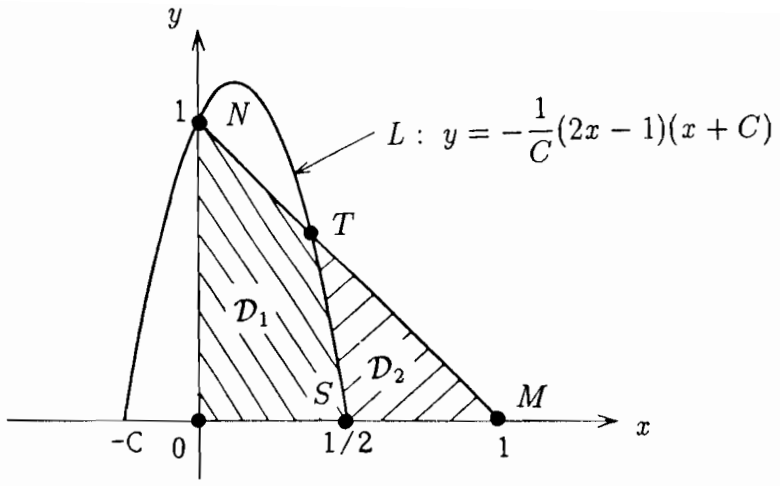

Figure 5.5: A candidate $\mathcal{D}_+ = \mathcal{D}_1 \cup \mathcal{D}_2$ and a curve L with $0 < C \leq 1$

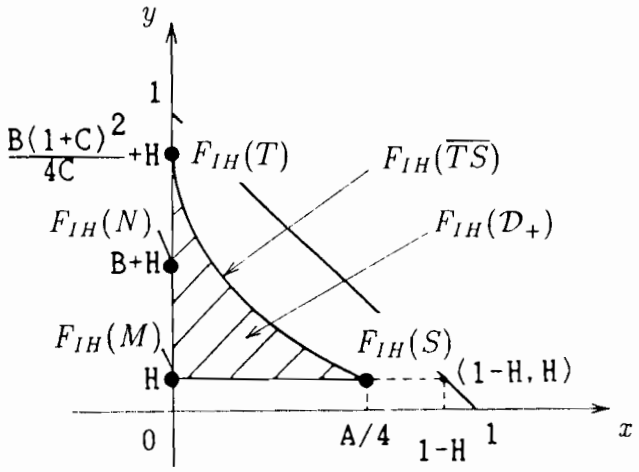

Figure 5.6: the image $F_{IH}(\mathcal{D}_+)$ of the candidate $\mathcal{D}_+$ with $H > 0$

From Fig.5.6, it is obtain that if the condition

$$F_{IH}(\overline{TS}) = \overline{F_{IH}(T)F_{IH}(S)} \subset \mathcal{D}_+$$

holds, then

$$F_{IH}(\mathcal{D}_+) \subset \mathcal{D}_+,$$

i.e., the candidate $\mathcal{D}_+$ is the invariant domain $\mathcal{D}$. Furthermore, noting that the curve $\overline{F_{IH}(T)F_{IH}(S)}$ is concave, if conditions

$$\text{the } y \text{ coordinate of the point } F_{IH}(T) < 1 \tag{5.30}$$

$$\text{the } x \text{ coordinate of the point } F_{IH}(S) < 1 - H \tag{5.31}$$

hold, then the candidate $\mathcal{D}_+$ is the invariant domain $\mathcal{D}$. From

$$F_{IH}(T) = \left(0, \frac{B(1+C)^2}{4C} + H\right)$$

and the condition (5.30), we obtain

$$H < 1 - \frac{B(1+C)^2}{4C}.$$

From

$$F_{IH}(S) = \left(\frac{A}{4}, 1 - H\right)$$

and the condition (5.31), we obtain

$$H < 1 - \frac{A}{4}.$$

Thus the proof of (i) is completed. The proof of (ii) is similar to that of (i). **(Q.E.D)**

(b) the case where $H < 0$: (Harvesting of predators)

In this case, as shown in Fig.5.7, the image $F(\mathcal{D}_+)$ of the candidate $\mathcal{D}_+$ has the area $\mathcal{B}$, which is not included in the first quadrant of the x-y plane. Hence, the invariant domain $\mathcal{D}$ is given by

$$\mathcal{D} = \mathcal{D}_+ - \bigcup_{k=1}^{\infty} F^{-k}(\mathcal{B}).$$

However, it is extremely difficult to obtain the shape of the invariant domain through theoretical analyses and numerical experiments are useful for demonstrating the shape of the invariant domain $\mathcal{D}$.

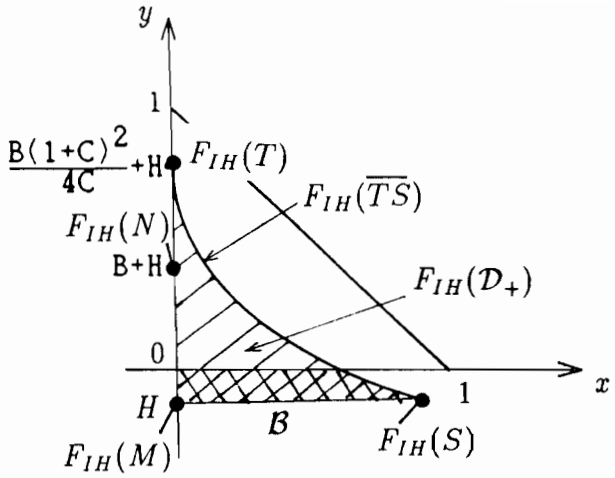

Figure 5.7: the image $F_{IH}(\mathcal{D}_+)$ of the candidate $\mathcal{D}_+$ with $H < 0$

5.2.5 Numerical Experiments

(a) Lyapunov Exponent

An important dynamical information of solution processes is provided by the Lyapunov exponent [BGS76] [SN79], defined as follows:

Definition 5.2 *(Lyapunov Exponent) In the dynamical system of the form*

$$(x_{n+1}, y_{n+1}) = F(x_n, y_n), \quad F : \mathbf{R}^2 \to \mathbf{R}^2,$$

letting $\mathbf{d}_n$ *be*

$$\mathbf{d}_n = F^n(x_0 + \delta x_0, y_0 + \delta y_0) - F^n(x_0, y_0),$$

then Lyapunov exponent Λ *is defined by*

$$\Lambda = \lim_{\substack{n \to \infty \\ \|\mathbf{d}_0\| \to 0}} \frac{1}{n} \log \frac{\|\mathbf{d}_n\|}{\|\mathbf{d}_0\|}, \tag{5.32}$$

where $\|\cdot\|$ *denotes Euclidean norm in* $\mathbf{R}^2$ *and* $\mathbf{d}_0 = (\delta x_0, \delta y_0)$ *is a two-dimensional vector.*

From the definition (5.32), it can be obtained that, for a sufficiently large n,

$$\|F^n(x_0 + \delta x_0, y_0 + \delta y_0) - F^n(x_0, y_0)\| \simeq \|(\delta x_0, \delta y_0)\| \cdot \exp(n\Lambda).$$

Therefore, if $\Lambda > 0$, the difference between $F^n(x_0 + \delta x_0, y_0 + \delta y_0)$ and $F^n(x_0, y_0)$ grows exponentially with increasing n. This phenomenon is called *sensitive dependence on initial condition* and is one of qualitative features presented by chaotic behavior.

As shown in Appendix 5B, the Lyapunov exponent Λ is approximately calculated by

$$\Lambda \simeq \frac{1}{n} \sum_{i=0}^{n-1} \log \|DF(x_i, y_i) \cdot \mathbf{e}_i\|, \tag{5.33}$$

where

$$\mathbf{e}_{i+1} = \frac{DF(x_i, y_i) \cdot \mathbf{e}_i}{\|DF(x_i, y_i) \cdot \mathbf{e}_i\|}$$

and $\mathbf{e}_0$ is a two-dimensional vector satisfying $\|\mathbf{e}_0\| = 1$.

(b) Asymptotic Behavior and Invariant Domains

Digital computer experiments are carried out in Eq.(5.3) for a set of fixed parameter values A, B and C and various values of the control term H. Parameters A, B and C are set as $A = 3.9$, $B = 0.3$ and $C = 0.1$ respectively and the control term H decreases from 0 to -0.16. Successive 50000 iterations $\{(x_n, y_n) : 5001 \leq n \leq 55000\}$, produced by Eq.(5.3), are plotted in Figs.5.8(a) to 5.11(a) for different $H \leq 0$, where in each figure the initial condition (x_0, y_0) is set as $(x_0, y_0) = (0.5, 0.25)$ and where the first 5000 iterations are regarded as a transient path and are not plotted.

Since, from discussions in subsec.5.2.4, the invariant domain $\mathcal{D}$ can not analytically be obtained expect for $H = 0$, the numerical procedure shows the shape of the invariant domain $\mathcal{D}$ which is shown in Fig.5.8(b) to 5.11(b) respectively. In Figs.5.8(b) and 5.11(b), the solution processes, starting from the blank region, eventually escape from the first quadrant of the x-y plane.

(i) Figure 5.11(a) illustrates the attractor of the system (5.3) with $H = 0$. The equilibrium z_3 is given by $z_3 = (0.2333\cdots,\ 0.5102\cdots)$ and the absolute value of complex eigenvalues at z_3 are calculated as

$$|\lambda(z_3)| = 1.2177 > 1,$$

which shows the instability of z_3. In this case, Marotto's Theorem [Mar78] can be applied and the existence of chaos is assured [SMYN87]. From Eq.(5.33), Lyapunov exponent Λ

is numerically calculated from a sample run as $\Lambda = 0.1394 > 0$, which means chaotic motions appear from Eq.(5.3). Figure 5.8(b) plots the invariant domain $\mathcal{D}$, which is a set $\mathcal{D}_+$ defined by Eq.(5.29).

(ii) The existence of negative control input $H = -0.07$ makes the invariant domain reduced from $\mathcal{D}_+ = \{(x, y) : \ x > 0, \ y > 0, \ 1 - x - y > 0\}$ to the black area shown in Fig.5.9(b). The equilibrium $z_3 = (0.2474\cdots, 0.4961\cdots)$ is unstable, which is assured by the absolute value of eigenvalues at z_3 as follows:

$$|\lambda(z_3)| = 1.1844 > 1.$$

Lyapunov exponent is numerically calculated as $\Lambda = 0.0884 > 0$. Hence, the (x_n, y_n)-process exhibits chaotic motions. It should be noted that since (x_n, y_n) starting from the neighborhood of z_3 never return back to z_3, namely, there does not exist a snap-back repeller. Therefore, in this case, chaos is examined through numerically calculated Lyapunov exponent.

(iii) As H decreases, the invariant domain $\mathcal{D}$ becomes smaller, as shown in Fig.5.10(b) and the asymptotic behavior shows a closed curve called limit cycle, around the equilibrium $z_3 = (0.2602\cdots, 0.4833\cdots)$ (Fig.5.10(a)). In the case where a limit cycle appears, Lyapunov exponent is numerically calculated as $\Lambda = 0$.

(iv) For $H < -0.152394$, eigenvalues at the equilibrium z_3 is less than 1 in the absolute value. Therefore the equilibrium z_3 is asymptotically stable and solution processes starting from the black region in Fig.5.11(b) converge to equilibrium z_3. In the case where $H = -0.16$, the position of the equilibrium $z_3 = (0.2668\cdots, 0.4766\cdots)$ is plotted in Fig.5.11(a). Numerically calculated absolute value of eigenvalues $|\lambda(z_3)| = 0.9603 < 1$ and Lyapunov exponent $\Lambda = -0.0404 < 0$ both indicate that the equilibrium z_3 is asymptotically stable.

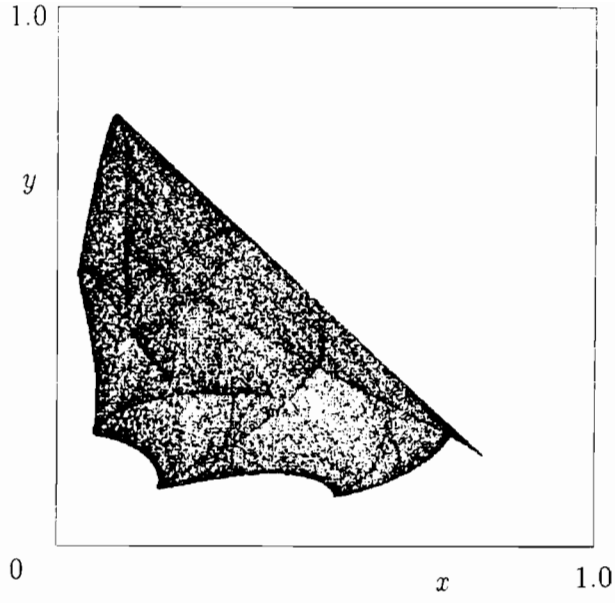

(a) Asymptotic behavior

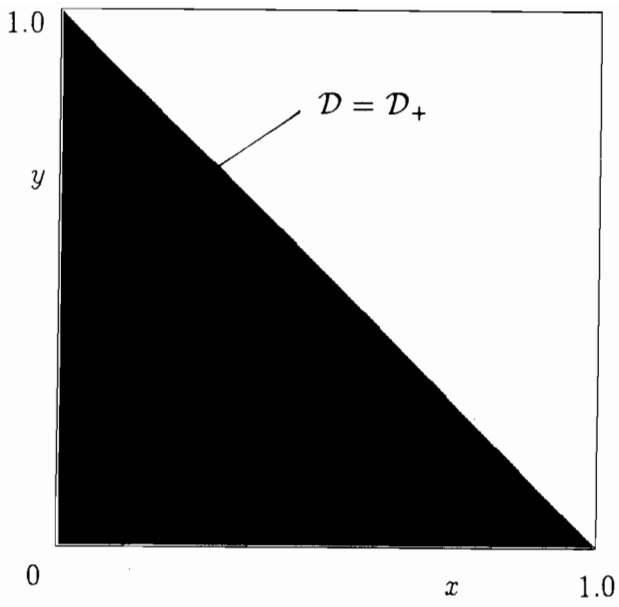

(b) Invariant domain

Figure 5.8: Asymptotic behavior and invariant domain of the uncontrolled system Σ_I with $A = 3.9$, $B = 0.3$ and $C = 0.1$

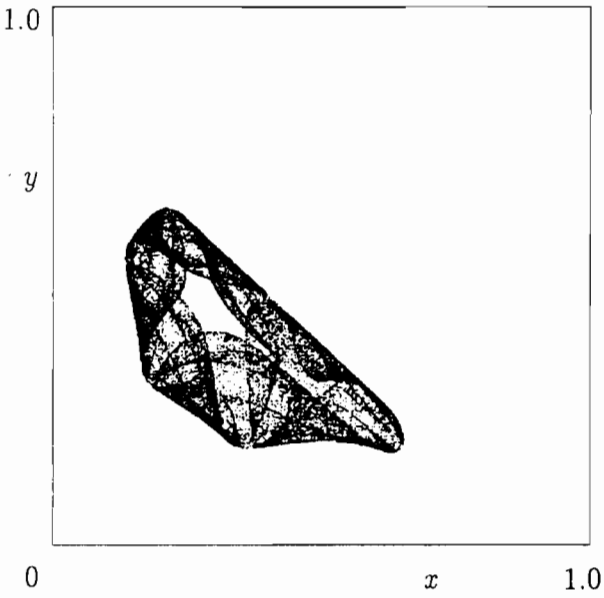

(a) Asymptotic behavior

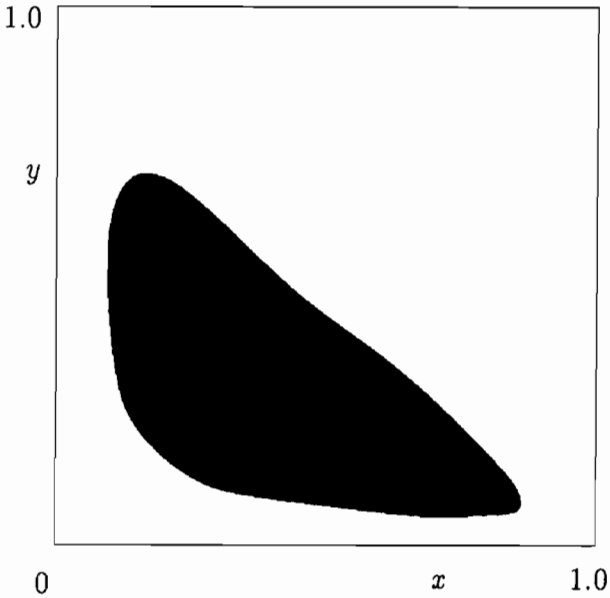

(b) Invariant domain

Figure 5.9: Asymptotic behavior and invariant domain of the controlled system Σ_{IH} with $A = 3.9$, $B = 0.3$, $C = 0.1$ and $H = -0.07$

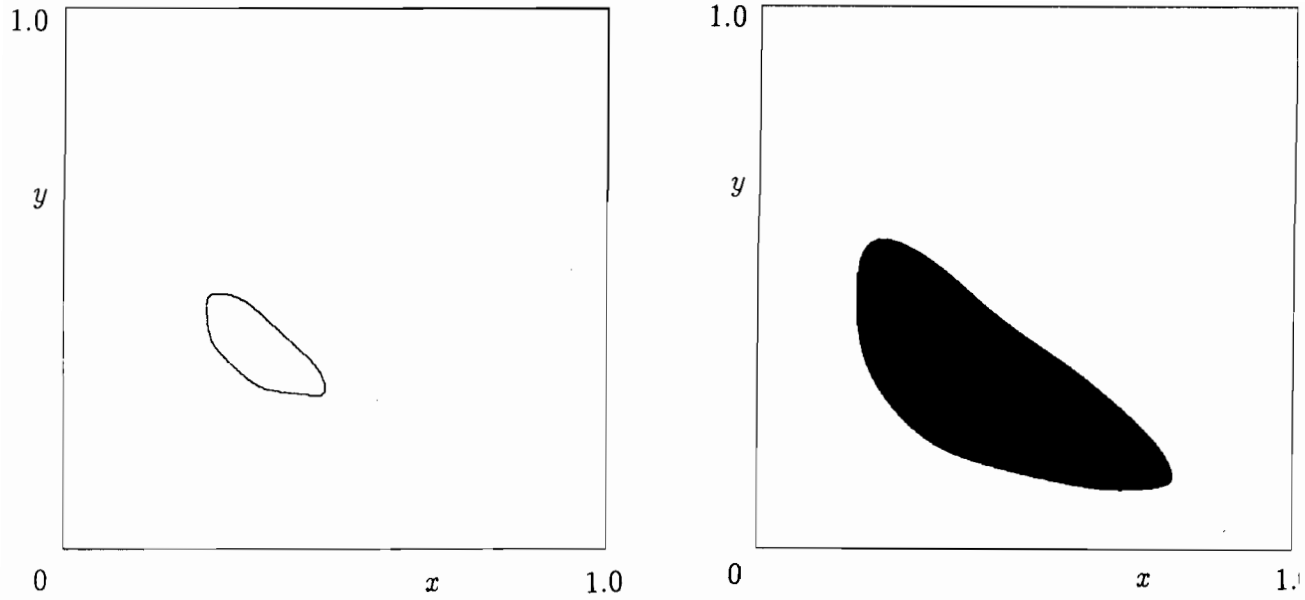

(a) Asymptotic behavior (b) Invariant domain

Figure 5.10: Asymptotic behavior and invariant domain of the controlled system Σ_{IH} with $A = 3.9$, $B = 0.3$, $C = 0.1$ and $H = -0.13$

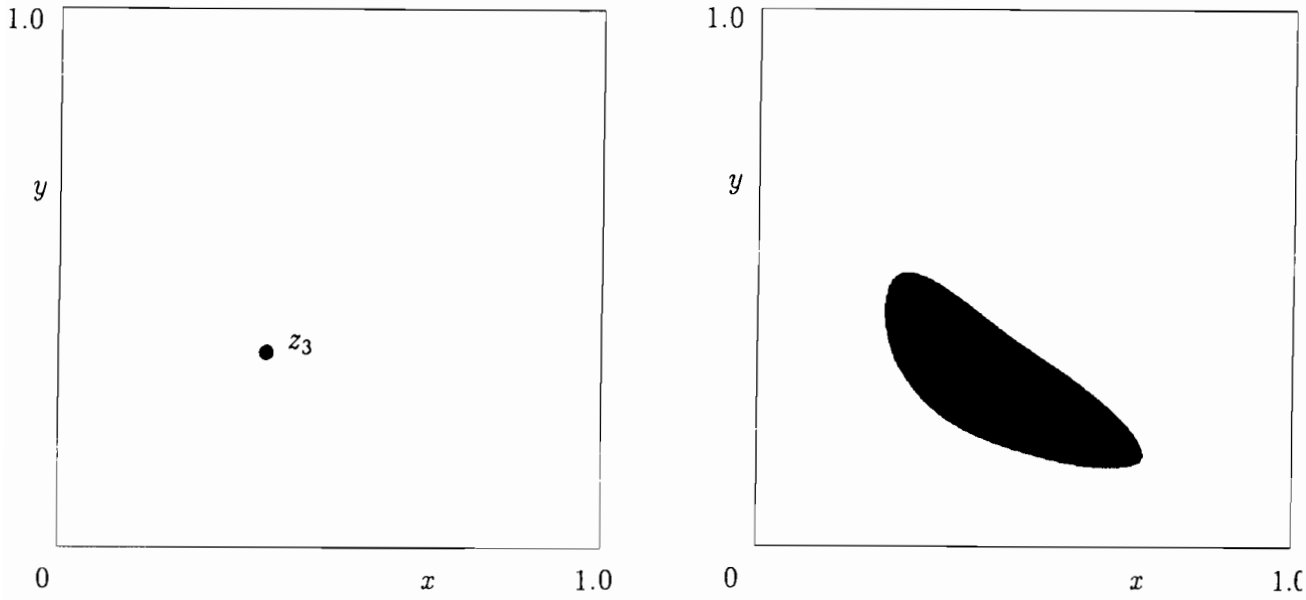

(a) Asymptotic behavior (b) Invariant domain

Figure 5.11: Asymptotic behavior and invariant domain of the controlled system Σ_{IH} with $A = 3.9$, $B = 0.3$, $C = 0.1$ and $H = -0.16$

5.3 Stabilization of Type II Predator-Prey Systems

In this section, our attention is concentrated on the nonlinear dynamics of the type II predator-prey system, described by Eq.(5.4) [YS90], [Yas91]. A topic of this section is effects of the constant harvesting of predators on fractal boundaries of the invariant domain, observed in the system (5.4).

5.3.1 Location of Equilibriums

The controlled system (5.4) has the following three equilibriums

$$\begin{aligned} z_1 &= \left(0, \frac{-H}{1+B}\right), \\ z_2 &= \left(\frac{1}{2}\left(\alpha + \sqrt{\beta^2 + \frac{4CH}{B}}\right), \frac{1}{2}\left(\beta - \sqrt{\beta^2 + \frac{4CH}{B}}\right)\right), \\ z_3 &= \left(\frac{1}{2}\left(\alpha - \sqrt{\beta^2 + \frac{4CH}{B}}\right), \frac{1}{2}\left(\beta + \sqrt{\beta^2 + \frac{4CH}{B}}\right)\right), \end{aligned} \tag{5.34}$$

where

$$\alpha = 1 - \frac{1}{A} + C\left(\frac{1}{B} + 1\right), \quad \beta = 1 - \frac{1}{A} - C\left(\frac{1}{B} + 1\right). \tag{5.35}$$

5.3.2 Stability of Equilibriums

The useful stabilization is carried out by using the equilibrium z_3. The stability of the equilibrium z_3 of the controlled system Σ_{IIH} is examined by the following theorem:

Theorem 5.4 *The equilibrium point z_3 of the controlled system Σ_{IIH} is locally asymptotically stable, if and only if*

(i) *for $AC \geq B$,*

$$0 < p_3 < \frac{C(3-B)}{AC-B}, \tag{5.36}$$

$$\begin{aligned} \max\left\{p_3 - C\left(\frac{1}{B}+1\right), \left(1 - \frac{2}{Ap_3}\right)\left\{p_3 + C\left(\frac{1}{B}-1\right)\right\}\right\} \\ < q_3 < p_3 - \left(C + \frac{1}{A}\right) + \frac{C}{Ap_3}\left(\frac{1}{B}+1\right) \end{aligned} \tag{5.37}$$

(ii) *for* $AC < B$,

$$0 < p_3 < \frac{C(B+1)}{B - AC}, \tag{5.38}$$

$$p_3 - C\left(\frac{1}{B}+1\right) < q_3 < p_3 - \left(C + \frac{1}{A}\right) + \frac{C}{Ap_3}\left(\frac{1}{B}+1\right), \tag{5.39}$$

where p_3 *and* q_3 *are the* x *and* y *coordinates of* z_3 *respectively.*

(Proof) Eigenvalues of Jacobian $DF_{\mathit{II}H}(x,y)$ at the equilibrium z_3 are calculated by

$$\begin{aligned}\lambda_{\pm}(z_3) &= \frac{1}{2}\left[A(1-2p_3-q_3) + B\left(-1+\frac{p_3}{C}\right)\right. \\ &\left. \pm\sqrt{\left\{A(1-2p_3-q_3) - B\left(-1+\frac{p_3}{C}\right)\right\}^2 - \frac{4AB}{C}p_3q_3}\right],\end{aligned} \tag{5.40}$$

where p_3 and q_3 are the x and y coordinates of z_3 respectively. From Eq.(5.34), it is obtained that p_3 and q_3 satisfy that

$$q_3 = 1 - \frac{1}{A} - p_3. \tag{5.41}$$

Substituting Eq.(5.41) into Eq.(5.40), Equation (5.40) becomes

$$\lambda_{\pm}(z_3) = \frac{1}{2}\left[1 - Ap_3 + B\left(-1+\frac{p_3}{C}\right) \pm \sqrt{\left\{(1 - Ap_3 - B\left(-1+\frac{p_3}{C}\right)\right\}^2 - \frac{4AB}{C}p_3q_3}\right]. \tag{5.42}$$

Noting that z_3 is asymptotically stable, if and only if $|\lambda_{\pm}(z_3)| < 1$, conditions in this theorem are derived from Eq.(5.42). **(Q.E.D.)**

From Theorem 5.4, the equilibrium z_3 is asymptotically stable, if and only if z_3 is included in the hatched region in Fig.5.12. This hatched region, determined by conditions (5.36) to (5.39), is called the stable area of the equilibrium z_3. If the equilibrium

$$z_{30} = z_3|_{H=0} = \left(C\left(\frac{1}{B}+1\right), 1 - \frac{1}{A} - C\left(\frac{1}{B}+1\right)\right), \tag{5.43}$$

of the uncontrolled system Σ_{II} is located outside the stable area as shown in Fig.5.12, then we need the constant control, by which z_{30} is transposed into the hatched region. On the other hand, if the equilibrium z_{30} is included in the stable area, then the system dose not require any control.

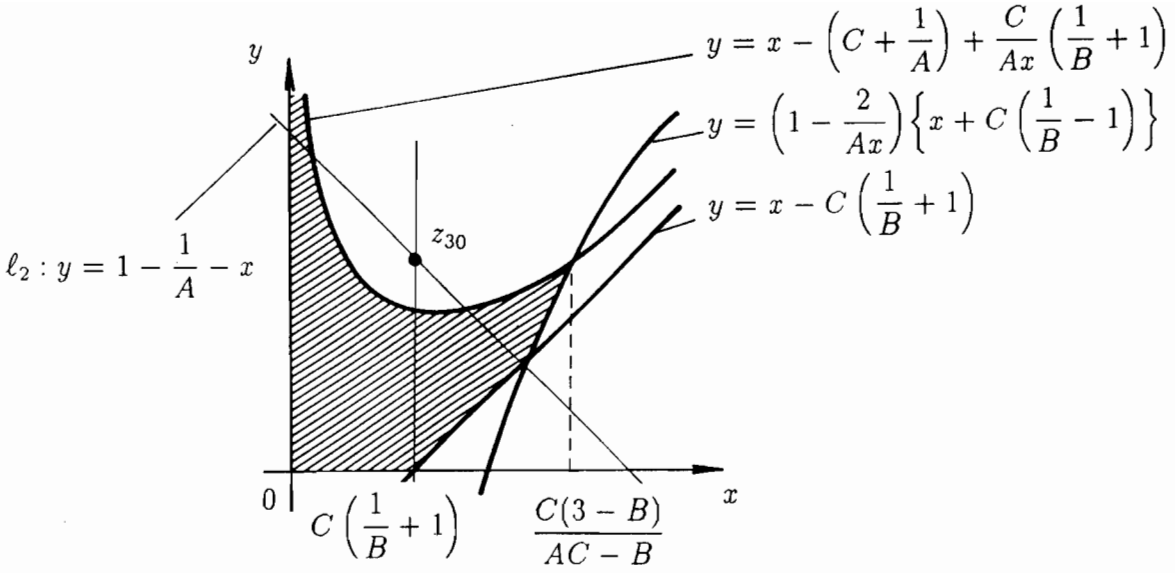

(a) $AC \geq B$

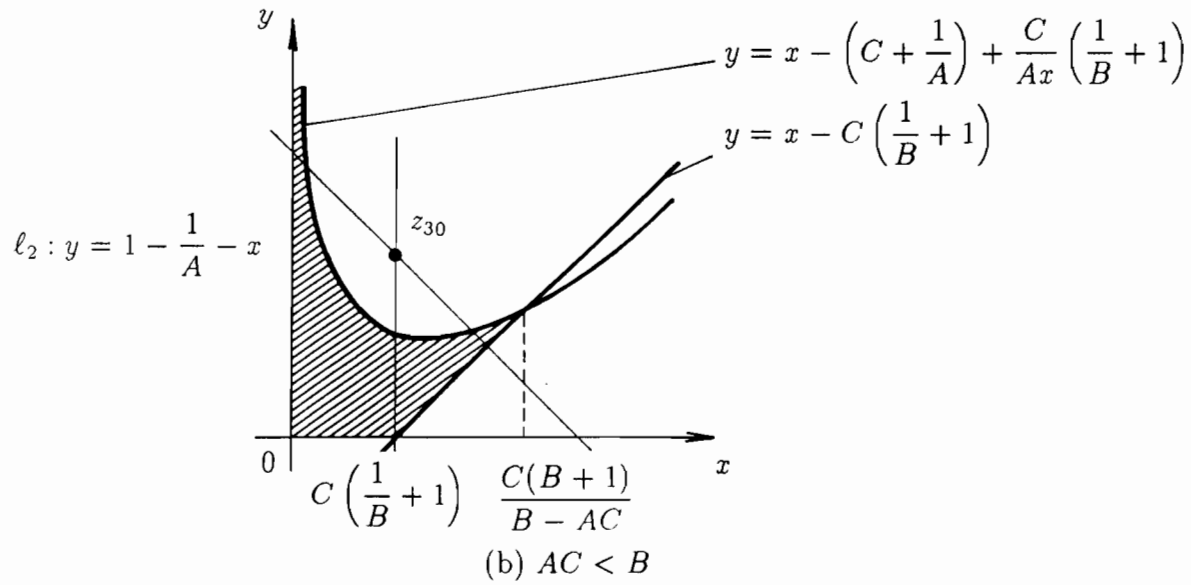

(b) $AC < B$

Figure 5.12: The stable area of the equilibrium z_3 of the controlled system Σ_{IIH}

5.3.3 Effects of Constant Harvesting on Fractal Boundaries

The system Σ_{IIH} with constant control is described by the nonlinear function,

$$F_{IIH}(x,y) = \left(Ax(1-x-y),\ \ By\left(-1+\frac{x}{C}\right)+H\right). \tag{5.44}$$

For the controlled system Σ_{IIH} with constant control, the domain

$$\mathcal{D}_- = \{(x,y):\ x > C,\ y > 0,\ Ax(1-x-y) > C\},$$

defined by Eq.(4.9), is adopted once again as a candidate of the invariant domain

$$\mathcal{D} = \{(x_0,y_0) : x_n > 0,\ y_n > 0,\ n = 0,1,2,\cdots\}.$$

In the case where $H < 0$, instead of Fig.4.6, the image $F_{IIH}(\mathcal{D}_-)$ becomes as shown in Fig.5.13. Due to the existence of the constant control the cross-hatched area $\mathcal{A}_h$ and the hatched area $\mathcal{B}_h$, which are not included in $\mathcal{D}_-$, appear.

For any $k \geq 1$, solution processes with initial conditions included in $F_{IIH}^{-k}(\mathcal{A}_h)$ or $F_{IIH}^{-k}(\mathcal{B}_h)$ are eventually escape from the first quadrant of the x-y plane. Therefore, the invariant domain $\mathcal{D}$ is given by

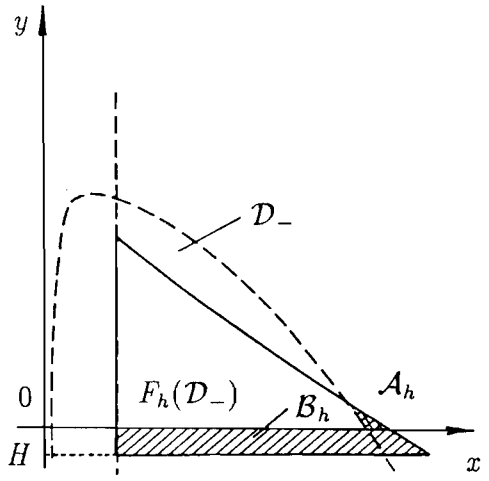

Figure 5.13: Image $F_{IIH}(\mathcal{D}_-)$ with regions $\mathcal{A}_h$ and $\mathcal{B}_h$

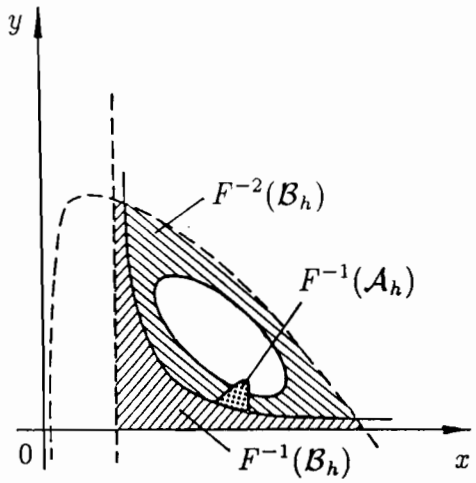

Figure 5.14: Inverse image $F_{\mathit{II}H}^{-1}(\mathcal{A}_h)$ and $F_{\mathit{II}H}^{-1}(\mathcal{B}_h)$

$$\mathcal{D} = \mathcal{D}_- - \bigcup_{k=1}^{\infty} F_{\mathit{II}H}^{-k}(\mathcal{A}_h) - \bigcup_{k=1}^{\infty} F_{\mathit{II}H}^{-k}(\mathcal{B}_h).$$

Thus, the following facts are obtained:

(i) For any $H > 0$, it can be shown that

$$F_{\mathit{II}H}^{-1}(\mathcal{A}_h) \subset F^{-1}(\mathcal{A}).$$

(ii) As shown in Fig.5.14, $F_{\mathit{II}H}^{-k}(\mathcal{B}_h), k = 1, 2, \cdots$ produce smooth boundaries and the tongue $F_{\mathit{II}H}^{-k}(\mathcal{A}_h)$ is buried in $F_{\mathit{II}H}^{-m}(\mathcal{B}_h), m > k$.

In view of the above two facts, it is concluded that in the controlled system $\Sigma_{\mathit{II}H}$, if the amount of the constant harvesting of predators H increases, fractal boundaries of the invariant domain $\mathcal{D}$ become smooth, i.e., the complexity of fractal boundaries decreases.

5.3.4 Numerical Experiments

To show the validity of results presented in the previous subsections 5.3.2 and 5.3.3, numerical experiments are carried out. As a typical example, parameters A, B and C in the system Σ_{II} are selected as $A = 3.9$, $B = 0.5$ and $C = 0.12$. Then, in the uncontrolled

system Σ_{II}, the equilibrium $z_3 = (0.36,\ 0.384\cdots)$ is unstable and the solution process exhibits chaotic behavior (See Fig.5.15(a)). Furthermore, conditions in Theorem 4.1 hold and the invariant domain $\mathcal{D}$ exhibits fractal boundaries, which is plotted in Fig.5.15(b). The solution process with the initial condition included in the dark region exhibits chaotic behavior. The white region of Fig.5.15(b) is the set of points,which eventually escape from the first quadrant of the x-y plane.

In view of Theorem 5.4, the constant harvesting of predators with the amount of the harvesting $H = -0.142$ is considered, in order to stabilize the chaotic behavior of the uncontrolled system. Under the constant harvesting $H = -0.142$, the equilibrium $z_3 = (0.500\cdots,\ 0.244\cdots)$ is included in the stable area depicted in Fig.5.12 and is asymptotically stable. Figure 5.16(b) plots the invariant domain $\mathcal{D}$ of the controlled system Σ_{IIH} with $H = -0.142$, where the boundary is smooth. Solution processes originating in the dark region are attracted to the equilibrium z_3 (Fig.5.16(a)). Figure 5.16(b) reveals that under the constant harvesting, fractal boundaries disappear and the small invariant domain with smooth boundaries appear.

5.4 Concluding Remarks

In this chapter, solution behavior of controlled predator-prey systems Σ_{IH} and Σ_{IIH} have been studied. The control term was adopted as the harvesting or supplying of predators in the system. Dynamics of solution processes were theoretically analyzed through the stability analysis of equilibriums and, with the aid of the concept of Lyapunov exponents, chaos, limit cycle and asymptotically stable equilibrium were also numerically examined. Through these investigation, it has been shown that both constant harvesting or supplying of predators are useful for preventing the oscillation of populations.

Furthermore, our investigations has been extended to the shape of the invariant domain of the system. Especially, the effect of the constant harvesting on fractal boundaries of the invariant domain, observed in the system Σ_{II}, are discussed and the following results are demonstrated: under the constant harvesting, fractal boundaries of the invariant

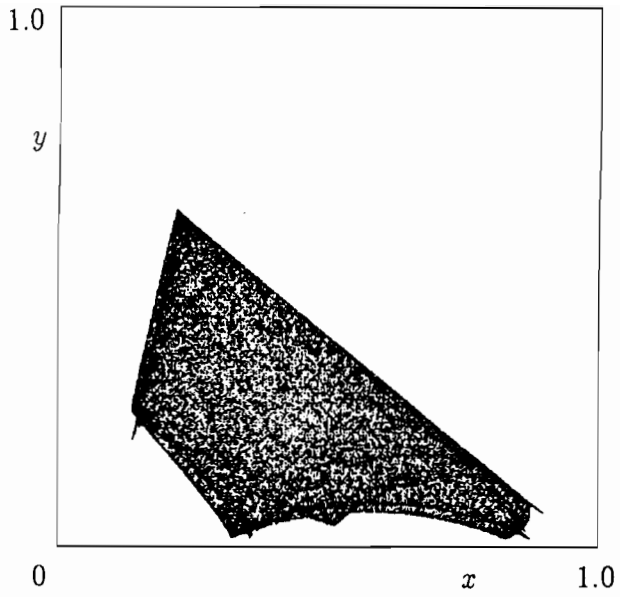

(a) Strange attractor

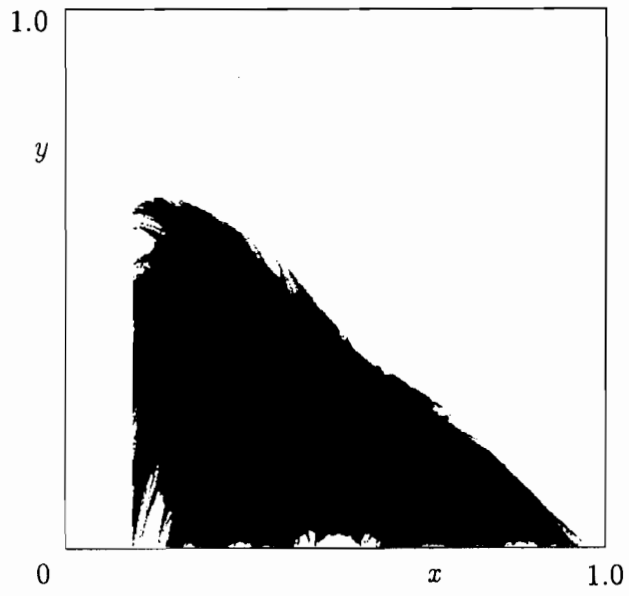

(b) Invariant domain

Figure 5.15: Strange attractor and invariant domain with fractal boundaries of the uncontrolled system Σ_{II} where $A = 3.9$, $B = 0.5$ and $C = 0.12$

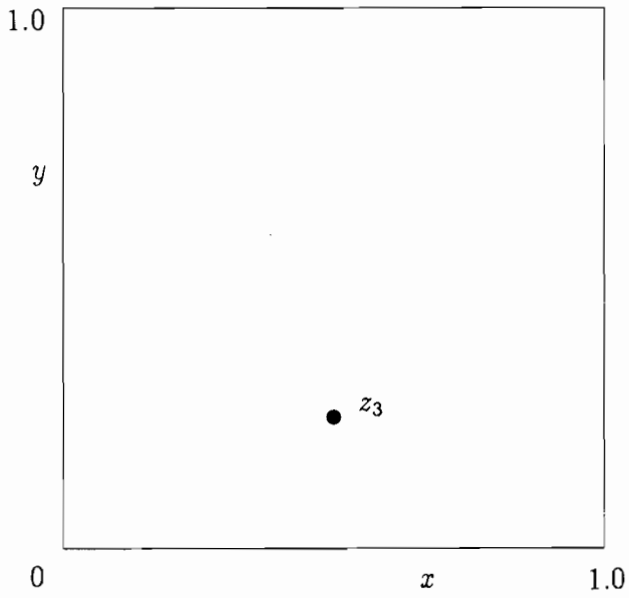

(a) Asymptotically stable equilibrium z_3

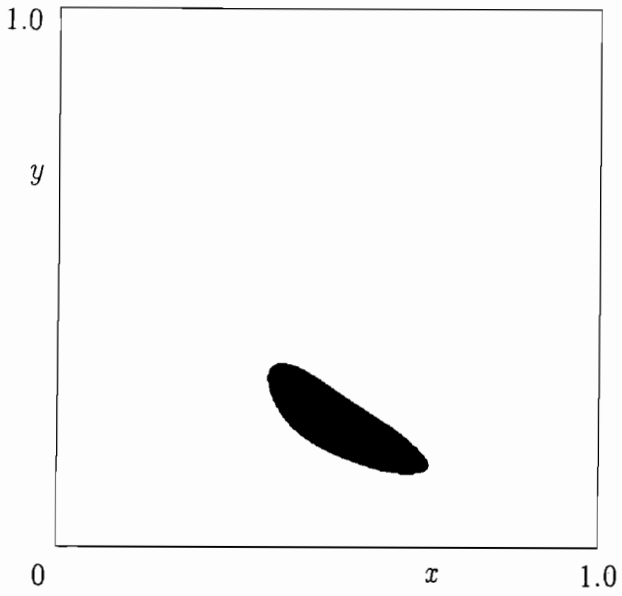

(b) Invariant domain

Figure 5.16: Asymptotically stable equilibrium z_3 and invariant domain with smooth boundaries of the controlled system Σ_{IH} where $A = 3.9$, $B = 0.5$, $C = 0.12$ and $H = -0.142$

domain become smooth, but the invariant domain becomes small, as the amount of the harvesting of predators increases. Hence, it is easy to decide the coexistence or extinction of population, however there exist many initial conditions led to the extinction of populations.

Appendix 5A: Derivation of Controlled Systems

For convenience of descriptions, introducing the nonlinear functions $f : \mathbf{R}^2 \to \mathbf{R}^1$ and $g : \mathbf{R}^2 \to \mathbf{R}^1$ defined by

$$f(x, y) = Ax(1 - x - y), \tag{5.45}$$

$$g(x, y) = By\left(1 + \frac{x}{C}\right), \tag{5.46}$$

the uncontrolled system (5.1) is rewritten by

$$\begin{cases} x_{n+1} = f(x_n, y_n) \\ y_{n+1} = g(x_n, y_n). \end{cases} \tag{5.47}$$

In the case where, at the n-th generation, the harvesting or supplying of predators H_n changes the population of predators y_n into z_n:

$$z_n = y_n + H_n, \tag{5.48}$$

the number of predators at the (n+1)-st generation y_{n+1} is determined by the number of preys x_n and predators z_n at the n-th generation:

$$y_{n+1} = g(x_n, z_n). \tag{5.49}$$

Furthermore, if the harvesting or supplying of predators are carried out before predators eat preys, then the population of predators which eat prey is given by $z_n = y_n + H_n$. Namely, x_{n+1} depends on x_n and z_n:

$$x_{n+1} = f(x_n, z_n). \tag{5.50}$$

Noting that

$$z_{n+1} = y_{n+1} + H_{n+1} = g(x_n, z_n) + H_{n+1}$$

and combining Eqs.(5.50), we obtain the controlled system of the form

$$\begin{cases} x_{n+1} = f(x_n, z_n) \\ z_{n+1} = g(x_n, z_n) + H_{n+1}. \end{cases} \tag{5.51}$$

In this chapter, it has been assumed that the amount of the harvesting or supplying of predators is constant, i.e., $H_n = H$. In the sequel, by using Eqs.(5.45) and (5.46) and by converting z_n into y_n, Equation (5.51) yields the controlled system of the form:

$$\Sigma_{IH} \begin{cases} x_{n+1} = Ax_n(1 - x_n - y_n) \\ y_{n+1} = By_n \left(1 + \dfrac{x_n}{C}\right) + H. \end{cases}$$

The similar procedure brings us the controlled system $\Sigma_{\mathit{II}H}$.

In the case where the amount of the harvesting or supplying of predators is proportional to the number of predators y_n, i.e., $H_n = Ey_n$, substituting

$$H_{n+1} = Ey_{n+1} = Eg(x_n, z_n) \tag{5.52}$$

into Eq.(5.51), we obtain

$$\begin{cases} x_{n+1} = f(x_n, z_n) \\ z_{n+1} = (1 + E)g(x_n, z_n). \end{cases} \tag{5.53}$$

By using Eqs.(5.45) and (5.46) and by converting z_n into y_n, Equation (5.53) yields the controlled system of the form:

$$\Sigma_{IE} \begin{cases} x_{n+1} = Ax_n(1 - x_n - y_n) \\ y_{n+1} = B(1 + E)y_n \left(1 + \dfrac{x_n}{C}\right) \end{cases}$$

and

$$\Sigma_{\mathit{II}E} \begin{cases} x_{n+1} = Ax_n(1 - x_n - y_n) \\ y_{n+1} = B(1 + E)y_n \left(-1 + \dfrac{x_n}{C}\right). \end{cases}$$

These models are explored in the next chapter 6.

Appendix 5B: Numerical Technique for Calculating Lyapunov Exponent

Noting that

$$\frac{\|\mathbf{d}_n\|}{\|\mathbf{d}_0\|} = \frac{\|\mathbf{d}_1\|}{\|\mathbf{d}_0\|} \cdot \frac{\|\mathbf{d}_2\|}{\|\mathbf{d}_1\|} \cdot \frac{\|\mathbf{d}_3\|}{\|\mathbf{d}_2\|} \cdots \frac{\|\mathbf{d}_n\|}{\|\mathbf{d}_{n-1}\|},$$

the definition (5.32) of Lyapunov exponent can be rewritten by

$$\Lambda = \lim_{\substack{n \to 0 \\ \|\mathbf{d}_0\| \to 0}} \frac{1}{n} \sum_{i=0}^{n-1} \log \frac{\|\mathbf{d}_{i+1}\|}{\|\mathbf{d}_i\|}. \tag{5.54}$$

From the definition of $\mathbf{d}_n$, it follows that

$$\begin{aligned} \mathbf{d}_{i+1} &= F^{i+1}(x_0 + \delta x_0, y_0 + \delta y_0) - F^{i+1}(x_0, y_0) \\ &= F(x_i + \delta x_i, y_i + \delta y_i) - F(x_i, y_i) \\ &= F(x_i + \delta x_i, y_i + \delta y_i) - F(x_i, y_i + \delta y_i) \\ &+ F(x_i, y_i + \delta y_i) - F(x_i, y_i). \end{aligned} \tag{5.55}$$

Since δx_i and δy_i are sufficiently small, the following approximations are obtained:

$$\begin{aligned} F(x_i + \delta x_i, y_i + \delta y_i) - F(x_i, y_i + \delta y_i) &= \frac{\partial F}{\partial x}(x_i, y_i) \cdot \delta x_i, \\ F(x_i, y_i + \delta y_i) - F(x_i, y_i) &= \frac{\partial F}{\partial y}(x_i, y_i) \cdot \delta y_i. \end{aligned} \tag{5.56}$$

Substituting Eqs.(5.56) into Eq.(5.55), it follows that

$$\mathbf{d}_{i+1} = \frac{\partial F}{\partial x}(x_i, y_i) \cdot \delta x_i + \frac{\partial F}{\partial y}(x_i, y_i) \cdot \delta y_i = DF(x_i, y_i) \cdot \mathbf{d}_i. \tag{5.57}$$

Letting $\mathbf{e}_i = \mathbf{d}_i / \|\mathbf{d}_i\|$, Equation (5.57) brings us

$$\begin{aligned} \|\mathbf{d}_{i+1}\| &= \|DF(x_i, y_i) \cdot \mathbf{d}_i\| \\ &= \|DF(x_i, y_i) \cdot \mathbf{e}_i \cdot \|\mathbf{d}_i\|\| \\ &= \|DF(x_i, y_i) \cdot \mathbf{e}_i\| \cdot \|\mathbf{d}_i\|. \end{aligned} \tag{5.58}$$

Substituting Eq.(5.58) into (5.54), we obtain Eq.(5.33).

Chapter 6

Chaotic Behavior and Fractal Boundaries of a Discrete Predator-Prey System with a Constant Rate Control

6.1 Introductory Remarks

In this chapter, it is assumed that the predator-prey systems are controlled by the harvesting or supplying of predators, and furthermore, assumed that the amount of harvesting or supplying at the n-th generation is proportional to the number of predators at the n-th generation. Under these assumptions, in Appendix 5A, the following mathematical models of controlled predator-prey systems have been already derived through the stock-recruitment model approach:

$$\Sigma_{IE} \begin{cases} x_{n+1} = Ax_n(1 - x_n - y_n) \\ y_{n+1} = B(1+E)y_n(1 + \dfrac{x_n}{C}) \end{cases} \tag{6.1}$$

and

$$\Sigma_{IIE} \begin{cases} x_{n+1} = Ax_n(1 - x_n - y_n) \\ y_{n+1} = B(1+E)y_n(-1 + \dfrac{x_n}{C}). \end{cases} \tag{6.2}$$

If a constant E is negative, then the predator is harvested, namely, the parameter E denotes the effort of harvesting and the amount of harvest Ey_n is proportional to the number of predators under a constant effort harvesting. Since the amount of harvest can not exceed the number of predators, the parameter E satisfies that $E > -1$.

Dynamics of the systems (6.1) and (6.2) depend on a constant E. In this chapter, the influence of the constant rate harvesting or supplying of predators on the behavior of the population number is investigated and the control scheme, which prevents oscillations of population number, is discussed [SMYH87], [YS90].

First, in order to stabilize oscillations of populations observed in systems (6.1) and (6.2), the relation between the stability of equilibriums and the parameter E is discussed. Furthermore, our investigations are extended to the shape of the invariant domain corresponding to controlled predator-prey systems and influences of the constant rate harvesting of predators on fractal boundaries are clarified [YS90], [Yas91].

6.2 Stabilization of Type I Predator-Prey Systems

6.2.1 Existence of Equilibriums

Dynamical properties of the solution process to Eq.(6.1) are closely related to the stability of equilibriums of the system (6.1). In order to find the control scheme which prevents the oscillation of populations, the stability of equilibriums are investigated.

From Eq.(6.1), the prey isoclines are given by

$$\ell_1 : \ x = 0 \tag{6.3}$$

and

$$\ell_2 : \ y = 1 - \frac{1}{A} - x, \tag{6.4}$$

which are depicted in Fig.6.1, where the axis of abscissa is the number of preys and the axis of ordinate is the number of predators. Similarly, from Eq.(6.1), the predator isoclines are given by

$$\ell_3 : \ y = 0 \tag{6.5}$$

and

$$\ell_4 : \ x = C \left\{ \frac{1}{B(1+E)} - 1 \right\}. \tag{6.6}$$

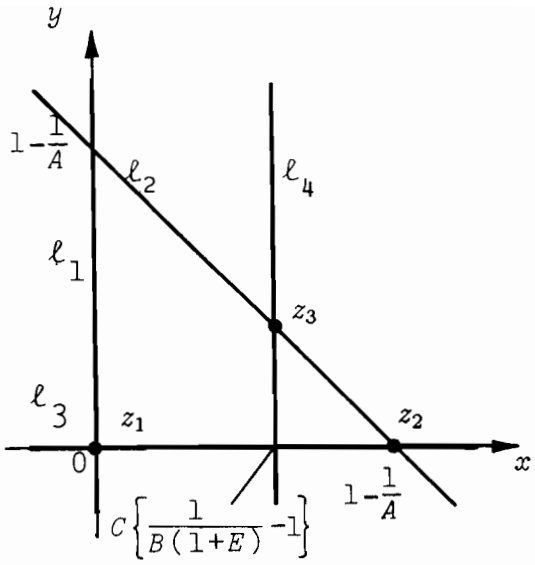

Figure 6.1: Predator and prey isoclines and equilibriums

Equilibriums of the system (6.1) are determined by intersections of prey isoclines and predator ones. Three equilibriums of the system (6.1) are given by

$$\begin{aligned} z_1 &= (0,0), \\ z_2 &= \left(1-\frac{1}{A},0\right), \\ z_3 &= \left(C\left\{\frac{1}{B(1+E)}-1\right\}, 1-\frac{1}{A}-C\left\{\frac{1}{B(1+E)}-1\right\}\right). \end{aligned} \tag{6.7}$$

Because of the interpretation of the coordinates x and y as population sizes which are necessarily nonnegative, equilibriums must lie in the first quadrant of the x-y plane.

Lemma 6.1 **(E1)** *The equilibrium z_1 is always in the first quadrant of the x-y plane.*
(E2) *The equilibrium z_2 is in the first quadrant of the x-y plane under the following condition:*

$$A \geq 1. \tag{6.8}$$

(E3) *The equilibrium z_3 is in the first quadrant of the x-y plane under the following conditions:*

$$\begin{aligned} &A \geq 1, \\ &\frac{AC}{B(AC+A-1)} - 1 \leq E \leq \frac{1}{B} - 1. \end{aligned} \tag{6.9}$$

Lemma 6.1 is derived from coordinates of equilibriums given by (6.7).

6.2.2 Stability of Equilibriums

For economy of notations, a nonlinear function $F_{IE} : \mathbf{R}^2 \to \mathbf{R}^2$ defined by

$$F_{IE}(x, y) = \left(Ax(1 - x - y),\ B(1 + E)y\left(1 + \frac{x}{C}\right)\right) \tag{6.10}$$

is introduced.

It is well known that the qualitative nature of equilibriums $z_i, i = 1, 2, 3$ of the system (6.1) is almost completely determined by the eigenvalues of the Jacobian $DF_{IE}(z_i)$ about the equilibrium z_i. A straightforward calculation brings us the eigenvalues $\lambda_{\pm}(z_i)$ of the Jacobian $DF_{IE}(z_i)$:

$$\begin{aligned}\lambda_{\pm}(z_i) = \ & \frac{1}{2}\left[A(1 - 2p_i - q_i) + B(1 + E)\left(1 + \frac{p_i}{C}\right)\right. \\ & \left. \pm\sqrt{\left\{A(1 - 2p_i - q_i) - B(1 + E)\left(1 + \frac{p_i}{C}\right)\right\}^2 - \frac{4AB(1 + E)}{C}p_i q_i}\right],\end{aligned} \tag{6.11}$$

where p_i and q_i denote the x and y coordinates of the equilibrium z_i, $i = 1, 2, 3$ respectively.

Theorem 6.1 (S1) *The equilibrium z_1 is locally asymptotically stable, if and only if the following conditions hold:*

$$A < 1, \quad E < \frac{1}{B} - 1. \tag{6.12}$$

(S2) *The equilibrium z_2 is locally asymptotically stable, if and only if the following conditions hold:*

$$1 < A < 3, \quad E < \frac{AC}{B(AC + A - 1)} - 1. \tag{6.13}$$

(S3) *The equilibrium z_3 is locally asymptotically stable, if and only if the following conditions hold:*

(i) for $1 < A \leq 3$,

$$\frac{AC}{B(AC + A - 1)} - 1 < E < \min\left\{\frac{1}{B} - 1, \frac{2AC}{B(AC + A - 1)} - 1\right\}. \tag{6.14}$$

(ii) for $A > 3$,

$$\frac{AC}{2B(AC+A-1)}\left\{4AC+A+3-\sqrt{(4AC+A+3)^2-12AC(AC+A-1)}\right\}-1 < E < \min\left\{\frac{1}{B}-1, \frac{2AC}{B(AC+A-1)}-1\right\}. \tag{6.15}$$

In order to prove Theorem 6.1, the following Lemma is useful:

Lemma 6.2 *The equilibrium* z_3 *is locally asymptotically stable, if and only if the following conditions hold:*

$$p_3 > 0, \tag{6.16}$$

$$\max\left\{0, \frac{2C}{B(1+E)}\left(1-\frac{2}{Ap_3}\right)\right\} < q_3 < \frac{C}{B(1+E)}, \tag{6.17}$$

where p_3 *and* q_3 *denote* x *and* y *coordinates of* z_3 *respectively.*

(Proof) From (6.7), p_3 and q_3 satisfy that

$$p_3 = C\{\frac{1}{B(1+E)}-1\}, \tag{6.18}$$

$$q_3 = 1-\frac{1}{A}-p_3. \tag{6.19}$$

From Eqs.(6.18) and (6.19), it follows that

$$B(1+E)(1+\frac{p_3}{C}) = 1, \tag{6.20}$$

$$A(1-2p_3-q_3) = 1-Ap_3. \tag{6.21}$$

Substituting Eqs.(6.20) and (6.21) into

$$\lambda_\pm(z_3) = \frac{1}{2}\left[A(1-2p_3-q_3)+B(1+E)\left(1+\frac{p_3}{C}\right) \pm\sqrt{\left\{A(1-2p_3-q_3)-B(1+E)\left(1+\frac{p_3}{C}\right)\right\}^2-\frac{4AB(1+E)}{C}p_3q_3}\right],$$

which is derived from (6.11), we obtain

$$\lambda_\pm(z_3) = \frac{1}{2}\left\{(2-Ap_3)\pm\sqrt{(Ap_3)^2-\frac{4AB(1+E)}{C}p_3q_3}\right\}. \tag{6.22}$$

From Eq.(6.22), if the following conditions hold:

$$\max\left\{0, \frac{2C}{B(1+E)}\left(1-\frac{2}{Ap_3}\right)\right\} < q_3 \leq \frac{AC}{4B(1+E)}p_3, \tag{6.23}$$

then $\lambda_{\pm}(z_3)$ is real and $|\lambda_{\pm}(z_3)| < 1$ holds. Furthermore, if

$$\frac{AC}{4B(1+E)}p_3 < q_3 < \frac{C}{B(1+E)} \tag{6.24}$$

then $\lambda_{\pm}(z_3)$ is imaginary and $|\lambda_{\pm}(z_3)| < 1$ holds. From (6.23) and (6.24), Lemma 6.2 is obtained. **(Q.E.D.)**

(Proof of Theorem 6.1) Conditions **(S1)** and **(S2)** are derived by substituting the x and y coordinates of equilibriums z_1 and z_2 into Eq.(6.11) and by calculating the condition under which $|\lambda_{\pm}(z_i)| < 1, \quad i = 1, 2$ holds.

The straightforward derivation of the condition **(S3)** is very complicated, so that the Lemma 6.2 is used. Substituting the x coordinate of z_3 into (6.16) of Lemma 6.2, we obtain

$$E < \frac{1}{B} - 1. \tag{6.25}$$

Substituting the y coordinate of z_3 into the latter half of Ineq.(6.17), we obtain

$$E < \frac{2AC}{B(AC+A-1)} - 1. \tag{6.26}$$

From Ineqs.(6.25) and (6.26), the upper limit of E, described in the condition **(S3)**, is obtained. Furthermore, noting that

$$\max\{0, \frac{2C}{B(1+E)}(1-\frac{2}{Ap_3})\} = \begin{cases} 0 & \text{for } 1 < A \leq 3 \\ \frac{2C}{B(1+E)}(1-\frac{2}{Ap_3}) & \text{for } 3 < A, \end{cases} \tag{6.27}$$

the lower limit of E in Ineq.(6.17) becomes

$$\begin{aligned} &0 < q_3, && \text{for } 1 < A \leq 3, \\ &\frac{2C}{B(1+E)}(1-\frac{2}{Ap_3}) < q_3, && \text{for } 3 < A. \end{aligned} \tag{6.28}$$

Substituting the x and y coordinates of the equilibrium z_3 into Ineqs.(6.28), the lower limit of E, described in the condition **(S3)** is obtained. **(Q.E.D)**

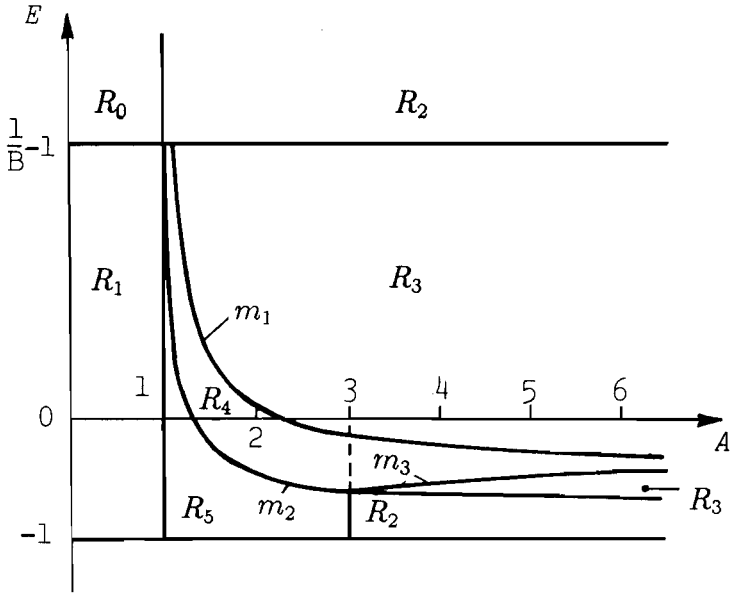

R_0 : z_1 exists and is unstable.
R_1 : z_2 exists and is stable.
R_2 : z_1 and z_2 exist and are unstable.
R_3 : z_1, z_2 and z_3 exist and are unstable.
R_4 : z_1, z_2 and z_3 exist and z_1 and z_2 are unstable, z_3 is stable.
R_5 : z_1 and z_2 exist and z_1 is unstable, z_2 is stable.

$$m_1 \ : E = \frac{2AC}{B(AC + A - 1)} - 1$$

$$m_2 \ : E = \frac{AC}{B(AC + A - 1)} - 1$$

$$m_3 \ : \frac{AC}{2B(AC + A - 1)} \left\{ 4AC + A + 3 - \sqrt{(4AC + A + 3)^2 - 12AC(AC + A - 1)} \right\} - 1$$

Figure 6.2: The A-E parameter space for existence and stability of equilibriums

Lemma 6.1 and Theorem 6.2 bring us Fig.6.2, which shows the existence and the stability of equilibrium solutions in the A-E parameter space.

If the equilibrium z_3 is unstable, then the solution of the system (6.1) goes around the equilibrium z_3 in the x-y plane and exhibits periodic solutions, limit cycles or chaotic behavior. Hence, in order to prevent oscillations of populations, namely, to make the solution converge to an equilibrium z_3, the equilibrium z_3 is stabilized by the harvesting or supplying of predators.

6.2.3 Stabilizability

No use is made for stabilizing the equilibrium z_1 or z_2, because the convergence to the equilibrium z_1 or z_2 means the extinction of preys or predators. Hence, the useful stabilization of the system (6.1) is realized by stabilizing the equilibrium z_3. The following theorem presents the control scheme which converts the system with oscillating behaviors into the one whose solution converges to the equilibrium z_3.

Theorem 6.2 *(i) The unstable equilibrium z_3 of the controlled system (6.1) is converted into the stable one by decreasing E, if the following conditions hold:*

$$\begin{cases} 1 < A, & \text{for } C \geq 1, \\ 1 < A < \dfrac{9}{1-C}, & \text{for } C < 1 \end{cases} \tag{6.29}$$

and

$$B \geq \frac{2AC}{(1+E)(AC+A-1)}. \tag{6.30}$$

(ii) The unstable equilibrium z_3 of the controlled system (6.1) is converted into the stable one by increasing E, if conditions (6.29) and the following condition hold:

$$B \leq \frac{1}{2(1+E)(AC+A-1)}\{4AC+A+3-\sqrt{(4AC+A+3)^2-12AC(AC+A-1)}\}. \tag{6.31}$$

Corollary 6.2 *(i) The unstable equilibrium z_3 of the uncontrolled system (5.1) is converted into the stable one by the harvesting of predators, if conditions (6.29) and the following*

condition hold:

$$B \geq \frac{2AC}{AC + A - 1}. \tag{6.32}$$

(ii) The unstable equilibrium z_3 of the uncontrolled system (5.1) is converted into the stable one by the supplying of predators, if conditions (6.29) and the following conditions hold:

$$B \leq \frac{1}{2(AC + A - 1)}\{4AC + A + 3 - \sqrt{(4AC + A + 3)^2 - 12AC(AC + A - 1)}\}. \tag{6.33}$$

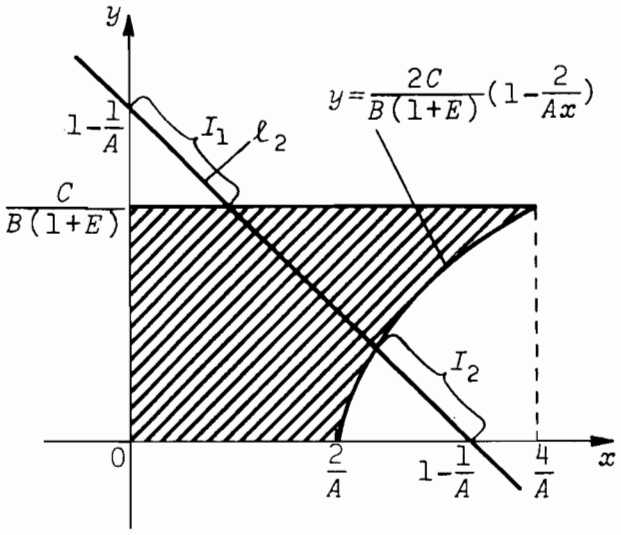

Figure 6.3: Stable area of the equilibrium z_3 in the x-y plane

(Proof) If conditions (6.29) hold, then the parameter E satisfying Ineqs.(6.14) or (6.15) exists. Hence, the unstable equilibrium z_3 can be stabilized whenever conditions (6.29) hold.

By using Lemma 6.2, the stable area of the equilibrium z_3 is depicted in Fig.6.3. Namely, the equilibrium z_3, included in the shaded area of Fig.6.3, satisfies conditions (6.16) and (6.17) in Lemma 6.2 and is asymptotically stable. On the other, the unstable equilibrium z_3 is contained in intervals I_1 or I_2 on the prey isocline ℓ_2.

Noting that the x coordinate of z_3 increases as E decreases, the unstable equilibrium z_3, contained in I_1, can be stabilized by decreasing E. On the other hand, the unstable equilibrium z_3, contained in I_2, can be stabilized by increasing E.

Inequality (6.30) gives the condition that the equilibrium z_3 is contained in the interval I_1 and Inequality (6.31) gives the condition that the equilibrium z_3 is contained in the interval I_2.

Corollary 6.2 is given by substituting $E = 0$ into Ineqs.(6.30) and (6.31). **(Q.E.D.)**

Theorem 6.2 indicates that:

- If the growth rate B of the predator is large, then the harvesting of predators is useful for preventing the oscillation of populations.
- If the growth rate B of the predator is small, then the supplying of predators is useful for preventing the oscillation of populations.

The amount of the effort for the harvesting or supplying, which converts the unstable equilibrium z_3 into the stable one, is obtained by Theorem 6.1.

6.2.4 Invariant Domain

Associated with the invariant domain

$$\mathcal{D} = \{(x_0, y_0) : x_n > 0,\ y_n > 0,\ n = 0, 1, 2, \cdots\},$$

the following result is derived:

Theorem 6.3 *The set*

$$\mathcal{D}_+ = \{(x, y) : x > 0,\ y > 0,\ 1 - x - y > 0\},$$

is the invariant domain of a nonlinear function F_{IE}, if the following conditions hold:
(i) for $0 < C \leq 1$,

$$0 < A < 4,$$
$$-1 < E < \frac{4C}{B(1+C)^2} - 1.$$

(ii) for $1 < C$,

$$0 < A < 4,$$
$$-1 < E < \frac{1}{B} - 1.$$

The proof of Theorem 6.3 is similar to that of Theorem 5.3.

Except for the case where $0 > 4C/B(1+C)^2 - 1$, Theorem 6.3 indicates that, for any harvesting effort E with $-1 < E < 0$, the invariant domain $\mathcal{D}$ is the set $\mathcal{D}_+$. The invariant set $\mathcal{D}_+$ is the largest one. Hence, Theorem 6.3 shows that the population does not die out under the constant effort harvesting.

6.2.5 Numerical Experiments

Numerical experiments are demonstrated to show the validity of results presented in Subsecs.6.2.2 to 6.2.4.

Figures 6.4(a) and (b) show the behavior of the uncontrolled system

$$\Sigma_I \begin{cases} x_{n+1} = Ax_n(1 - x_n - y_n) \\ y_{n+1} = By_n\left(1 + \dfrac{x_n}{C}\right), \end{cases}$$

calculated by the digital computer, where growth rates of the prey and predator are set as $A = 3.9$ and $B = 0.3$ respectively and the dependence of the predator on the prey is set as $C = 0.1$. In Fig.6.4(b), the 50,000 number of successive solutions are plotted in the x-y plane after 5000 iterations. Figures 6.4 show that the solution process to the uncontrolled system exhibits chaotic behavior in the case where $A = 3.9, B = 0.3$ and $C = 0.1$.

From Theorem 6.2, if the proportional constant E holds the condition

$$-0.5111\cdots < E < -0.2097\cdots,$$

then the equilibrium z_3 is locally asymptotically stable. Figure 6.5 shows the solution process to the controlled system (6.1) with a proportional constant of control $E = -0.4$, where $A = 3.9, B = 0.3$ and $C = 0.1$. Figure 6.5 indicates that if the predator is harvested with the proportional constant $E = -0.4$, then the solution process converges to an equilibrium $z_3 = (0.4555\cdots, 0.2880\cdots)$. Numerical experiments demonstrated in Figs.6.4 and 6.5 show the validity of Theorem 6.2.

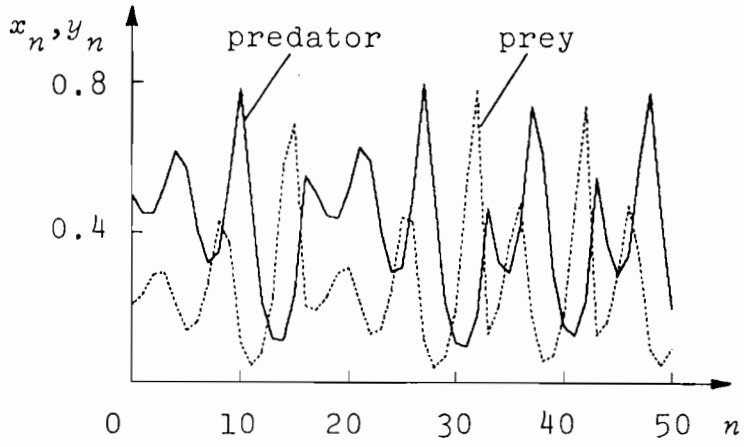

(a) Chaotic behavior

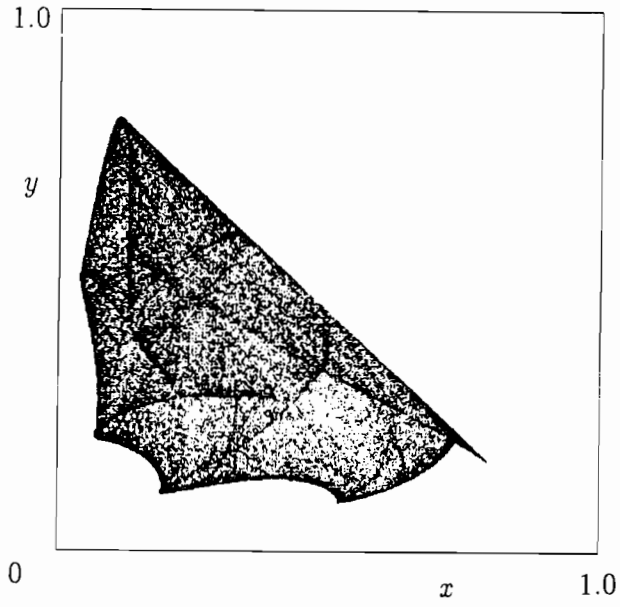

(b) Chaotic attractor

Figure 6.4: Chaotic behavior observed in the uncontrolled predator-prey system Σ_I with $A = 3.9$, $B = 0.3$ and $C = 0.1$

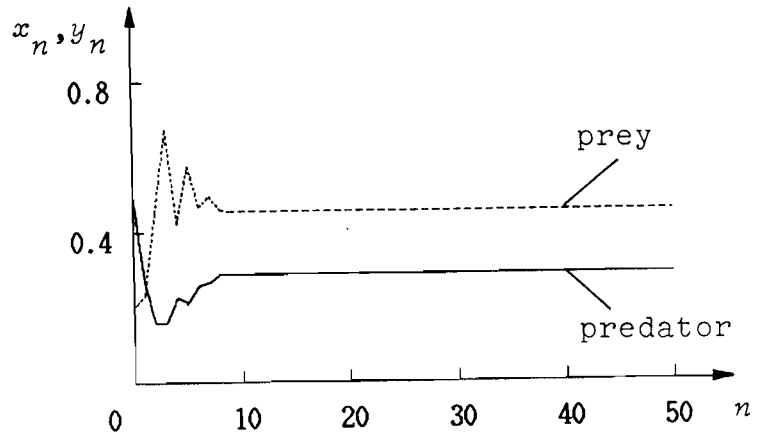

Figure 6.5: The Convergence to stable equilibrium z_3 observed in the controlled predator-prey system Σ_{IE} with $A = 3.9$, $B = 0.3$, $C = 0.1$ and $E = -0.4$

6.3 Stabilization of Type II Predator-Prey Systems

In this section, nonlinear dynamics of the type II Predator-Prey system Σ_{IIE} and the effects of constant rate harvesting on fractal boundaries of the invariant domain are discussed [YS90], [Yas91].

6.3.1 Location of Equilibriums

The controlled system (6.2) has the following three equilibriums

$$\begin{aligned} z_1 &= (0,0), \\ z_2 &= \left(1 - \frac{1}{A}, 0\right), \\ z_3 &= \left(C\left\{\frac{1}{B(1+E)} + 1\right\}, 1 - \frac{1}{A} - C\left\{\frac{1}{B(1+E)} + 1\right\}\right). \end{aligned} \tag{6.34}$$

6.3.2 Stability of Equilibriums

The stability of the equilibrium z_3 of the system Σ_{IIE} with the constant rate control is shown by the following theorem:

Theorem 6.4 *The equilibrium z_3 is locally asymptotically stable, if and only if*

(i) for $1 < A \leq 3$,

$$\frac{2AC}{B(A-AC-1)} - 1 < E < \max\left\{\frac{1}{B} - 1, \frac{2AC}{B(A-AC-1)} - 1\right\}. \tag{6.35}$$

(ii) for $3 < A$,

$$\frac{2AC}{B(A-AC-1)}\{(4AC+A+3) - \sqrt{(4AC+A+3)^2 - 12(A-AC-1)}\} - 1$$
$$< E < \max\left\{\frac{1}{B} - 1, \frac{2AC}{B(A-AC-1)} - 1\right\}. \tag{6.36}$$

Corollary 6.4 *The equilibrium* z_3 *is locally asymptotically stable, if and only if conditions*

$$p_3 > 0, \tag{6.37}$$

$$\max\left\{0, \frac{2C}{B(1+E)}(1 - \frac{2}{Ap_3})\right\} < q_3 < \frac{C}{B(1+E)} \tag{6.38}$$

hold, where p_3 *and* q_3 *are the* x *and* y *coordinates of the equilibrium* z_3 *respectively.*

6.3.3 Effects of Constant Rate Harvesting on Fractal Boundaries

For convenience of discussions, we introduce

$$F_{IIE}(x,y) = \left(Ax(1-x-y),\ \ B(1+E)y\left(-1+\frac{x}{C}\right)\right). \tag{6.39}$$

For the controlled system Σ_{IIE}, we also adopt the set

$$\mathcal{D}_- = \{(x,y):\ x > C,\ y > 0,\ Ax(1-x-y) > C\}$$

as a candidate of the invariant domain $\mathcal{D}$. Figure 6.6 shows images $F(\mathcal{D}_-)$, which is equal to $F_{IIE}(\mathcal{D}_-)$ with $E = 0$, and $F_{IIE}(\mathcal{D})$ with $E < 0$. As shown in Fig.6.6, for any $E < 0$, $F_{IIE}(\mathcal{D})$ is included in $F(\mathcal{D})$. Namely, the mapping F_{IIE} with $E < 0$ squeezes the domain $\mathcal{D}_-$ vertically rather than the mapping F. Hence, the inverse mapping F_{IIE}^{-1} stretches the area $\mathcal{A}_e$ vertically rather than the inverse mapping F^{-1} and the tongue $F_{IIE}^{-k}(\mathcal{A}_e)$ becomes longer than the tongue $F^{-k}(\mathcal{A})$. Therefore, it is proposed that fractal boundaries produced by

$$\mathcal{D}_- - \bigcup_{k=1}^{\infty} F_{IIE}^{-k}(\mathcal{A}_e)$$

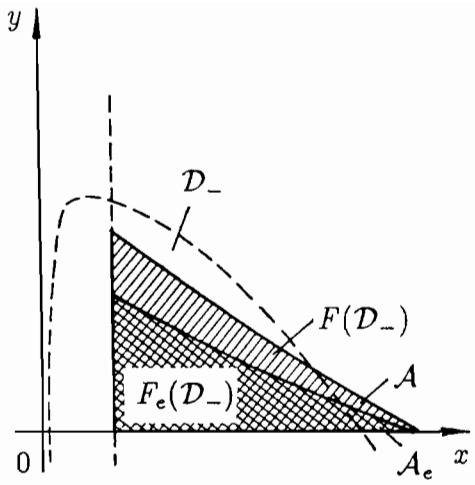

Figure 6.6: Images $F(\mathcal{D})$ and $F_{IE}(\mathcal{D})$

is more complicated than that by

$$\mathcal{D}_- - \bigcup_{k=1}^{\infty} F^{-k}(\mathcal{A}).$$

Hence, in the controlled system Σ_{IE}, as the constant E decreases, the complexity of fractal boundaries of the invariant domain $\mathcal{D}$ increases.

6.3.4 Numerical Experiments

(a) Definition of Capacity Dimension

In order to evaluate the complexity of fractal boundaries, it is useful to calculate the capacity dimension, which is one of the fractal dimension, defined as follows:

Definition 6.1 *[MGOY85a], [Tak86] The capacity dimension* $\dim_C(\partial\mathcal{D})$ *of the boundary* $\partial\mathcal{D}$ *of the domain* $\mathcal{D}$ *is defined by*

$$\dim_C(\partial\mathcal{D}) = \lim_{\delta \to 0} \frac{\ln N(\delta)}{\ln \frac{1}{\delta}}, \tag{6.40}$$

where $N(\delta)$ *is the minimum number of squares of side* δ *required to cover the boundary of the domain* $\mathcal{D}$ *[MGOY85a], [Tak86] .*

If the boundary is smooth, then the capacity dimension is given by $\dim_C(\partial\mathcal{D}) = 1$. On the other hand, if the boundary is fractal, the the capacity dimension satisfies that

$$1 < \dim_C(\partial\mathcal{D}) < 2.$$

Furthermore, when the complexity of the boundary increases, the capacity dimension of the boundary also increases [MGOY85a], [Tak86]. Numerical technique calculating the capacity dimension is demonstrated in Appendix 6A.

(b) Capacity Dimension of Fractal Boundaries

To show the validity of results presented in previous subsections, parameters are selected as $A = 3.9$, $B = 0.5$ and $C = 0.12$ for the uncontrolled system Σ_{II}. In this case, the solution process exhibits chaotic behavior and the invariant domain $\mathcal{D}$ exhibits fractal boundaries, which are already shown in Figs.5.15 of Chapter 5.

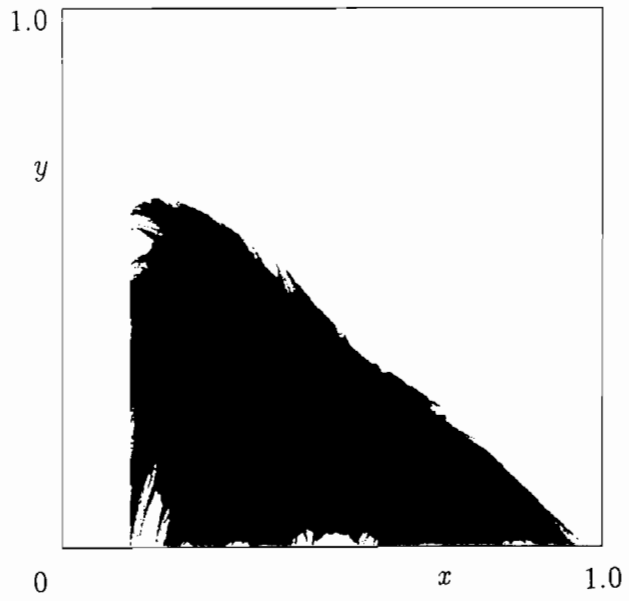

Figure 6.7: The invariant domain with fractal boundaries of the controlled predator-prey system Σ_{IIE} with $A = 3.9$, $B = 0.5$, $C = 0.12$ and $E = -0.368$

Based on Theorem 6.2, in order to stabilize the chaotic oscillation, the effort for the harvesting E is set as $E = -0.368$. Then, the equilibrium $z_3 = (0.500\cdots, 0.244\cdots)$ is asymptotically stable. The invariant domain $\mathcal{D}$ of the controlled system Σ_{IIE} with $E = -0.368$ is plotted in Fig.6.7, where fractal boundaries of the invariant domain are

demonstrated. In order to compare the complexity of fractal boundaries observed in the systems Σ_{II} and Σ_{IIE}, the capacity dimension is numerically calculated as follows (See Appendix 6A):

$$\Sigma_{II}(\text{ i.e., } E = 0) \quad : \dim_C(\partial D) = 1.576$$
$$\Sigma_{IIE} \text{ with } E = -0.368 \quad : \dim_C(\partial D) = 1.706.$$

These numerical experiments indicate that, under the constant rate harvesting of predators, the complexity of fractal boundaries increases.

6.4 Conclusions

It has been shown that chaotic behavior of a class of discrete predator-prey systems are stabilized by the constant rate harvesting or supplying of predators. For a large B, namely, when the growth rate of the predator is large, we can stabilize the system by the harvesting of predators. For a small B, namely, when the growth rate of the predator is small, we can stabilize the system by the supplying of predators.

From viewpoints of the conservation of ecosystems, the control using the constant rate harvesting has an advantage rather than that using the constant harvesting, because the invariant domain of the constant rate harvesting is larger than that of the constant harvesting.

Theoretical and numerical approach developed here should be useful in pursuing the answers to stabilization problems in discrete predator-prey systems with a constant rate harvesting or supplying.

Appendix 6A: Numerical Technique for Calculating Capacity Dimension

(a) Capacity Dimension and Uncertain Exponent

In order to calculate the capacity dimension, the concept of final state sensitivity is introduced [MGOY85a]. Consider a two dimensional phase space, as shown in Fig.6.8. The region $\mathcal{D}$ is the invariant domain and its boundary is denoted by $\partial\mathcal{D}$. Now, consider the situation that initial conditions are measured and the measurement has an uncertainty ε in the sense that the actual initial condition might be anywhere in a disc of radius ε centered at the measured value. Hence if the measured initial condition is a point p_1 in Fig.6.8, then the true initial condition is certainly included in the invariant domain $\mathcal{D}$ and the solution process certainly remains in the invariant domain $\mathcal{D}$. On the other hand, if the measured initial condition is a point p_2, then the true initial condition may be included in the invariant domain $\mathcal{D}$ or may not be included in the invariant domain $\mathcal{D}$. Hence, the point p_2 is called the uncertain initial condition.

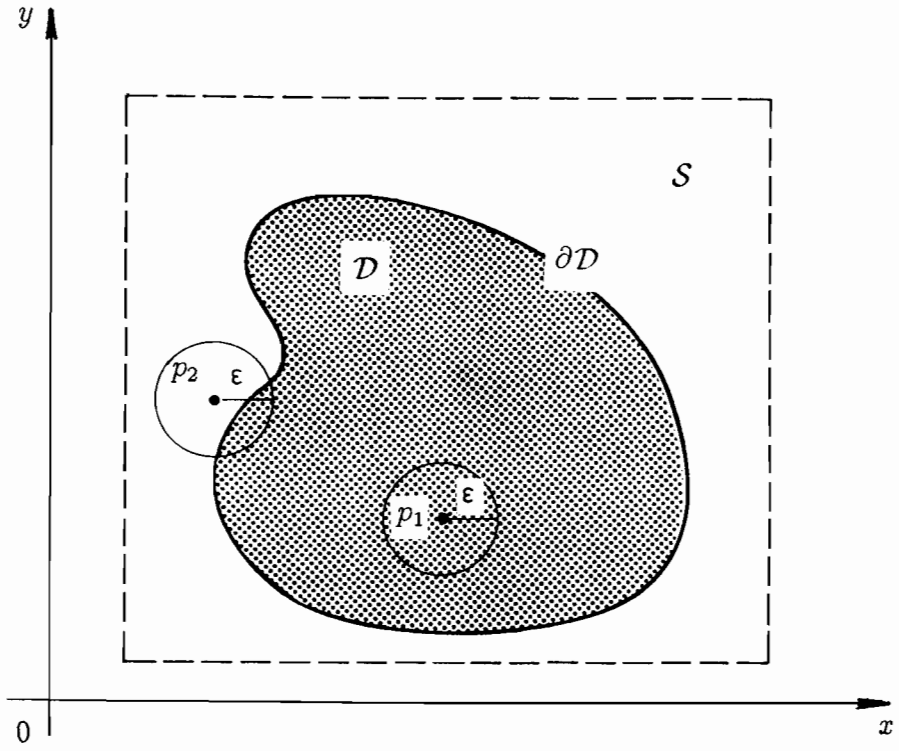

Figure 6.8: The uncertain initial condition

Assuming that the initial condition is uniformly distributed in the area $\mathcal{S}$ depicted by the broken line in Fig.6.8, we can consider the fraction $h(\varepsilon)$ that the measured initial condition is uncertain. The fraction $h(\varepsilon)$, indeed, depends on the uncertainty ε. When the boundary of the invariant domain is smooth, the fraction $h(\varepsilon)$ is proportional to ε, i.e.,

$$h(\varepsilon) \sim \varepsilon.$$

On the other hand, when the boundary of the invariant domain is fractal, the fractal $h(\varepsilon)$ satisfies

$$h(\varepsilon) \sim \varepsilon^{\alpha}, \quad 0 < \alpha < 1.$$

The constant α is called the uncertain exponent. It has been shown that the capacity dimension $\dim_{\mathrm{C}}(\partial\mathcal{D})$ of the boundary $\partial\mathcal{D}$ satisfies [MGOY85a]

$$\dim_{\mathrm{C}}(\partial\mathcal{D}) = 2 - \alpha.$$

Therefore, in order to obtain the capacity dimension $\dim_{\mathrm{C}}(\partial\mathcal{D})$, it is necessary to calculate the uncertain exponent α with the aid of digital computer.

(b) Numerical Technique calculating Uncertain Exponent

In order to calculate the uncertain exponent α, the following procedures are carried out:

(i) The interval $[0, 1]$ in x and y axes is equally divided into 200 segments. By drawing the vertical and horizontal lines through dividing points, the mesh is constructed in the x-y plane. (See Fig.6.9) The intersection between vertical and horizontal lines included into the area

$$\{(x, y) : x \geq 0, y \geq 0, 1 - x - y \geq 0\} \tag{6.41}$$

is selected as the initial condition.

(ii) Each initial condition is iterated two hundred times by Eq.(6.2) and if the solution process does not leave from the first quadrant until 200 step iteration, then the initial condition is regarded as a point included in the invariant domain $\mathcal{D}$.

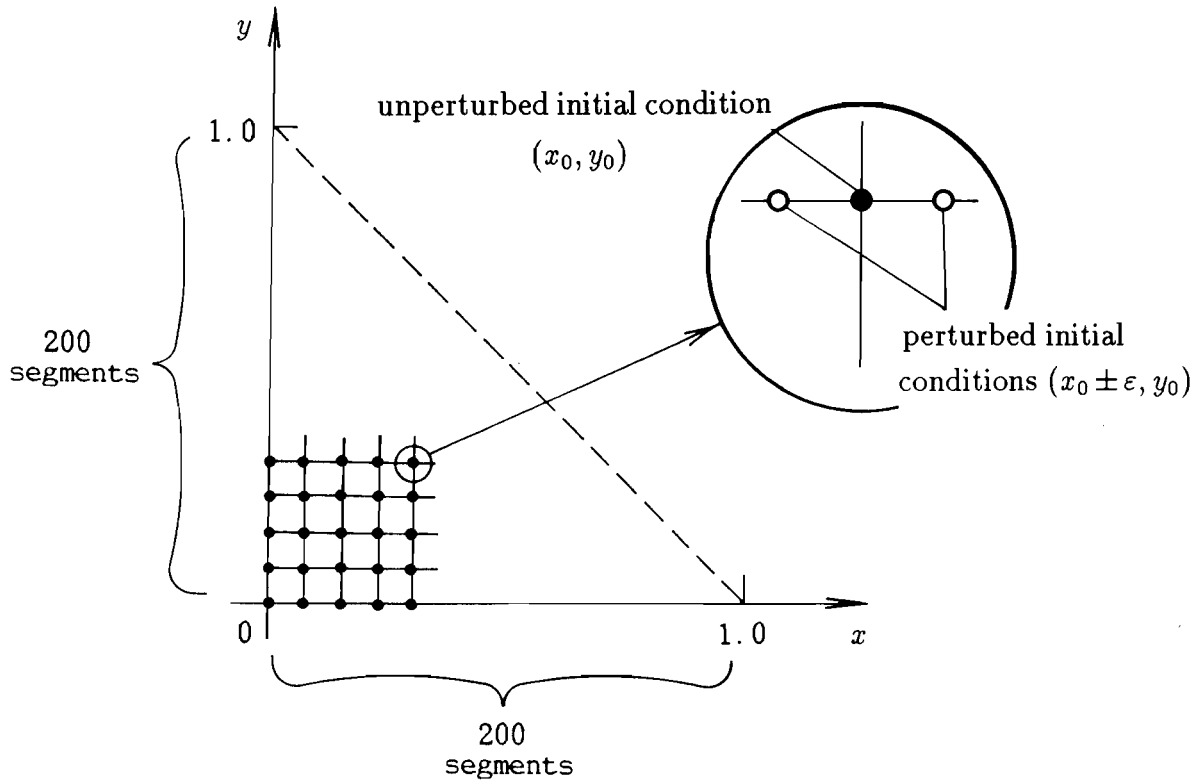

Figure 6.9: Unperturbed and perturbed initial conditions

(iii) For an initial condition (x_0, y_0), two perturbed initial conditions $(x_0 \pm \varepsilon, y_0)$ are made and are iterated two hundred times by Eq.(6.2), in order to decide whether perturbed initial conditions are included in the invariant domain or not. This result is compared with that for the unperturbed initial condition. If either of perturbed initial conditions has the different result from that for the unperturbed initial condition, then the unperturbed initial condition is regard as the uncertain initial condition.

(iv) For all 20301 unperturbed initial condition, the procedure presented in (iii) is done and we record the number of the uncertain initial condition. The fraction $h(\varepsilon)$ is given by

$$h(\varepsilon) = \frac{\text{the number of the uncertain initial condition}}{20301}, \tag{6.42}$$

where 20301 is the total number of the unperturbed initial conditions.

(v) For various values of the error ε, the uncertain fraction $h(\varepsilon)$ is calculated and the relation between $\log \varepsilon$ and $\log h(\varepsilon)$ are plotted as shown in Fig.6.12. The slope of the graph indicates the uncertain exponent α.

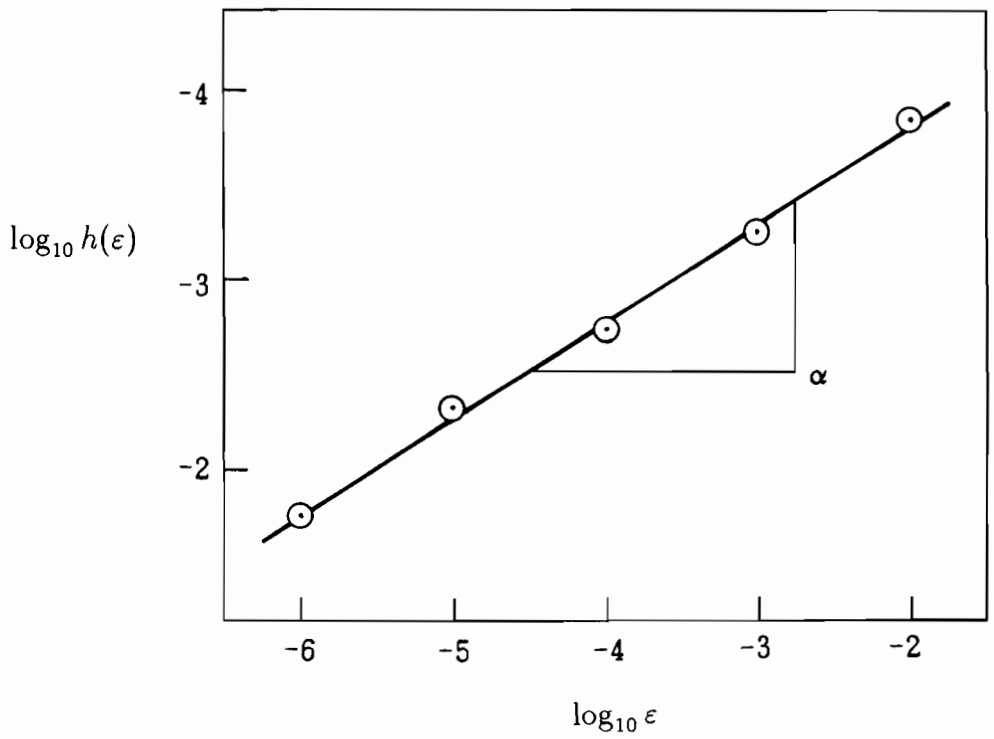

Figure 6.10: $\log \varepsilon$ vs $\log h(\varepsilon)$

Chapter 7

Conclusions

In this thesis, chaotic and fractal phenomena have been investigated, concerned with one and two dimensional nonlinear discrete dynamical systems.

A contribution was provided by theoretical analysis using Hausdorff dimension. Namely, it has been demonstrated that the existence of the periodic point with period three implies the existence of fractal boundaries, concerned with a class of one-dimensional discrete dynamical systems. By applying the results obtained by theoretical analyses, fractal boundaries, observed in a class of sampled-data control systems, were investigated. In illustrative examples, the existence of fractal boundaries of the set of initial conditions, under which solution processes are bounded, was shown and furthermore fractal basin boundaries of coexisting final state were also discussed.

The fractal set generated by contraction mappings was already investigated and the excellent results were obtained [Huc81]. However, in the previous results [Huc81], the set itself is fractal, hence the Lebesgue measure of the fractal set is zero. In engineering dynamical systems, including control systems, this fact means that the fractal basin of an equilibrium has the zero Lebesgue measure and, for almost all initial conditions, state variables do not converge to the equilibrium. Therefore, in engineering systems, the existing conditions of fractal basin boundaries are valuable, rather than those of the fractal set.

Secondly, mechanisms yielding fractal boundaries of the invariant set of nonlinear functions were investigated by using the notation of the symbolic dynamics, and the

existence of five different mechanisms were shown.

These results, in one-dimensional dynamical systems, provide a tool for investigating complicated boundaries of the invariant domain, which is the set of initial conditions generating nonnegative solution processes, concerned with a class of two-dimensional dynamical system describing a class of predator-prey systems. Through a fundamental approach constructed by the following procedures:

(Step 1) Find a candidate of the invariant domain.

(Step 2) Consider the image of the selected candidate, generated by the nonlinear function describing the system dynamics.

(Step 3) Consider inverse images of subsets of the image, which are not included in the candidate.

mechanisms yielding complicated boundaries exhibiting self-similar structures were clarified by using the notation of the symbolic dynamics and existing conditions of fractal boundaries were obtained.

The other topic of the thesis is concerned with the stabilization scheme of oscillation of the population, observed in a class of predator-prey systems, demonstrated in Chaps.5 and 6. The control term was adopted as both harvesting and supplying of predators. Solution properties were analyzed through the stability analysis of equilibriums and it has been shown that both constant and constant rate harvesting or supplying of predators are useful for preventing the oscillation of populations.

Furthermore, investigations has been extended to explore effects of the control input on fractal boundaries. Under the constant harvesting, fractal boundaries became smooth but the size of the invariant domain becomes small, as the amount of the harvesting of predators increases. Hence, it is easy to decide the coexistence or extinction of population, but there exist many initial conditions led to the extinction of populations by the constant harvesting. On the other hand, under the constant rate harvesting, as the effort to harvest

increases, the complexity of fractal boundaries increases. Hence, it is needed to carefully decide the coexistence or extinction of populations.

From viewpoints of the conservation of ecosystems, the control using the constant rate harvesting has an advantage rather than that using the constant harvesting, because the invariant domain under the constant rate harvesting is larger than that under the constant harvesting.

Nonlinear dynamics, yielding chaotic behavior of the system, often exhibits fractal phenomena. However, this situation is not usual. An example was shown in Chap.6, i.e., chaotic oscillations of populations are stabilized by the constant rate harvesting of predators, on the other hand, the complexity of fractal boundaries of the invariant domain increases under the constant rate harvesting.

Bibliography

[AA68] V. I. Arnold and A. Avez. *Ergodic Problems of Classical Mechanics.* Benjaminn, New York, 1968.

[AAR87a] F. Argoul, A. Arneodo, and P. Richetti. Experimental evidence for homoclinic chaos in the Balousov-Zhabotinski reactor. *Phys. Lett. A*, 120(6):269–275, 1987.

[AAR*87b] F. Argoul, A. Arneodo, P. Richetti, J. C. Roux, and H. L. Swinney. Chemical chaos: from hints to confirmation. *Acc. Chem. Res.*, 20:436–442, 1987.

[ABK91] H. D. I. Abarbanel, R. Brown, and M. B. Kennel. Lyapunov exponents in chaotic systems: their importance and their evaluation using observed data. *Mod. Phys. Lett. B*, 1991.

[adHW83] Uwe an der Heiden and H. O. Walther. Existence of chaos in control systems with delayed feedback. *Journal of Differential Equations*, 47:273–295, 1983.

[Arn63] V. I. Arnold. Small denominators *II*, proof of a theorem of A. N. Kolmogolov on the preservation of conditionally-periodic motions under a small perturbation of the Hamiltonian. *Russ. Math. Surveys*, 18:5, 1963.

[ATT90] K. Aihara, T. Tanabe, and M. Toyoda. Chaotic neural networks. *Phys. Lett. A*, 144(6 & 7):333–340, 1990.

[Bar88] M. Barnsley. *Fractal Everywhere.* Academic Press, New York, 1988.

[BBW80] J. Baillieul, R. W. Brockett, and R. B. Washburn. Chaotic motion in nonlinear feedback systems. *IEEE Trans. on Circuits and Systems*, CAS-27(11):990–997, 1980.

[BC91] M. Benedicks and L. Carleson. The dynamics of the Hénon map. *Annals of Mathematics*, 133(1):73–169, 1991.

[BDMP80] P. Bergé, M. Dubois, P. Manneville, and Y. Pomeau. Intermettency Rayleigh-Benard convection. *J. Phys. Lett.*, 41(15):L341–L345, 1980.

[Bel90] V. V. Beletzky. Nonlinear effects in dynamics of controlled two-legged walking. *in Nonlinear dynamics in Engineering Systems, W. Schielen(ed.), Springer-Verlag, Berlin*, 17–26, 1990.

[BFL75] J. R. Beddington, C. A. Free, and J. H. Lawton. Dynamic complexity in predator-prey models framed in difference equations. *Nature*, 255:58–60, 1975.

[BGS76] G. Benettin, L. Galgani, and J. -M. Strelcyn. Kolmogorov entropy and numerical experiments. *Physical Review A*, 14(6):2338–2345, 1976.

[Bil65] P. Billingsley. *Ergodic Theory and Information.* Wiley, New York, 1965.

[Bir35] G. D. Birkhoff. Nouvelles recherches sur les systèms dynamiques. *Mém. Pont. Acad. Sci. Novi. Lyncaei.*, 1:85, 1935.

[Blo78] L. Block. Homoclinic points of mappings of the interval. *Proc. Am. Math. Soc.*, 72:576–580, 1978.

[BPV84] P. Bergé, Y. Pomeau, and C. Vidal. *Order within Chaos Towards a Deterministic Approach to Turbulence.* Jhon Wiley and Sons, New York, 1984.

[Bra76] F. Brauer. De-stabilization of predator-prey systems under enrichment. *Int. J. Control*, 23(4):541–552, 1976.

[BS79] F. Brauer and A. C. Soudack. Stability regions and transition phenomena for harvested predator-prey systems. *J. Math. Biology*, 7:319–337, 1979.

[BS85] F. Brauer and A. C. Soudack. Optimal harvesting in predator-prey systems. *Int. J. Control*, 41(1):111–128, 1985.

[BS87] A. Brandstater and H. L. Swinney. Strange attractors in weakly turbulent Couette-Taylor flow. *Phys. Rev. A*, 35(5):2207–2220, 1987.

[BSJ76] F. Brauer, A. C. Soudack, and H. S. Jarosh. Stabilization and destabilization of predator-prey systems under harvesting and nutrient enrichment. *Int. J. Control*, 23(4):553–573, 1976.

[BSS*83] A. Brandstater, A. Swift, H. L. Swinney, A. Wolf, J. D. Farmer, E. Jen, and J. P. Crutchfield. Low-dimensional chaos in a hydrodynamics system. *Phys. Rev. Lett.*, 51(6):1442–1445, 1983.

[BSSW84] A. Brandstater, A. Swift, H. L. Swinney, and A. Wolf. A strange attractor in a Couette-Taylar experiment. *in Turbulence and Chaotic Phenomena Fluids, Proceedings of the IUTAM symposium (Kyoto), T. Tatsumi (ed.), North-Holland, Amsterdam*, 1984.

[Can83] G. Cantor. Über unendliche, lineare Punktmannigfaltigkeiten V. *Mathematische Annalen*, 21:545–591, 1883.

[CE80] P. Collet and J. P. Eckmann. *Iterated Maps on the Interval as Dynamical Systems.* Birkhauser, Boston, 1980.

[CG85] S. Ciliberto and J. P. Gollub. Chaotic mode competition in parametrically forced surface waves. *J. Fluid Mech.*, 158:381–398, 1985.

[Che88] P. Chen. Empirical and theoretical evidence of economic chaos. *System Dynamics Review*, 4:81–108, 1988.

[Che91] G. Cherbit, editor. *Fractals, Non-integral Dimensions and Applications.* Jhon Wiley & Suns, Chichester, 1991.

[CKM86] L. O. Chua, M. Komuro, and T. Matsumoto. The double scroll family. *IEEE Trans. Circuits and Syst.*, CAS-33:1072, 1986.

[CL45] M. L. Cartwright and J. E. Littlewood. On nonlinear differential equations of the second order: I the equation $y'' - k(1 - y^2)y' + y = bk\cos(t + d), k$ large. *J. London Math. Soc.*, 20:180–189, 1945.

[CL89] J. M. Carlson and J. S. Langer. Properties of earthquakes generated by fault dynamics. *Phys. Rev. Lett.*, 62(22):2632–2635, 1989.

[Cla76] C. W. Clark. *Mathematical Bioeconomics: The Optimal Management of Renewable Resources.* John Wiley & Sons, New York, 1976.

[CM90] J. P. Cusumano and F. C. Moon. Low dimensional behavior in chaotic nonplanar motions of a forced elastic rod: experiment and theory. *Proc. IUTAM Symposium on Nonlinear dynamics in Engineering Systems, W. Schiehlen (ed.), Springer-Verlag, Berlin*, 59–66, 1990.

[CP82] M. Cirillo and N. F. Pedersen. On bifurcations and transitions to chaos in a Josephson junction. *Phys. Lett.*, 90A:150, 1982.

[CS90] R. J. Comparin and R. Singh. An analytical study of automotive neural gear rattle. *J. Mech. design*, 112:237–245, 1990.

[DBC82] M. Dubois, P. Bergé, and V. Croquette. Study of nonsteady convective regimes using Poincaré sectionsd. *J. Phys. Lett.*, 43:L295–298, 1982.

[DBHL82] D. D'humieres, M. R. Beasly, B. A. Humbermann, and A. Libchaber. Chaotic states and routes to chaos in the forced pendulum. *Phys. Rev.*, 26A:3483, 1982.

[Dev89] R. L. Devaney. *An Introduction to Chaotic Dynamical Systems, Second Edition.* Addison-Wesley, Redwood City, 1989.

[Dev90] R. L. Devaney. *Chaos, Fractals, and Dynamics.* Addison-Wesley, Menlo Park, 1990.

[DHF87] H. Degn, A. V. Holder, and L. Folsen. *Chaos in Biological Systems.* Plenum Press, New York, 1987.

[Dia76] P. Diamond. Chaotic behavior of systems of differince equations. *Internat. J. Systems Sci.*, 7:953–956, 1976.

[DP86] E. H. Dowell and C. Pezeshki. On the understanding of chaos in Duffing's equation including a comparison with experiment. *J. Appl. Mech.*, 53(1):5–9, 1986.

[EC88] T. Endo and L. O. Chua. Chaos from phase-locked loops. *IEEE Trans. Circuits & Syst.*, CAS-35(8):987–1003, 1988.

[EC89] T. Endo and L. O. Chua. Chaos from phase-locked loops, Part II: high-dissipation case. *IEEE Trans. Circuits & Syst.*, CAS-36(2):255–263, 1989.

[EC90] T. Endo and L. O. Chua. Bifrucation diagrams and fractal basin boundaries of phase-locked loop circuits. *IEEE Trans. Circuits & Syst.*, CAS-37(4):534–540, 1990.

[Edg90] G. Edger. *Measures, Topology and Fractal Geometry.* Springer-Verlag, New York, 1990.

[EIC90] T. Endo, M. Imai, and L. O. Chua. Phase-locked loops can be chaotic. *Trans. IEICE*, E73(6):825–827, 1990.

[End90] T. Endo. Homoclinic orbits, fractal basin boundaries and bifurcations of phase-locked loop circuits. *Trans. IEICE*, E73(6):828–835, 1990.

[ES90] T. Endo and T. Saito. Chaos in electrical and electrotic circuits and systems. *Trans. IEICE*, E73(6):763–771, 1990.

[Fal85] K. Falconer. *Geometry of Fractal Sets.* Cambridge University Press, Cambridge, 1985.

[Fal90] K. Falconer. *Fractal Geometry.* John Wiley & Suns, Chichester, England, 1990.

[Fed88] J. Feder. *Fractals.* Plenum Press, New York, 1988.

[Fei78] M. J. Feigenbaum. Quantitative universality for a class of nonlinear transformations. *J. Stat. Phys.*, 19:25–32, 1978.

[FM89] B. F. Feeny and F. C. Moon. Autocorelation on symbol dynamics for a chaotic dry-friction oscillator. *Phys. Lett.*, 141:397–400, 1989.

[FM92a] B. F. Feeny and F. C. Moon. Bifurcation sequences of a Coulomb friction oscillator. *Nonlin. Dynam.*, 1992.

[FM92b] B. F. Feeny and F. C. Moon. Chaos in a forced dry-friction oscillator: experiments and numerical modeling. *J. Sound. Vib.*, 1992.

[FOY83] J. D. Farmer, E. Ott, and J. A. Yorke. The dimension of chaotic attractors. *Physica*, 7D:153–180, 1983.

[GH83] J. Guckenheimer and P. Holmes. *Nonlinear Oscillations, Dynamical systems, and Bifurcations of Vector Fields.* Springer-Verlag, 1983.

[Gib88] V. Gibiat. Phase space representations of acoustical musical signals. *J. Sound Vib.*, 123(3):529–536, 1988.

[GM80] I. Gumowski and C. Mira. *Recurrences and Discrete Dynamical Systems. Springer Lecture Notes in Mathematics*, Springer-Verlag, New York, 1980.

[GM88] L. Glass and M. C. Mackey. *From Clocks to Chaos: The Rhythms of Life.* Princeton University Press, Princeton, NJ., 1988.

[GM91] M. F. Golnaraghi and F. C. Moon. Experimental evidence for chaotic response in a feedback system. *J. Dynam. Syst. Meas. Control*, 113:183–187, 1991.

[GOI77] J. Guckenheimer, G. Oster, and A. Ipaktchi. The dynamics of density dependent popultion models. *J. Math. Biology*, 4:101–147, 1977.

[GOY83] C. Grebogi, E. Ott, and J. A. Yorke. Fractal basin boundaries, long lived chaotic transients and unstable-unstable pair bifurcation. *Phys. Rev. Lett.*, 50(13):935–938, 1983.

[GOY86] C. Grebogi, E. Ott, and J. A. Yorke. Metamorphoses of basin boundaries in nonlinear dynamical systems. *Phys. Rev. Lett.*, 56(10):1011–1014, 1986.

[GP83] P. Grassberger and I. Proccacia. Characterization of strange attractors. *Phys. Rev. Lett.*, 50:346–349, 1983.

[GP84] P. Grassberger and I. Proccacia. Dimensions and entropies of strange attractors from a fluctuation dynamics approach. *Physica 13D*, 34–54, 1984.

[GPL90] K. Geist, U. Parlitz, and W. Lauterborn. Comparison of different methods for computing Lyapunov exponents. *Prog. Theo. Phys.*, 83(5):875–893, 1990.

[Gra86] I. Grabec. Chaos generated by the cutting process. *Phys. Lett. A*, 117(8):384–386, 1986.

[Gra88] I. Grabec. Chaotic dynamics of the cutting process. *Int. J. Mach. Tools Manufact*, 28(1):19–32, 1988.

[Guc79] J. Guckenheimer. Sensitive dependence on initial conditions for one-dimensional maps. *Comm. Math. Phys.*, 70:133–160, 1979.

[Guc80] J. Guckenheimer. Dynamics of the Van der Pol equation. *IEEE Trans. on Circuits & Systems*, CAS-27(11):983–989, 1980.

[GW85] E. G. Gwinn and R. M. Westervelt. Intermittent chaos and low-frequency noise in the driven damped pendulum. *Phys. Rev. Lett.*, 54(15):1613–1616, 1985.

[HA88] K. Hirai and T. Adachi. Coexistence of periodic points and chaos. *Technical Report of IEICE*, NLP88-9:1–6, 1988.

[Hak75] H. Haken. Analogy between higher instabilities in fluids and lasers. *Phys. Lett.*, 53A:77, 1975.

[Hak85] H. Haken. *Light, Vol.2: Laser Light Dynamics.* North-Holland, Amsterdam, 1985.

[Hat90] M. Hata. Euler's finite difference scheme and chaos in R^n. *Proc. Jap. Acad.*, 58(Ser.A):178–181, 1990.

[Hau19] F. Hausdorff. Dimension und äusseres Mass. *Mathematische Annalen*, 79:157–179, 1919.

[Hay80] S. Hayama. Dynamics of a discrete prey-predator model, and chaos. *Biophysics*, 20(3):57–65, 1980. (in Japanese).

[HB86] R. G. Harrison and D. J. Biswas. Chaos in light. *Nature*, 22:394–401, 1986.

[HE87] H. Haucke and R. E. Ecke. Mode-locking and chaos in Rayleigh-Benard convection. *Physica*, D, 1987.

[Hen76] M. Hénon. A two-dimensional mapping with a strange attractor. *Commun. Math. Phys.*, 50:69–77, 1976.

[Hen83] F. Hendriks. Bounce and chaotic motion in print hammers. *IBM J. Res. Dev.*, 27(3):273–280, 1983.

[HH86] K. Hockett and P. J. Holmes. Josephson junction, annulus maps, Birkhoff attractors, horseshoes and rotation sets. *Ergod. Th. and dynam. Sys.*, 6:205–239, 1986.

[HH87] K. Hockett and P. J. Holmes. Nonlinear oscillations, iterated maps, symbolic dynamics, and knotted orbits. *Proc. IEEE*, 75:1071–1080, 1987.

[HH91] T. Hogg and B. A. Huberman. Controlling chaos in distributed systems. *IEEE Trans. Sys., Man, and Cyber.*, SMC-21(6):1325–1332, 1991.

[Hil91] D. Hilbert. Über die stetige abbildung einer linie auf ein Flächenstück. *Mathematische Annalen*, 38:459–460, 1891.

[Hir90] K. Hirai. Coexistence of periodic points and chaos in a nonlinear discrete-time system. *Nonlinear Dynamics in Engineering Systems, IUTAM Symposium Stuttgart/Germany 1989*, 107–116, 1990.

[HKGS82] F. A. Hopf, D. L. Kaplan, H. M. Gibbs, and R. L. Shoemaker. Bifurcations to chaos in optical bistability. *Phys. Rev.*, 25A:2172, 1982.

[HM83] P. J. Holmes and F. C. Moon. Strange attractors and chaos in nonlinear mechanics. *J. Appl. Mech.*, 50:1021–1032, 1983.

[Hol82] P. J. Holmes. The dynamics of repeated impacts with a sinusoidally vibrating table. *J. Sound Vib.*, 84:173–189, 1982.

[Hol85] P. J. Holmes. Dynamics of nonlinear oscillator with feedback control. *J. Dynam. Syst. Meas. Control*, 107:159–165, 1985.

[HU90] K. Hirai and T. Ushio. Chaos and control. *J. SICE*, 32(11):944–951, 1990. (in Japanese).

[Huc81] J. E. Huchinson. Fractals and self-similarity. *Indiana Univ. J.*, 30(5):713–747, 1981.

[IM92] M. Itoh and H. Murakami. Chaos synchronization and secure communications in discrete dynamical systems. *Technical Report of IEICE*, NLP92-50:25–31, 1992.

[IM93] M. Itoh and H. Murakami. Chaos synchronization in discrete-time dynamical systems and secure communication. *Proc. of the 11th European Conference on Circuit Theory and Design, Davos*, 611–614, 1993.

[IMHC93] M. Itoh, H. Murakami, K.S. Halle, and L.O. Chua. Transmission of signals by chaos synchronization. *Technical Report of IEICE*, NLP93-27:89–93, 1993.

[Jul18] G. Julia. Mémoire sur l'iteration des fonctions rationnelles. *Journal de Math. Pure et Appl.*, 8:47–245, 1918.

[Kal56] R. E. Kalman. Nonlinear aspects of sampled data control systems. *Proc. Symp. on Nonlinear Circurit Analysis*, VI:273–312, 1956.

[KHE*92] L. Kocarev, K.S. Halle, K. Eckert, U. Parlitz, and L.O. Chua. Experimental demonstration of secure communications via chaos synchronization. *Int. J. Bifurcaton and Chaos*, 2(3):709–713, 1992.

[Kol54] A. N. Kolmogorov. On conservation of conditionally-periodic motions for a small change in Hamilton's function. *Dokl. Akad. Nauk. USSR*, 98:525, 1954.

[KP91a] K. Karagiannis and F. Pfeiffer. Theoretical and experimental investigations of gear-rattling. *Nonlin. Dyn.*, 2:367–387, 1991.

[KP91b] A. Kunert and F. Pfeiffer. Description of chaotic motion by an invariant distribution at the example of the driven Duffing oscillator. *Int. Series Num. Math.*, 97:225–230, 1991.

[KSK*93] K. Konishi, Y. Shirao, H. Kawabata, T. Nagahara, and Y. Inagaki. Controlling chaos in the maxwell-bloch equations with time delay. *IEICE Trans.*, E76-A(7):1121–1125, 1993.

[KY78] J. L. Kaplan and J. A. Yorke. Chaotic behavior of multidimensional difference equation. *in Springer Lecture Notes in Mathematics, No.730*, 228, 1978.

[LC81] W. Lauterborn and E. Cramer. Subharmonic route to chaos observed in acoustics. *Phys. Rev. Lett.*, 47(20):1145, 1981.

[Lev49] N. Levinson. A second order differential equation with singular solutions. *Ann. Math.*, 50:127–153, 1949.

[LH91] W. Lauterborn and J. Holzfuss. Acoustic chaos. *Int. J. Bifurcation Chaos*, 1(1):13–26, 1991.

[Lib87] A. Libchaber. From chaos to turbulence in Bérnard convection. *Proc. Roy. Soc. London*, A413:633–, 1987.

[Lin81] P. S. Linsay. Period doubling and chaotic behavior in a driven anharmonic oscillator. *Phys. Rev. Lett.*, 47(19):1349–1352, 1981.

[Lin85] P. S. Linsay. The structure of chaotic behavior in a pn junction oscillator. *MIT, Department of Physics Report*, 1985.

[LK81] P. W. Levin and B. P. Koch. Chaotic behavior of parametrically excited damped pendulum. *Phys. Lett. A*, 86(2):71–74, 1981.

[LL83] A. J. Lichtenberg and M. A. Liebermann. *Regular and Stochstic Motion.* Springer, Berlin-Heidelberg-New York-Tokyo, 1983.

[LM85] A. Lasota and M. Mackey. *Probabilistic Properties of Deterministic Systems.* Cambridge University Press, New York, 1985.

[LM90a] G.-X. Li and F. C. Moon. Criteria for chaos of a three-well potential oscillator with homoclinic and heteroclinic orbits. *J. Sound Vib.*, 136:17–34, 1990.

[LM90b] G.-X. Li and F. C. Moon. Fractal basin boundaries in a two-degree-of-freedom nonlinear system. *Nonlin. dynam.*, 1:209–219, 1990.

[Lor63] E. N. Lorenz. Deterministic non-periodic flow. *J. Atmos. Sci.*, 20:130–141, 1963.

[Lot25] A. J. Lotka. *Elements of Physical Biology.* Williams and Wilkins, Baltimore, 1925.

[LPC81] V. S. L'vov, A. A. Predtechensky, and A. I. Chernykh. Bifurcation and chaos in a system of Taylor vortices: a natural and numerical experiment. *Soviet Phys.*, JETP 53:562, 1981.

[Lud79] D. Ludwig. Optimal harvesting of a randomly fluctuating resource. I: Application of perturbation methods. *SIAM J. Appl. Math.*, 37(1):166–184, 1979.

[LV79] D. Ludwig and J. M. Varah. Optimal harvesting of a randomly fluctuating resource. II: Numerical methods and results. *SIAM J. Appl. Math.*, 37(1):185–205, 1979.

[LY75] T. Y. Li and J. A. Yorke. Period three implies chaos. *Amer. Math. Mon.*, 82:985–992, 1975.

[MABD83] G. Malraison, P. Atten, P. Bergé, and M. Dubois. Dimension of strange attractors: an experimental determination of the chaotic regime of two, convective systems. *J. Phys. Lett.*, 44:897–902, 1983.

[Mag83] K. Maginu. Spatially homogineous and inhomogineous oscillations and chaotic motion in the active Josephson junction line. *SIAM J. apple. Math.*, 43:225–243, 1983.

[Man75] B. B. Mandelbrot. *Les Objets Fractals: Forme, Hasard et Dimension.* Flammaison, Paris, 1975.

[Man77] B. B. Mandelbrot. *Fractals: Form, Chance, and Dimension.* W. H. Freeman, San Francsisco, 1977.

[Man82] B. B. Mandelbrot. *The Fractal Geometry of Nature.* W. H. Freeman, New York, 1982.

[Mar78] F. R. Marotto. Snap-back repellers imply chaos in $\mathbf{R}^n$. *J. Math. Anal. Appl.*, 63:199–223, 1978.

[Mar88] P. S. Marcus. Numerical simulation of Jupiter's great red spot. *Nature*, 331:693–696, 1988.

[Mat84] T. Matsumoto. A chaotic attractor from Chua's circuit. *IEEE Trans. Circuits & Syst.*, CAS-31(12):1055–1058, 1984.

[May73] R. M. May. *Stability and Complexity in Model Eco-systems.* Princeton University Press, 1973.

[May74] R. M. May. Biological population with nonoverlapping generations: stable points, stable cycles, and chaos. *Science*, 186:645–647, 1974.

[May76] R. M. May. Simple mathematical models with very complicated dynamics. *Nature*, 261:459–467, 1976.

[May87] R. M. May. Chaos and the dynamics of biological populations. *Proceedings of the Royal Society*, A413, 1987.

[MB86] I. M. Y. Mareels and R. R. Bitmead. Nonlinear dynamics in adaptive control: chaotic and periodic stabilization. *Automatica*, 22:641–655, 1986.

[MB88] I. M. Y. Mareels and R. R. Bitmead. Nonlinear dynamics in adaptive control: chaotic and periodic stabilization – anaysis. *Automatica*, 24(4):485–497, 1988.

[MCH87] F. C. Moon, J. Cusumano, and P. J. Holmes. Evidence for homoclinic orbits as a precursor to chaos in a magnetic pendulum. *Physica 24D*, 383–390, 1987.

[Mcl81] J. B. Mclaughlin. Period-doubling bifurcations and chaotic motion for parametrically forced pendulum. *J. Stat. Phys.*, 24(2):375–388, 1981.

[MCL86] C. Maganza, R. Caussé, and F. Laloe. Bifurcations, period doubling and chaos in clarinetlike systems. *Europhys. Lett.*, 1(6):295–302, 1986.

[MCT84] T. Matsumoto, L. O. Chua, and S. Tanaka. Simplest chaotic nonautonomous circuit. *Phys. Rev. A.*, 30(2):1155–1984, 1984.

[MCT85] T. Matsumoto, L. O. Chua, and S. Tanaka. The double scroll. *IEEE Trans. Circuits & Syst.*, CAS-32(8):798–818, 1985.

[Mel63] V. K. Melnikov. On the stability of the center for time periodic perturbations. *Trans. Moscow Math. Soc.*, 1–57, 1963.

[MGOY85a] S. W. McDonald, C. Grebogi, E. Ott, and J. A. York. Fractal basin boundaries. *Physica 17D*, 125–153, 1985.

[MGOY85b] S. W. McDonald, C. Grebogi, E. Ott, and J. A. York. Structure and crises of fractal basin boundaries. *Phys. Lett.*, 107A:19, 1985.

[MH79] F. C. Moon and P. J. Holmes. A magnetoelastic strange attractor. *J. Sound Vib.*, 65(2):275–296, 1979.

[MH81] G. Mayer-Kress and H. Haken. The influence of noise on the logistic model. *J. Statistical Physics*, 26(1):149–171, 1981.

[MH85] F. C. Moon and W. T. Holmes. Double Poincaré sections of a quasiperiodically forced, chaotic attractor. *Phys. Lett. A*, 111(4):157–160, 1985.

[Mil84a] J. Miles. Resonant motion of spherical pendulum. *Physica 11D*, 309–323, 1984.

[Mil84b] J. Miles. Resonant, nonlpanar motion of a stretched string. *J. Acoust. Soc.*, 75(5):1505–1510, 1984.

[Mir87] C. Mira. *Chaotic Dynamics.* World Scientific, Singapore, 1987.

[ML85a] F. C. Moon and G.-X. Li. Fractal basin boundaries and homoclinic orbits for periodic motion in a two-well potential. *Phys. Rev. Lett.*, 55(14):1439–1442, 1985.

[ML85b] F. C. Moon and G.-X. Li. The fractal dimension of the two-well potintial strange attractor. *Physica 17D*, 99–108, 1985.

[Moo80a] F. C. Moon. Experimental models for strange attractor vibration in elastic systems. *in New Approaches to Nonlinear Problems in Dynamics, P. J. Holomes (ed.)*, 487–495, 1980.

[Moo80b] F. C. Moon. Experiments on chaotic motions of a forced nonlinear oscillator: Strange attractors. *ASME J. Appl. mech.*, 47:638–644, 1980.

[Moo84] F. C. Moon. Fractal boundary for chaos in a two state mechanical oscillator. *Phis. Rev. Lett.*, 53(60):962–964, 1984.

[Moo92] F. C. Moon. *Chaotic and Fractal Dynamics, An Introduciton for Applied Scientists and Engineers.* John Wiley & Sons, New York, 1992.

[Mos67] J. Moser. Convergent series expansions of quasi-periodic motions. *Math. Ann*, 169:163, 1967.

[MS83] F. C. Moon and S. W. Shaw. Chaotic vibration of a beam with nonlinear boundary condition. *J. Nonlinear Mech.*, 18:465–477, 1983.

[MSA87] P. W. Milonni, M.-L. Shih, and J. R. Ackerhalt. *Chaos in Laser-Matter Interactions.* World Scientific, Singapore, 1987.

[MSS89] S. D. Meyers, J. Sommeria, and H. L. Swinney. Laboratory study of the dynamics of Jovian-type vortices. *Physica D*, 37:515–530, 1989.

[MY91] Y. Morita and T. Yasuda. Chaos in one-dimensiona nonlinear systems with small random perturbations. *Systems and Control (ed. T.Ono and F.Kozin), Mita Press*, 215–214, 1991.

[NS89] A. H. Nayfeh and N. E. Sanchez. Bifurcations in a forced softening Duffing oscillator. *Int. J. NonLinear Mechanics*, 24(6):483–497, 1989.

[OGY90] E. Ott, C. Grebogi, and J. A. Yorke. Controlling chaos. *Phys. Rev. Lett.*, 64:1196–1199, 1990.

[OO80] Y. Oono and M. Osikawa. Chaos in nonlinear difference equations. I – Qualitative study of (formal) chaos. *Prog. Theo. Phys.*, 64:54–67, 1980.

[ORr91] O. M. O'Rrelly. Grobal bifurcations in the force vibration of a damped string. *Int. J. Non-Linear Mech.*, 1991.

[Ose68] V. I. Oseledic. A multiplicative ergodic theorem Lyapunov characteristic numbers for dynamical systems. *Trans. Moscow Math. Soc.*, 19:197–231, 1968.

[Ott81] E. Ott. Strange attractors and chaotic motions of dynamical systems. *Rev. Modern Phys.*, 53-41:655–671, 1981.

[PC90] L.M. Pecora and T.L. Carroll. Syncronization in chaotic systems. *Physical Review Letters*, 64(8):821–824, 1990.

[Pea90] G. Peano. Sur une courbe, qui remplit toute une aire plane. *Mathematische Annalen*, 36:157–160, 1890.

[PK90] F. Pfeiffer and A. Kunert. Rattling models from deterministic to stochastic processes. *Nonlinear Dynam.*, 1:63–74, 1990.

[PMM88] B. Poddar, F. C. Moon, and S. Mukherjee. Chaotic motion of an elastic-plastic beam. *J. Appl Mech.*, 55:185–189, 1988.

[Poi90a] H. Poincaré. *Mémoire sur Céurbes Définies par les équations Différentieele I-VI, Oeuvre I.* Gauthier-Villar, Paris, 1880-90.

[Poi90b] H. Poincaré. Sur les équations de la dynamique et le probléme de rois corps. *Acta Math.*, 13:1–270, 1890.

[Poi99] H. Poincaré. *Les Methodes Nouvelles de la Mecanique Celeste, 3 Vols.* Gauthier-Villar, Paris, 1899.

[PR86] H.-O. Peitgen and P. H. Richter. *The Beauty of Fractals.* Springer-Verlag, Berlin, 1986.

[Pre83] C. Preston. *Iterates of Maps on an Interval. Springer Lecture Notes in Mathematics*, Springer-Verlag, Berlin, 1983.

[PS88] H.-O. Peitgen and D. Saupe, editors. *The Science of Fractal Images.* Springer-Verlag, 1988.

[PS90] K. Popp and P. Stelter. Nonlinear oscillations of structures induced by dry friction. *in Nonlinear Dynamics Engineering Systems, W. Schielen (ed.), Springer-Verlag, Berlin*, 233–240, 1990.

[PT86] L. Pietronero and E. Tosatti, editors. *Fractals in Physics.* North-Holland, Amsterdam, 1986.

[RAC85] F. R. Rubio, J. Aracil, and E. F. Camacho. Chaotic motion in an adaptive control system. *Int. J. Control*, 42(2):353–360, 1985.

[RGOD92] F. J. Romeriras, C. Grebogi, E. Ott, and W. P. Dayawansa. Controlling chaotic dynamical systems. *Physica*, D 58:165–192, 1992.

[RH82] R. W. Rollins and E. R. Hunt. Exactly solvable model of a physical system exhibition universal chaotic behavior. *Phys. Rev. Lett.*, 49(18):1295–1298, 1982.

[Rmb76a] O. E. Rössler. Chemical turbulence: Chaos in a small reaction-diffusion system. *Z. Naturforsch*, 31:1168–1172, 1976.

[Rmb76b] O. E. Rössler. An equation for continuous chaos. *Phys. Lett. A*, 57:397, 1976.

[RS84] P. H. Richter and H.-J. Scholz. Chaos in classical mechanics: the double pendulum. *in Stochastic Phenomena and Chaotic Behavior in Complex Systems, P. Schuster (ed.), Springer-Verlag, Berlin*, 86–97, 1984.

[RT71] D. Ruelle and F. Takens. On the nature of turbulence. *Comm. Math. Phys.*, 20:167–192, 1971.

[Sar64] A. Sarkovskii. Coexistence of cycles of a continuous map of a line into itself. *Ukranian Math. J.*, 16:61–71, 1964.

[SB88] F. M. A. Salam and S. Bai. Complicated dynamics of a prototype continuous-time adaptive control systems. *IEEE Trans. Circuits and Syst.*, CAS-35:842, 1988.

[Sch84] H. G. Schuster. *Deterministic Chaos.* Physik-Verlag, Weinheim, 1984.

[SGOY93] T. Shinbrot, C. Grebogi, E. Ott, and J. A. Yorke. Using small perturbations to control chaos. *Nature*, 363-3:411–417, 1993.

[Sha81] R. Shaw. Strange attractors, chaotic behavior and information flow. *Z. Naturforsch. A*, 36:80–112, 1981.

[Sha84] R. Shaw. *The Dripping Faucet as a Model Chaotic System.* Aerial Press, Santa Cruz, CA, 1984.

[Sie16] W. Sierpinski. Sur une courbe contorienne qui content une image biunivoquet et continue detoute courbe donneé. *C. R. Acad. Paris*, 162:629–632, 1916.

[Sin78] D. Singer. Stable orbits and bifurcations of maps of the interval. *SIAM J. Appl. Math.*, 35:260–267, 1978.

[SK79] K. Shiraiwa and M. Kurata. A generalization of a theorem of Marotto. *Proc. Japan Acad.*, 55(Ser. A):286–289, 1979.

[Sma67] S. Smale. Differentiable dynamical systems. *Bull. Amer. Math. Soc.*, 73:747–817, 1967.

[SMY84] Y. Sunahara, Y. Morita, and T. Yasuda. On sensitive dependence on initial condition of nonlinear dynamical systems with additive random perturbations. *System and Control*, 28(9):616–622, 1984. (in Japanese).

[SMY88] Y. Sunahara, Y. Morita, and T. Yasuda. Chaos in nonlinear systems subjected to small random perturbations. In *Nonlinear Stochastic Dynamical Engineering Systems, Proc. of IUTAM Symposium Innsbruck/Igls, Austria*, pages 217–228, Springer-Verlag Berlin Heidelberg, 1988.

[SMYH87] Y. Sunahara, Y. Morita, T. Yasuda, and H. Hisada. Chaotic behavior in a class of discrete predator-prey systems with constant rate control. *Trans. SICE*, 23(9):941–948, 1987. (in Japanese).

[SMYK83] Y. Sunahara, Y. Morita, T. Yasuda, and M. Kimura. On chaotic systems with small random perturbations. *Trans. SICE*, 20(5):389–395, 1983. (in Japanese).

[SMYN87] Y. Sunahara, Y. Morita, T. Yasuda, and H. Nishigami. Chaotic behavior in a class of discrete predator-prey systems with constant control. *Trans. SICE*, 23(6):611–618, 1987. (in Japanese).

[SMYY87] Y. Sunahara, Y. Morita, T. Yasuda, and T. Yamahori. Chaos and fractal boundaries in controlled predator-prey systems. In *Preprints of 16th SICE Symp. on Control Theory*, pages 147–150, 1987.

[SN79] I. Shimada and T. Nagashima. A numerical approach to ergodic problem of dissipative dynamical systems. *Progress of Theoretical Physics*, 61(6):1605–1616, 1979.

[SOGY90] T. Shinbrot, E. Ott, C. Grebogi, and J. A. Yorke. Using chaos to direct trajectories to targets. *Phys. Rev. Lett.*, 26:3215–3218, 1990.

[Spa80] C. T. Sparrow. Bifurcation and chaotic behaviour in simple feedback systems. *J. Theor. Biol.*, 83:93–105, 1980.

[Spa81] C. T. Sparrow. Chaos in a three-dimensional single loop flow system with a piecewise linear feedback function. *J. Math. Anal. A*, 83:275–291, 1981.

[SS80] A. Shibata and N. Saito. Time delays and chaos in two competing species. *Mathematical Biosciences*, 51:199–211, 1980.

[SS85] F. M. A. Salam and S. S. Sastry. Dynamics of the forced Josephson junction circuit: the regions of chaos. *IEEE Trans. Circuits and Syst.*, CAS-32:784–796, 1985.

[SS89] J. Show and S. W. Show. The onset of chaos in a two-degree-of-freedom impacting system. *Trans. ASME*, 56:168–174, 1989.

[SV81] J. G. Sinai and E. B. Vul. Hyperbolicity conditions for the Lorenz model. *Physica 2D*, 3–7, 1981.

[Swi83] H. L. Swinney. Observations of order and chaos in nonlinear systems. *in Order and Chaos, D. H.Campbell and H. A. Rose (eds.), North-Holland, Amsterdam*, 3–15, 1983.

[Swi85] H. L. Swinney. Observations of complex dynamic and chaos. *in Fundamental Problems in Statistical Mechanics VI, E.G.D.Cohen (ed.), Elsevier Science Publishers, New York*, 253–289, 1985.

[SWS82] R. H. Simoyi, A. Wolf, and H. L. Swinney. One dimensional dynamics in a multicomponent chemical reaction. *Phys. Rev. Lett.*, 49:245, 1982.

[SXC89] R. Singh, H. Xie, and R. J. Comparin. Analysis of automotive neutral gear rattle. *J. Sound Vib.*, 131(2):177–196, 1989.

[SY82] P. S. Symonds and T. X. Yu. Evidence for universal chaotic behavior in a driven nonlinear oscillator. *Phys. Rev. Lett.*, 48:714, 1982.

[SY85] P. S. Symonds and T. X. Yu. Counterintuitive behavior in a problem or elastic-plastic beam dynamics. *J. Appl. Mech.*, 52:517–522, 1985.

[SY89] Y. Sunahara and T. Yasuda. On mechanism yielding fractal invariant domain of one-dimensional discrete nonlinear systems. *Trans. ISCIE*, 2(12):431–439, 1989. (in Japanese).

[TA86] N. B. Tufillaro and A. M. Albano. Chaotic dynamics of a bouncing ball. *Am. J. Phys.*, 54(10):939–944, 1986.

[Tak86] H. Takayasu. *Fractal.* Asakura Shoten, 1986. (in Japanese).

[Tat86] T. Tatsumi. *Turbulence and Chaotic Phenomena in Fluids.* North-Holland, Amsterdam, 1986.

[TS86] J. M. T. Thomson and H. B. Stewart. *Nonlinear Dynamics and Chaos – Geometrical Methods for Engineers and Scientists.* John Wiley and Sons, 1986.

[UA81] Y. Ueda and N. Akamatsu. Chaotically transitional phenomena in the forced negative resistance oscillator. *IEEE Trans. Circuit and Syst.*, CAS-28(3):217–224, 1981.

[Ued79] Y. Ueda. Randomly transitional phenomena in the system governed by Duffing's equation. *J. Stat. Phys.*, 20:181–196, 1979.

[Ued80a] Y. Ueda. Explosion of strange attractors exhibited by Duffing's equation. *Ann. N. Y. Acad. Sci.*, 357:422–434, 1980.

[Ued80b] Y. Ueda. Steady motions exhibited by Duffing's equation: a picture book of regular and chaotic motions. *in New Approaches to Nonlinear Problems in Dynamics, P. J. Holmes (ed.), SIAM, Philadelpohia*, 311–322, 1980.

[Ued85] Y. Ueda. Random phenomena resulting from non-linearity in the system described by Duffing's equation. *Int. J. Non-Linear Mech.*, 20(56):481–491, 1985.

[UH83] T. Ushio and K. Hirai. Chaos in non-linear sampled-data control systems. *Int. J. Control*, 38(5):1023–1033, 1983.

[UH84] T. Ushio and K. Hirai. Chaos in peicewise-linear sampled-data control systems. *Trans. SICE*, 20(6):486–491, 1984. (in Japanese).

[UH85a] T. Ushio and K. Hirai. Chaotic behavior in piecewise-linear sampled-data control systems. *Int. J. Non-Linear Mechanics*, 20(5/6):493–506, 1985.

[UH85b] T. Ushio and K. Hirai. Chaotic behavior in pulse-width modulated feedback systems. *Trans. SICE*, 21(6):539–545, 1985. (in Japanese).

[UH87a] T. Ushio and C. S. Hsu. Chaotic rounding error in digital control systems. *IEEE Trans. Circuits and Syst.*, CAS-34(2):133–139, 1987.

[UH87b] T. Ushio and C. S. Hsu. Simple example of digital control systems with chaotic rounding errors. *Int. J. Control*, 45(1):17–31, 1987.

[UNHS88] Y. Ueda, H. Nakajima, T. Hikihara, and H. B. Stewart. Forced two-well potential Duffing equation. *in Dynamical System Approaches to Nonlinear Problems in Circuits and Systems, F. M. A. Salam and M. L. Levi (ed.), SIAM, Philadelphia*, 128–137, 1988.

[Ush82] S. Ushiki. Central difference scheme and chaos. *Physica 4D*, 407–424, 1982.

[Ush94] T. Ushio. Chaotic synchronization and control in one dimensional neural networks with bidirectional connections. *Technical Report of IEICE*, NLP93-76:95–102, 1994. (in Japanese).

[vK04] H. von Koch. Sur une courbe continue sans tangente, obtenue par une construction géometrique élémentaire. *Arkiv för Matematik*, 1:681–704, 1904.

[vK06] H. von Koch. Une méthode géométrique élémentaire pour l'etude de certaines questions de la théorie des courbes planes. *Acta Mathematica*, 30:145–174, 1906.

[Vol26] V. Volterra. Variazioni e fluttuazioni del numero d'individui in spoecie animali conviventi. *Mem. Acad. Lincei.*, 2:31–113, 1926.

[VRS90] J. A. Vastano, T. Russo, and H. L. Swinney. Bifurcation to spatially induced chaos in a reaction-diffusion system. *Physica 46D*, 23–42, 1990.

[WB81] L. A. Wood and K. P. Byrne. Analysis of a random repeated impact process. *J. Sound Vib.*, 82:329–345, 1981.

[WSSV85] A. Wolf, J. B. Swift, H. L. Swinney, and J. A. Vasano. Determining Lyapunov exponents from a time series. *Physica 16D*, 285–317, 1985.

[Yas91] T. Yasuda. Chaos and fractal of a predator-prey system with control inputs. *Systems and Control (ed. T.Ono and F.Kozin), Mita Press*, 439–448, 1991.

[YM79] M. Yamaguchi and H. Matano. Euler's finite difference scheme and chaos. *Proc. Jap. Acad.*, 55(Ser. A):78–80, 1979.

[YS90] T. Yasuda and Y. Sunahara. Stabilization of a chaotic predator-prey system considering fractal boundaries. In *Proc. of the 11th World Congress of IFAC*, pages 379–384, 1990.

[YS91a] T. Yasuda and Y. Sunahara. Fractal dimension of invariant domain of a class of one-dimensional discrete non-linear dynamical system. In *Preprints of the 23rd ISCIE Symposium on Stochastic Systems Theory and its Applications*, pages 109–112, 1991.

[YS91b] T. Yasuda and Y. Sunahara. Fractal domain with positive Lebesgue measure of a one-dimensional discrete nonlinear system. In *Preprints of the 13rd Dynamical System Symposium*, pages 247–250, 1991.

[YS91c] T. Yasuda and Y. Sunahara. Fractal invariant domain and symbolic dynamics of nonlinear dynamical systems. In *Recent Advances in Mathematical Theory of Systems, Control, Networks and Signal Processing II, Proc. of International Symp. MTNS-91*, pages 395–400, Mita Press, Tokyo, 1991.

[YS93] T. Yasuda and Y. Sunahara. Hausdorff dimension of fractal basin boundaries of a class of one-dimensional nonlinear sampled-data control systems. In *Proc. of the 12th World Congress of IFAC*, 1993. (in press).

[YS94a] T. Yasuda and Y. Sunahara. Coexisting final states and fractal basin boundaries of a class of nonlinear sampled-data systems. In *Proc. of the Asian Control Conference*, pages 221–224, 1994.

[YS94b] T. Yasuda and Y. Sunahara. Existing conditions of fractal boundaries of invariant sets of a class of one-dimensional nonlinear discrete-time systems. *Trans. ISCIE*, 7(2):68–76, 1994. (in Japanese).

[YU81] M. Yamaguchi and S. Ushiki. Chaos in numerical analysis of ordinary differential equations. *Physica 3D*, 618–626, 1981.